Effect of Cyclodextrin on Preservative–Surfactant–Protein Interactions

Ruoyu Jia

DIVISION OF FOOD AND PHARMA/CHEMICAL ENGINEERING | DEPARTMENT OF PROCESS AND LIFE SCIENCE ENGINEERING FACULTY OF ENGINEERING LTH | LUND UNIVERSITY

2026

Effect of Cyclodextrin on Preservative–Surfactant–Protein Interactions

Ruoyu Jia

LUND
UNIVERSITY

Effect of Cyclodextrin on Preservative–Surfactant–Protein Interactions

Published by
Department of Process and Life Science Engineering
Faculty of Engineering LTH, Lund University
P.O. Box 118, SE-221 00 Lund, Sweden

Publicerad av
Institutionen för processteknik och tillämpad biovetenskap
Lunds Tekniska Högskola, Lunds universitet
Box 118, 221 00 Lund

Subject: KLGM06 Degree Project in Pharmaceutical Formulation

Division: Division of Food and Pharma/Chemical Engineering
Supervisor: Marie Wahlgren
Examiner: Lars Nilsson

Ämne: KLGM06 Masterexamensarbete i läkemedelsformulering

Avdelning: Avdelningen för livsmedel och läkemedel/kemiteknik
Huvudhandledare: Marie Wahlgren
Examinator: Lars Nilsson

Effect of Cyclodextrin on Preservative–Surfactant–Protein Interactions

by

Ruoyu Jia

Process and Life Science engineering

06 2026

Supervisor: Marie Wahlgren

Examiner: Lars Nilsson

Abstract

Particulate matter formation in parenteral protein formulations poses significant safety risks and quality challenges. In the multi-dose injectable products, therapeutic proteins, surfactants, and antimicrobial preservatives are present together, forming a complex system that is more prone to destabilizing interactions. Cyclodextrin (CD) has been proposed as a potential stabilizer, yet its role in such multiple-component systems remains insufficiently understood.

This project systematically investigated the effect of HP-β-CD on the interactions within a protein–surfactant–preservative model system, using bovine serum albumin (BSA) and human growth hormone (hGH) as model proteins, polysorbate 20 (PS20) as the surfactant, and phenol as the preservative. A stepwise experimental approach was adopted, progressing from binary to ternary systems. Instability was characterized by phenol- and salt-induced precipitation thresholds, detected simultaneously through absorbance, fluorescence, and light scattering signals using a Probe Drum titration instrument.

Results demonstrated that CD's effect on formulation stability is formulation-dependent, governed by the interplay of CD concentration, protein identity, and surfactant concentration. At high concentration, CD protected PS20 against phenol-induced clouding, whereas low CD concentration (10 mg/mL) showed destabilizing tendencies. Although CD slightly destabilized BSA, the overall performance of the CD-BSA ternary system was similar to that of PS20. CD provided no protective effect against phenol-induced hGH aggregation. In the hGH ternary systems, CD behaved as a destabilizer in the hGH system by disrupting PS20's protective role at intermediate surfactant concentrations. Consequently, in ternary systems, CD expressed its effect on formulation stability primarily through modulation of PS20 behavior.

These findings indicate that CD cannot be considered a universally beneficial stabilizer for complex protein formulations containing surfactants and preservatives, and its incorporation requires careful, case-by-case evaluation.

Acknowledgement

I would like to express my sincere gratitude to my supervisor, Marie Wahlgren, for her invaluable guidance, scientific insight, and continuous encouragement throughout this project. I am deeply grateful for her inspiring communications, unwavering support, and profound expertise in pharmaceutical formulation. Her guidance not only provided me with rewarding new experiences but also helped me successfully finish this interesting thesis, during which I acquired abundant knowledge and essential skills.

I am also grateful to my examiner and supervisor for their constructive feedback and academic oversight that enhanced the quality of this work.

Special thanks go to the Division of Food and Pharma/Chemical Engineering at Lund University for providing access to the laboratory facilities, the Probe Drum instrumentation, and all the necessary materials that made this project possible.

Besides, I would like to thank my parents and friends for their patience, encouragement, and company throughout these two years. Despite the geographical distance, their love and warmth have always been present. Talking with them was always the constant comfort that relieve my mental stress every single time. My heartfelt thanks also go to my fellow students during my Master's studies, whose admirable qualities taught me a lot.

Finally, I am profoundly grateful for this two-year Master's journey, 8000 km away from home. It has been an unforgettable experience that allowed me to explore an unknown world, promoted my personal growth, and granted me new insights into myself and life.

Thank you to everyone who crossed my path and supported me along the way.

Thank you for this beautiful chapter of my life.

Thank you for the new experiences in the world.

Table Of Contents

1 Background

Injectable or parenteral formulations are administered directly into the body, usually through several routes, including intravenous, intramuscular, and subcutaneous. Considering that, regulations and pharmacopeias lay strict requirements on the quality control of injectable formulations, involving sterility, particulate matter, pH value, and osmolality[1,2]. Among critical quality attributes, particulate matter is of particular concern.

Among these attributes, particulate matter has been regarded as a quality defect that brings safety risk to patients. As reported, particulate contamination is relevant to adverse clinical consequences, including irreversible lodging and embolization within the pulmonary vasculature initially, then provoking granulomatous inflammation[3,4], if the diameter of the particle is higher than the pulmonary capillary or blood vessel (approximately 10-15 um)[5]. This process may result in structural lung damage (micronodules) and, in severe or chronic cases, development of pulmonary arterial hypertension[5–7]. At the same time, it is also identified as a major cause of drug recalls. Approximately 22% of parenteral drug recalls between 2008 and 2012 were associated with particulate contamination[8]. The number of recall incidents soared in 2013 and 2014, with more than 20 occurrences each year, announced by the FDA[9]. Although the number decreased subsequently, such incidents continued to occur. Therefore, the importance of controlling particulate matter should be highlighted during production design.

This concern is especially critical for therapeutic proteins, which are widely administered parenterally. A great majority of therapeutic proteins employed in clinical practice are formulated as multi-dose injection solutions due to their advantages, particularly in production cost efficacy, minimizing protein waste, repeated administration convenience for health staff, and dosage flexibility[10,11]. In the multi-dose formulations, preservatives are required to maintain the system sterile and avoid microbial contamination[12] since repeated exposure to the potentially microbial-contaminated environment increases the infection risk, and the solution is deemed as expired if it has been opened for more than 24 hours without preservatives inside[13]. Another commonly used excipient is surfactant, providing protective and stabilizing effects to proteins[14]. These components coexist in multi-dose protein formulations and may interact not only with the protein but also with each other, forming a highly complex system.

Although during the process of drug design, development, and production, particles introduced externally, such as insoluble substances from packaging, raw materials, as well as microbial contamination, and generated in the internal solution have been as much as possible avoided to minimize such risks, in practical usage, dilution, and shipment, particle formation can still be observed. Such instability is often driven by competitive adsorption at interfaces and hydrophobic interaction[15–17]. Besides particulate matter, these interactions can also lead to protein denaturation, decreasing the effective protein concentration and inducing adverse immune responses[18,19]. That means purity and potency of therapeutic protein in the injectable solution also reduce[20], which are also critical quality attributes.

These challenges highlight the need for alternative approaches to alleviate the destabilization.

Under these circumstances, cyclodextrins (CDs), a class of cyclic oligosaccharides with a hydrophobic core and hydrophilic surface, which are mostly used for solubility enhancement of poorly soluble drugs, are considered potentially beneficial. An ideal binding is expected to take place between the CD's cavity and the hydrophobic amino acid residues on the protein surface, thereby resulting in occupation of the hydrophobic interaction site and reduction of destabilizing interactions with components in the system. However, some research demonstrated that CD-protein interactions might undermine protein stability[21,22]. At the same time, the behavior of cyclodextrins in multi-component protein formulations containing surfactants and preservatives remains insufficiently understood.

2 Aim of the thesis

The overall aim of this Master's thesis work is to systematically determine the effect of cyclodextrin in the complex formulation system (containing protein, surfactant, and preservative) and how cyclodextrin affects the known incompatibilities in these systems.

There are two destabilizing interactions in the system, surfactant-preservative interaction causing surfactant clouding and protein-preservative interaction leading to protein aggregation, the effects of cyclodextrin on which have not, to our knowledge, been elucidated. Therefore, the first objective of this work is to investigate the effect of cyclodextrin on the respective incompatibility phenomena, determine whether CD could protect surfactant or protein against phenol-induced instability and characterize how this effect varies with CD concentrations. Subsequently, the full complex protein-surfactant-preservative systems are used to study the impact of CD on the overall formulation stability. Together, these objectives aimed to provide a mechanistic understanding of how CD interacts with the individual components and the system as a whole, and to evaluate whether CD can be considered a beneficial stabilizer for complex multi-dose injectable protein formulations containing surfactants and phenolic preservatives.

3 Theoretical background

The United States Pharmacopeia (USP) and the European Pharmacopoeia (Ph. Eur.) define particulate matter as mobile, randomly-sourced, extraneous substances, other than gas bubbles, that cannot be quantified by chemical analysis due to the small amounts of material they represent and their heterogeneous composition[23,24]. In reality, particulate matter can be divided into visible and sub-visible particles. Visible particles are assessed as essentially absent through visual inspection in the solution, which should be conducted against a black or white background and at an illumination intensity between 2000 and 3750lux[25]. As for subvisible particles, there are two examining methods, the light obscuration particle count test and the microscopic particle count test[23,24], which apply to both large- and small-volume injections. Based on USP, particles of a diameter between 10 and 25 μm should be lower than 6000 in small-volume injections and 25 in large-volume injections. And the limit for larger particles (≥ 25 μm) is 600 per container for small-volume injections and 3 per mL for large-volume injections[23]. If the average number of particles exceeds the limit, solutions should undergo a microscopic test. In the small-volume injections, particles between 10 and 25 μm should be less than 3000, and the number of particles larger than 25 μm should not exceed 300 per container. Then, in the large-volume injections, particles between 10 and 25 μm should be less than 12, and the number of particles bigger than 25 μm should not exceed 2 per mL. Parenteral solutions that exceed the requirements are regarded as unqualified.

The source of injectable particulate is usually classified as external and internal. External particulate comes from the environment, including dust, fibers, and microorganisms[26]. Apart from the packaging-derived and process-related, internal particles also include aggregation, agglomerate, and degradants generated from interactions between protein and excipients or among excipients. Understanding and avoiding these interactions helps design and stabilize the formulations.

Regarding the strict requirement for particulate control, this issue becomes even more critical for therapeutic proteins. Protein is generally more prone to aggregation and precipitation than other excipients under a variety of environmental conditions[27], which depends on the intrinsic factor (such as protein structure) and extrinsic conditions (which impose protein stress that destabilizes it). The protein aggregation is a multistep process where proteins lose their native conformational stability and progressively associate into higher-order species. The protein aggregation pathway is initialized through conformational perturbations locally, including unfolding and misfolding[28]. These changes partially expose aggregation-prone sequence(s) or "hot spot(s)"[29], which usually possess high hydrophobicity, lack charges, and are prone to form β-sheets when paired with adjacent strands[30], and present in different regions of proteins. Exposed sequences increase protein-protein hydrophobic interaction, decrease electrostatic repulsion, and facilitate the formation of the hydrogen bond network of the intermolecular β-sheet, making the overall molecules more sustainable for initial aggregation (oligomerization)[28,29]. However, not all of the oligomers can be considered as nucleating species[27,28]. Many early dimers or trimers dissociate into the monomers reversibly, and therefore do not deliver aggregation. Only stable oligomers can continue to grow and act as nuclei.

Subsequently, small oligomeric nuclei associate into bigger clusters and polymers, and eventually form subvisible and visible particles due to limited solubility and/or sedimentation[27]. Here, late-stage aggregation or precipitation tends to be irreversible.

In this process, physical and chemical stresses trigger this pathway by destabilizing the native structure. Physical stresses include interfacial tension[15], freeze-thawing[31,32], shear force[33], and heating[34,35]. For example, interfacial tension is one of the major stresses. Since protein molecules are amphiphilic[36], it is more stable to keep hydrophobic regions at the liquid/air interface and liquid/solid interface, and hydrophilic regions remain in the liquid phase. At the same time, after proteins absorb to interfaces, the overall tension reduces[37], and proteins will spontaneously and irreversibly be attracted to the interface[38]. However, in this process, conformational change and cluster formation occur for proteins on the surface[15,39–41]. As for chemical degradation, oxidation[42], glycation[43], and cross-linking reaction (especially intermolecular disulfide bond formation)[27,44,45] can often change the physical properties of a protein, such as hydrophobicity and local structure, and therefore promote aggregation.

Another external factor that contributes to protein aggregation is colloidal stress, which functions by affecting intermolecular interactions rather than the native conformation. Colloidal factors include protein concentration, pH, ionic strength, buffer type, and addition of excipients[46–48], which regulate the balance between attractive and repulsive forces among protein molecules, and therefore promote protein-protein interactions and oligomer formation.

Besides external stresses (physical, chemical, and colloidal), the overall aggregation tendency also depends on the intrinsic properties of the protein itself, such as hydrophobicity, surface charge, and structural flexibility[49–51]. High hydrophobicity, low net charge (at a certain pH value), and high flexibility make native proteins more susceptible to slight disturbance and likely to aggregate.

Based on the multiple pathways and factors contributing to protein aggregation, formulation strategies are essential to relieve these effects and maintain protein stability. Among these, surfactants are employed to stabilize proteins against interfacial stress. The most extensively used surfactants in biopharmaceutical formulations are non-ionic surfactants, usually polysorbates 20 (Tween 20, PS 20), polysorbate 80 (Tween 80, PS 80), and poloxamer 188 (Figure 1.1)[52]. These surfactants have a hydrophobic fatty acid ester fragment and a hydrophilic poly-oxy-ethylene (PEO) segment, which helps the molecules be amphipathic. Therefore, on the air-liquid interface, hydrophobic tails face the non-polar phase, and PEO chains point towards the aqueous phase; that's why they possess surface activity and decrease interfacial tension. Once the interface is filled with surfactant monomer, all additional surfactants in the system will form micelles (thermodynamically stable nanostructures with inner hydrophobic cores and corona surface constructed from hydrophilic head groups[53]. This concentration, when the interface is saturated, is called the critical micelle concentration (CMC). Below CMC, the surface tension of the system is inversely proportional to the amount of the surfactant, whereas above CMC, surface tension almost plateau[54]. As reported, non-ionic surfactants avoid interface-induced aggregation for different types of protein[55–57] by competing absorption on the interface[52].

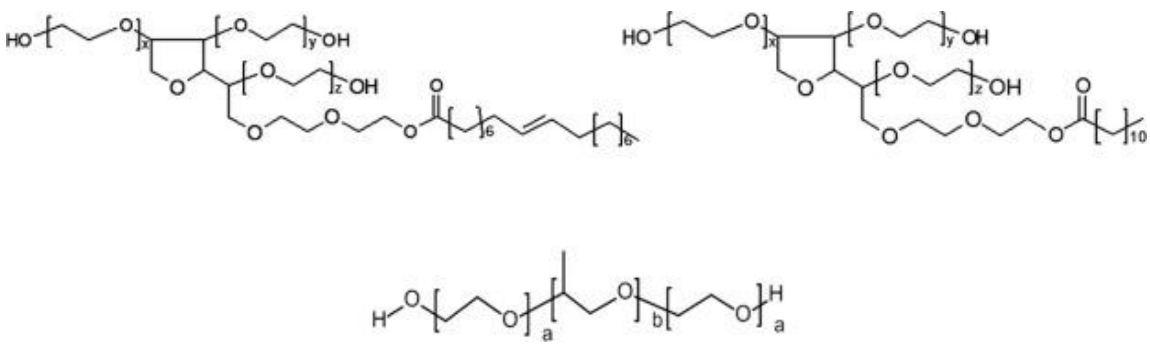

Figure 1.1. Structure of commonly used surfactants: polysorbate 80 (top left), polysorbate 20 (top right) x + y + z = 20; and poloxamer 188 (bottom) a = 80 and b = 2752.

Apart from interfacial benefits, non-ionic surfactants also protect proteins through direct interaction. This interaction is achieved through binding between hydrophobic patches exposed on the protein surface and fatty acid ester fragment of the surfactant, which causes the CMC changing of the surfactant and protein refolding[58,59], and thereby stabilizes the protein formulation. Although protein–surfactant interactions are generally weak[60], the binding affinity and specificity can vary substantially among different surfactants[58,59]. Such differences arise from variations in surfactant hydrophobic tail length and saturation[61,62], which determine how deeply and selectively each surfactant engages with accessible hydrophobic patches or pockets on the protein surface.

However, surfactants also pose a threat to the entire protein formulation. On the one hand, the main degradants of non-ionic surfactants (such as free fatty acids) released via oxidation or hydrolysis catalyze the protein aggregation[63], since the hydrophobicity and low solubility of degradants accelerate further aggregation and sedimentation of proteins[64]. On the other hand, surfactants are susceptible to physical instability, one notable example of which is clouding. Clouding behavior, also known as lower consolute behavior or coacervate phase behavior, is a physical change in the homogeneous solutions of amphiphilic substances, which represents the solution separation into a surfactant-rich and surfactant-poor phase at a certain temperature[65]. This temperature is also called the clouding point, above which the efficient dehydration of the hydrophilic portion of micelles happens. After losing the surrounding hydration layer and releasing the hydrophobic core, attraction between each other is enhanced, and then visible/subvisible cluster formation is promoted[66]. The extent of dehydration increases with temperature growth, which is also the reason why the solubility of surfactants decreases as the temperature rises. Besides temperature, clouding behavior is also influenced by pH value, salt concentration, and organic additives[65,67]. This behavior compromises formulation stability by reducing the effective surfactant concentration and weakening the protection effect. In addition, the increase in turbidity affects the quality of the formulation.

As described above, the preservative is necessary for the whole formulation. Commonly used preservatives for biological drugs are phenol, metacresol, and benzyl alcohol[66]. Their similarity is that there is a benzene ring in their structures (Figure 1.2), which is the crucial part that exerts antibacterial function. These lipophilic molecules permeate through the membrane, accompanied by entering and acidifying the cytoplasm, thereby causing the outflow of the cell contents and the death of the microbial cell[68]. However, precisely because of this

lipophilicity/hydrophobicity characteristic, it is impossible to avoid the destabilizing effects of these preservatives on other components within the formulation. Phenolic preservatives are well-known to affect the clouding point of surfactants[16,66,69] by enhancing hydrophobic attraction with micelles. They are also possible to bind to protein through hydrophobic association, leading to protein aggregation and unfolding[70,71]. Such incompatibility not only generates visible/subvisible particulate matter but also declines the antimicrobial efficacy of preservatives[10]. Consequently, two major destabilizing interactions arise in the system, the surfactant–preservative interaction and the protein – phenol interaction. Although all of these interactions might happen in the multi-component system are generally weak, the dominant pathway leading to precipitation varies depending on the specific protein involved[72]. Therefore, the choice and amount of excipients required for formulation stabilization must be determined case-by-case, as no universal formulation strategy applies.

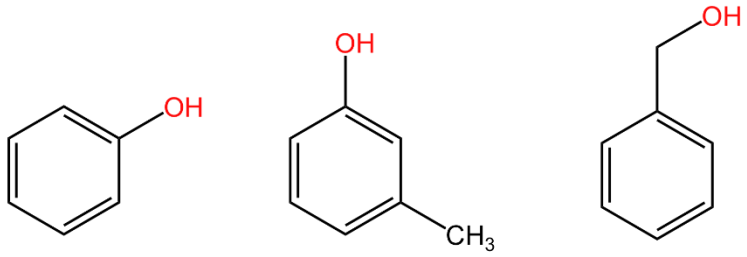

Figure 1.2. Structure of commonly used preservatives: phenol (left), metacresol (middle), and benzyl alcohol (right).

In that case, to protect the overall quality of formulations and avoid destabilizing effects (especially hydrophobic interactions), CD is selected as a potential stabilizer. Composed of glucose subunits in a ring, CD can be categorized into α- (6 subunits), β- (7 subunits), and γ-CD (8 subunits)[22], in Figure 1.3. These molecules are presented as "truncated" cones, whose size of internal cavities is determined by the number of subunits[73]. Considering that natural β-CD has very limited solubility, α-CD is associated with high renal toxicity, and γ-CD is approved by the FDA, but not by the EMA for parenteral use, the cyclodextrins most widely adopted in pharmaceutical formulations are the chemically modified β-CDs, such as HP-β-CD and SBE-β-CD[73–75].

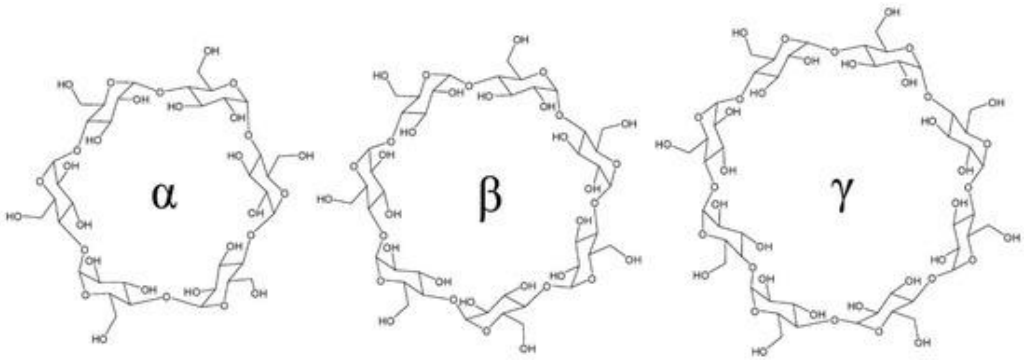

Figure 1.3. Structure of CD: α-CD (left), β-CD (middle), and γ-CD (right)76

CD molecules possess a hydrophilic outer surface and a hydrophobic internal cavity, enabling

them to form inclusion complexes with hydrophobic compounds. Through such hydrophobic interactions, CD can individually interact with proteins, preservatives, and surfactants, thereby potentially decreasing micelle clouding and protein aggregation, as well as improving formulation stability[73,77–79]. On the other hand, the presence of CD can also help depolymerization of protein aggregates through hydrophobic interactions, especially at sites in the protein-protein interface[79]. In addition, CD also contributes to the formulation stability by mitigating interfacial stresses[21,22]. However, CD has been observed to obtain a destabilizing effect on protein thermal stability through preferentially hydrophobic interactions with the folded state, which lowers the energy difference between native and unfolded state, resulting in reducing the thermal unfolding temperature[79,80]. This destabilizing effect on the protein is derived from interaction not only with hydrophobic residues, but also with polar amino acids, even the protein backbone, which also promotes protein unfolding.

In order to achieve the overall objectives of this project, a model system was established comprising bovine serum albumin (BSA) and human growth hormone (hGH) as representative proteins, polysorbate 20 (PS20) as the surfactant, phenol as the preservative, and hydroxypropyl-β-cyclodextrin (HP-β-CD) as a representative cyclodextrin.

The concentration of phenol, as an antibacterial preservative, is strictly limited to the range of 0.0715 – 0.5% for parenteral protein-based products[81]. In contrast, regulatory agencies do not specify the fixed concentration limits for PS20 and HP-β-CD in injectable formulations. Nevertheless, considering the safety of both patients and the formulation[63,74,80,82], the commonly used concentration for PS20 is 0.004 – 0.2% (w/v)[83], which remains above its CMC range (0.0018 – 0.009% at 25 ˚C). As for HP-β-CD, the maximum concentration in the FDA-approved product (SPORANOX®) is 400 mg/mL.

BSA is well-known in many protein researches[58] owing to its stable structure and robustness. BSA is a 66 kDa, highly stable monomeric protein containing 17 disulfide bonds and exhibiting a low isoelectric point (pI ≈ 4.7)[84]. In contrast, recombinant hGH, also called somatotropin, has been employed in parenteral treatment[85]. hGH is a small protein (191 amino acid residues, pI ≈ 5, and molecular weight of 22 kDa) stabilized by two disulfide bonds. When formulated in specific conditions including preservatives, it displays strong aggregation propensity[72,86]. Together, these two proteins (Figure 1.4) provide a complementary model system representing both stable and susceptible protein behaviors.

The detection of this project is based on the determination of the protein and surfactant stability threshold or incompatibility among all components under chemical disturbance from phenol and salt. The addition of phenol generates hydrophobic precipitation inside the system as described above. However, as for salt, increasing concentration of salt replaces the hydration shell around micelles and proteins and shields the surface charge, causing higher precipitation possibility, which can also be called salting out[87]. Once the threshold concentration is reached, the system undergoes loss of stability, leading to aggregation and visible precipitation.

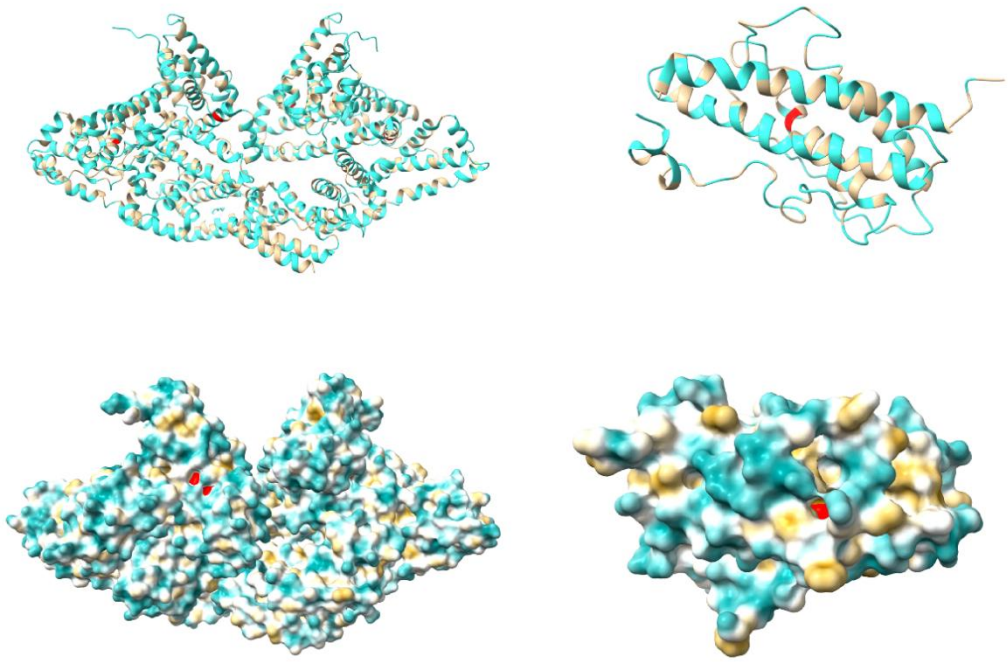

Figure 1.4. Structure of model protein: peptide chains of BSA (upper left), peptide chains of BSA (upper left), where yellow represents hydrophobic residues, and blue represents hydrophilic; surface hydrophobicity of BSA (lower left), surface hydrophobicity of hGH (lower right), where blue and yellow zones reflect hydrophilic and hydrophobic patches, respectively. In this figure, hydrophobic residue tryptophan (Trp) is labeled as red.

Moreover, in the detection process, three signals (absorbance, fluorescence, and light scattering) are simultaneously monitored. The absorbance at a certain wavelength reflects the effective concentration of protein remaining in the liquid phase, while fluorescence in the 300 – 400 nm emission range originates from the protein's intrinsic fluorescence of aromatic amino acid residues (primarily from tryptophan, Trp), which is also influenced by the polarity of their surrounding environment[88]. Light scattering corresponds to single-angle static light scattering measured at a certain wavelength and can be interpreted as a turbidity readout. It reflects the formation of protein aggregation or particles in the system. The scattering intensity depends on both particle number and particle size[89].

4 Material and Methods

4.1 Materials

Two model proteins used in this project were BSA and hGH, in which recombinant human growth hormone (hGH, Somatotropin) was provided by Ferring Pharmaceuticals, and BSA (lyophilized powder, ≥ 96%) was supplied by Sigma Aldrich. Before using, these two proteins experienced no further purification. Polysorbate 20 (super refined) was obtained from Croda (UK), phenol, sodium chloride (NaCl) and (2-Hydroxypropyl)-β-cyclodextrin were both purchased from Sigma Aldrich. All other chemicals were of Pro Analysis grade, and the water used was of Millipore grade.

The buffer used in all experiments was 25 mM phosphate buffer solution (PB) with a pH of 7.00, prepared by disodium hydrogen phosphate and monosodium dihydrogen phosphate (Reag. Ph Eur, Sigma Aldrich, US), kept at room temperature. For the stock solution, BSA, PS20, and CD were dissolved in PB and stored in the freezer. The hGH solution was always freshly prepared in PB before use. Phenol (4.40% and 6.13%, wt%) and NaCl (1 M) solutions were also prepared in PB and stored at room temperature.

4.2 Equipment

This project was conducted using titration in Probe Drum equipment (Labbot, Lund, Sweden) to determine the clouding point of surfactant and the precipitation point of proteins. Probe Drum allows for automatic concentration titration on a microliter scale, with temperature control, mixing of the sample, and simultaneous measurement of three signals (absorbance, fluorescence, and light scattering).

Absorbance spectra were collected in the range of 240 – 720 nm, and fluorescence signal was measured from 240 to 720 nm, with excitation at 280 nm and 4000 ms integration time. Additionally, a laser-based light scattering signal was detected at a 90˚ angle to the sample (red laser with the detector at 637 nm and 100 ms integration time).

4.3 Methods

4.3.1 Experimental design

To systematically investigate how (2-Hydroxypropyl)-β-cyclodextrin (CD) influences the instability of the protein-surfactant-preservative system, the experiments were designed in a stepwise manner from simple to complex systems.

First, the effects of CD on the PS20-phenol (surfactant-preservative) interaction and the BSA/hGH-phenol (protein-preservative) interactions were evaluated individually. Then, ternary combination systems (BSA/hGH-PS20-phenol), which reflected the formulation-like environment, were employed to determine the effect of CD under the more realistic conditions.

In the two mentioned experiments, phenol was employed as the titrant to investigate the concentration threshold for precipitation, serving as the primary destabilizing stress. Finally, an additional stress, ionic strength through NaCl titration was introduced as the supplementary evidence for the effect of CD when facing different stability stressors. In the salt-induced precipitation experiment, phenol was incorporated as a component of the formulation at a concentration below the precipitation threshold of the system, as determined in previous work. Then the system was titrated with 1M NaCl to see at what concentration precipitation will occurs. Considering that the added phenol has a negligible impact on the critical salt concentration at the point of precipitation[72], its operational concentration was set at 50% of the previously determined threshold, which was obtained from the same systems under phenol-stress conditions.

In all of the experiments, system instability was characterized by immediate precipitation and particle formation, represented by the onset of rapid light scattering signal increase at a certain point during the titration of phenol and NaCl solution. And the destabilizing

4.3.2 Sample preparation

Protein concentration was 10 mg/mL for both proteins in all samples.

For sample preparation, PB was first added to the container, followed by the addition of PS20 stock solution and CD stock solution. Subsequently, the protein solution was added to the container. All pipetting and mixing were performed gently to avoid bubble formation. For the salt titration samples, the mixture with protein was gradually added to the phenol solution to avoid too high a local phenol concentration.

Additionally, before being transferred to the cuvette, samples experienced syringe filtration through a 0.22 μm low-protein-binding membrane to remove visible exogenous impurities and minimize protein loss.

4.3.3 Titration procedure

Before the titration procedure, the equipment was blanked with PB.

In these experiments, the initial content of the cuvettes was 600 μL, and a total titrant volume of 200 μL (maximum to 220 μL) was added, with 5 μL of step volume. And the baseline experienced 10 seconds. The measurements were conducted at a temperature of 25 ˚C, with intermittent stirring. The stirring was set at speed setting 4 out of 7 available for the Probe Drum instrument, with a 20-second duration. After each titration step, the sample was equilibrated for 60 s before measuring. For all experiments, two replicates were performed.

4.3.4 Data analysis

The precipitation point was defined as the titrant concentration where the light scattering raw signal first showed a sharp and irreversible increase, as described in experimental design. Through the threshold of titrant concentration/volume at that point, the stability of each system would be compared, and the effect of CD on the stability would be investigated. No smoothing, fitting, or further post-processing was applied to the raw signals.

5 Results

5.1 Effect of CD on clouding interaction between surfactant and preservatives

To evaluate how CD modulates surfactant-preservative interactions during phenol titration, the clouding behavior of the PS20 was first examined. In Figure 2.1, the clouding point diagram at room temperature (25 ˚C) for PS20 with phenol in 25 mM PB is presented.

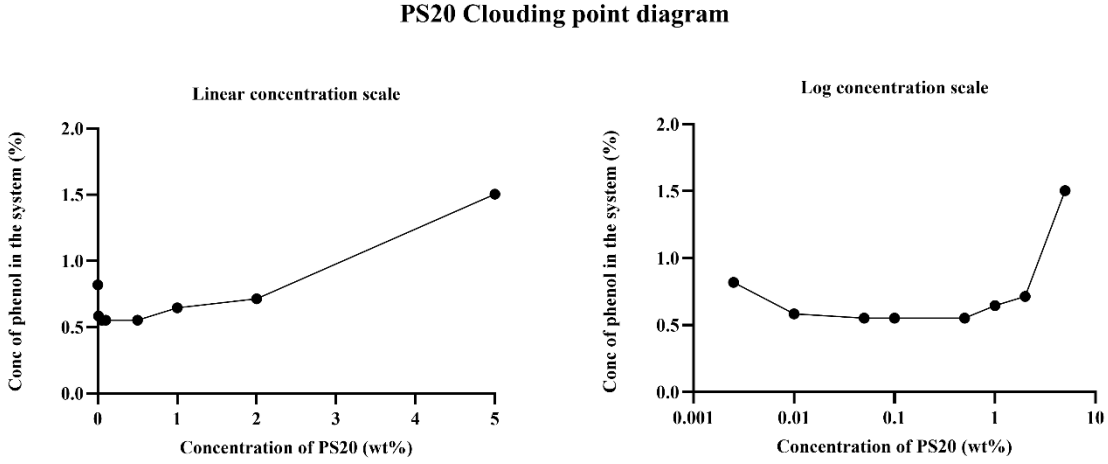

Figure 2.1. Clouding point diagram of PS20 (The left panel shows the phenol concentration (wt%) at which clouding occurred as a function of PS20 concentration (wt%). And the right panel presents the same data plotted against the logarithm of PS20 concentration (wt%).)

The result indicates that there is a compatibility region for any given concentration of PS20 (within the range tested) as long as the phenol concentration is below 0.55%. Overall, there are three distinct regions across the tested PS20 concentration range. Within the intermediate concentration (wt%) range of 0.01% to 0.5%, the phenol concentration causing clouding remained almost constant. When the concentration of PS20 was higher than 0.5%, the clouding-point phenol concentration increased with increasing PS20 concentration. While at PS20 concentrations below 0.01%, the phenol concentration required to induce clouding increased as PS20 decreased. Under a linear concentration scale, the increasing rate in the low PS20 concentration region was dramatically higher than that in the high PS20 concentration region. Another observation is the much lower light-scattering signal intensities and reduced turbidity inside the cuvette when the PS20 concentration was below 0.01% (Figure A.1.1 and Figure A. 1.2), suggesting that fewer particles of smaller size formed in the system.

Based on the identified three regions, four concentrations of PS20 representing different micelle conditions in the system were selected for subsequent investigation on the effect of different concentrations of CD: 0.0025%, 0.01%, 0.1%, and 1% (wt%), respectively. The left panel in

Figure 2.2 illustrates the influence of CD at three concentrations (10, 50, and 100 mg/mL) on the phenol-induced clouding behavior of PS20 compared to the native curve section without cyclodextrin. Except for 10 mg/mL CD, the remaining CD concentration groups maintained almost the similar trend and curve shape to the control (0 mg/mL CD). Both 50 and 100 mg/mL of CD increased the amount of phenol required for the clouding, indicating that cyclodextrin provided a protective effect on PS20 clouding behaviors at 50 mg/mL and 100 mg/mL, and this effect was concentration dependent. Whereas, 10 mg/mL CD overall showed a reduction in phenol concentration at clouding formation (while it exhibited an enhancing effect at 0.01% PS20), suggesting that CD actually possessed no protective effect and even obtained a destabilizing tendency at low concentrations.

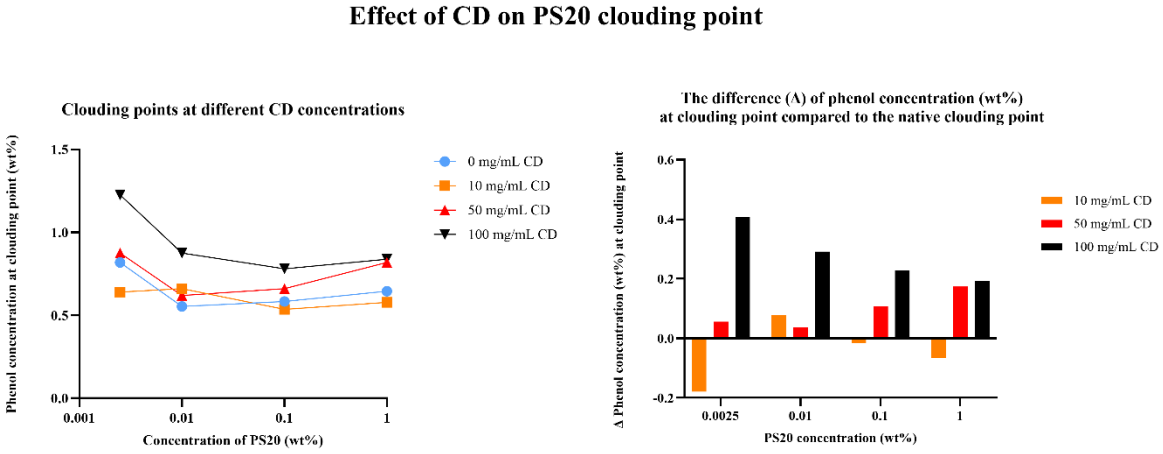

Figure 2.2. Influence of CD concentration on the phenol-induced clouding behavior of PS20. (The left panel shows the absolute phenol concentration at clouding point across different PS20 and CD concentration, and the right panel shows the differences in phenol concentration relative to the control (0 mg/mL CD), where colors represent different CD levels: blue – 0 mg/mL, orange – 10 mg/mL, red – 50 mg/mL, and black – 100 mg/mL in both panels.)

Comparing the differences in clouding phenol concentration at different PS20 concentrations and CD concentrations as present in the right panel in Figure 2.2, the changing trend across PS20 concentration varied distinctly among different CD concentration. Moreover, the lower PS20 concentration showed a higher increasing magnitude upon CD addition, demonstrating that more dilute PS20 system possessed a higher sensitivity in response to the CD effect.

5.2 Effect of CD on aggregation interaction between proteins and preservatives

After examining how CD modifies the surfactant-preservative interaction, the next experiment focused on its influence on protein-preservative interactions. The two proteins, BSA and hGH, exhibited distinct sensitivities and behaviors in response to phenol disturbance.

5.2.1 Effect of CD on BSA-phenol interaction

For BSA, within the tested range (up to 220 μL of 6.13% phenol), the light scattering intensity progressively increased with phenol addition (Figure A.1.20). In contrast, the fluorescence intensity was quenched at 340 nm (Figure A.2.1), reflecting changes in the environment of Trp and indicating the occurrence of hydrophobic interactions between phenol and those residues on the surface of BSA. But these interactions were not sufficiently strong to cause measurable BSA aggregation.

Precipitation points were still not observed when adding 10, 50, and 100 mg/mL of CD to 10 mg/mL of BSA within the tested phenol concentration (Figure A.1.21), because no precipitation occurred in the control sample (BSA alone), these light scattering results do not allow assessment of whether CD provides the protective or destabilizing effect to BSA.

In contrast, the fluorescence spectra show some changes compared to the original spectra without CD after adding 10 and 50 mg/mL CD. The maximum wavelength of the initial emission peak before phenol addition turned to a flat range around 330 to 350 nm. Subsequently, as phenol in the system became more, the wavelength shifted to 310 nm, accompanied with intensity decrease (Figure A.2.2 and Figure A.2.3). However, when the concentration of CD increased to 100, the fluorescence spectra was consistent with that when no CD was present (Figure A.2.4). This observation reflected that at 10 and 50 mg/mL CD, CD-BSA interactions affected the microenvironment of hydrophobic residues, while this influence disappeared when concentration increased to 100 mg/mL.

5.2.2 Effect of CD on hGH-phenol interaction

For hGH, the phenol-induced precipitation points at different CD concentrations are summarized in Table 2.1. The result illustrates that aggregation of hGH occurred at very low phenol concentration, suggesting a high sensitivity of hGH to phenol-induced destabilization. Moreover, there was no increasing trend in phenol concentration as CD concentration rose. Such an observation indicates that the presence of CD provides no protective effect on hGH-phenol interaction, nor does it aggravate the destabilization of hGH within the tested range.

Table 2.1. Precipitation points of hGH induced by phenol (4.40%)

hGH concentration	**10**			
CD concentration (mg/mL)	**0**	**10**	**50**	**100**
Phenol concentration at precipitation point (wt%)	0.107	0.107	0.107	0.090

Consistently, the intrinsic fluorescence measurement was complemented to assess the combination with hydrophobic residues. The wavelength of the emission peak blue shifted from a range (around 320 nm – 350 nm, such a flat peak is usually caused by too high protein concentration) to 326 nm, and subsequently to 314 nm (Figure A.2.5 to Figure A.2.8), also reflecting the occurrence of hydrophobic hGH-phenol interaction.

Another interesting observation from the light scattering data was that although the aggregation points for hGH were comparable at stock solutions of 4.40% and 6.13% phenol, the extent of increasing intensity differed between the two conditions. At 6.13%, the increase was sharper and subsequently reached a stable plateau (Figure A.1.22). This indicates that the critical concentration for phenol-induced aggregation depends on protein types, while the more intense changes of phenol concentration increase the subsequent aggregation rate and the degree of reversibility. Therefore, the phenol concentration used in the subsequent experiments with the systems containing hGH was 4.40% (wt%).

5.3 Effect of CD in the protein–surfactant–preservative systems

In order to further determine the more practical effect of CD on the basis of its individual influence on two destabilizing interactions, a more complex system containing all three components mentioned above was applied for both BSA and hGH.

5.3.1 Effect of CD in the BSA system

The results of light scattering obtained from the BSA-PS20-phenol system at different cyclodextrin concentrations are shown in the left panel of Figure 2.3. 100 mg/mL cyclodextrin provided the maximum increasing level of clouding phenol concentration compared to that without cyclodextrin, suggesting that a higher concentration of cyclodextrin provided a higher protection effect to the whole system, which was similar to the trend of effect of cyclodextrin on PS20-phenol interactions. However, for 10mg/mL CD, its destabilizing effect on the PS20-phenol interaction only appeared at 0.01% and was greatly weakened. And when the PS20 concentrations were at the remaining two levels, CD showed a comparable protective effect. Another similar observation to the effect of cyclodextrin on PS20-phenol interactions was that the sensitivity of PS20 towards cyclodextrin's protection was more notable at 0.01%, as indicated by the increasing magnitude of difference in phenol concentration when precipitating (the right panel of Figure 2.3).

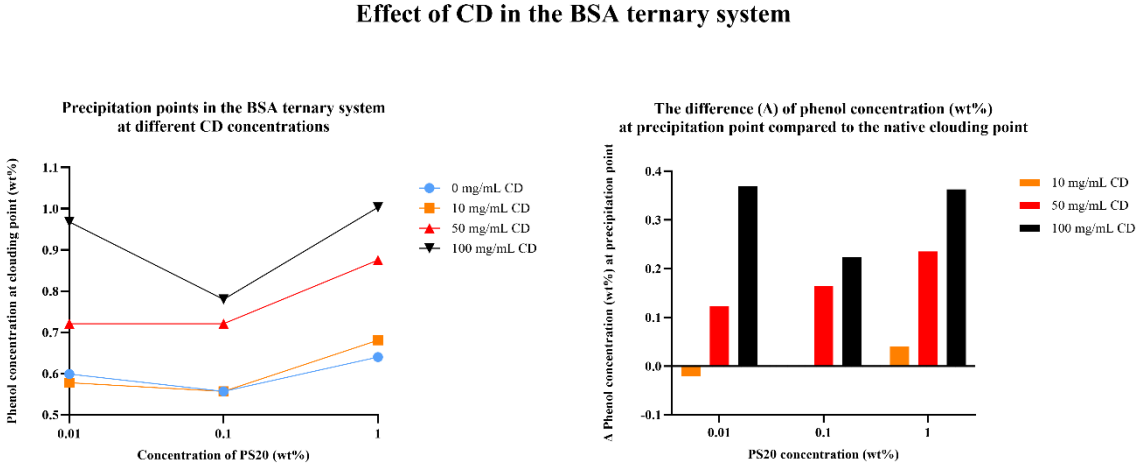

Figure 2.3. Influence of CD concentration on the precipitation behaviors in the BSA ternary system. (The left panel shows the absolute phenol concentration at precipitation point across

different PS20 and CD concentration, and the right panel shows the differences in phenol concentration relative to the control (0 mg/mL CD), where colors represent different CD levels: blue – 0 mg/mL, orange – 10 mg/mL, red – 50 mg/mL, and black – 100 mg/mL in both panels.)

The PS20-phenol and BSA-phenol systems without CD were further compared with this ternary system (BSA-PS20-phenol), no phenol-induced precipitation was observed in the BSA-phenol mixture, whereas visible precipitation appeared in the remaining two systems containing PS20. The distinct behaviors indicated that the precipitation in the ternary mixture was primarily derived from PS20 clouding induced by phenol, supporting why the effect of CD in the BSA-PS20-phenol system shared a comparable trend with the PS20-phenol system.

Additionally, phenol concentration at the point of precipitation differed between the two system types (with and without BSA), as shown in Figure 2.4, reflecting the amount of phenol bound to BSA. In the presence of CD, BSA in systems containing 0.1% PS20 always showed the highest amount of bound phenol, indicating that CD and PS20 affected the phenol-BSA interaction to some extent.

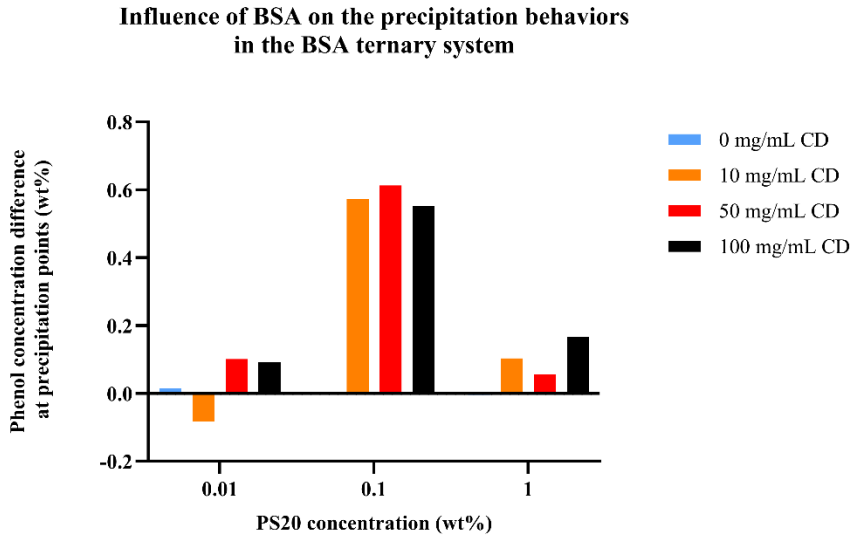

Figure 2.4. Influence of BSA on the precipitation behaviors in the BSA ternary system. (Colors represent different CD levels: blue – 0 mg/mL, orange – 10 mg/mL, red – 50 mg/mL, and black – 100 mg/mL.)

Furthermore, the fluorescence spectra at four different CD concentrations were collected as the complement to the analysis of protein interactions (from Figure A.2.9 to Figure A.2.20). Compared to then initial fluorescence before addition of phenol when only BSA was in the solution, the wavelength of initial fluorescence of solution containing 1%PS20 and 10 mg/mL BSA shifted from 340 nm to 330 nm, while the initial wavelength of the solution containing 0.1% and 0.01% PS20 stayed at 340 nm. This phenomenon indicated that higher PS20 concentration hydrophobically interacted with BSA. During the process of phenol titration, the intensity at the initial wavelength gradually decreased. And following the precipitation point, the wavelength shifted to 300 nm for all three PS20 concentrations.

However, when CD was present in the system, the initial wavelength of fluorescence emission peak showed a progressive red shift as the CD concentration (only happened in the 1%PS20 system). The wavelength shifted to 333 nm at 10 mg/mL CD, 335 nm at 50 mg/mL CD, and 340 nm at 100 mg/mL CD (which was the same as the native BSA). These shifts represented the changes in combination with hydrophobic residues on BSA, suggesting that CD decreased the combination of BSA with PS20, and this reducing effect was relevant to CD concentration.

5.3.2 Effect of CD in the hGH system

Phenol induced precipitation

The influence of PS20 on hGH precipitation induced by phenol was determined at three concentrations (1%, 0.1%, and 0.01%). The result is shown in Figure 2.5. Compared to the phenol concentration at the precipitation point of hGH itself, the addition of 1% PS20 and 0.1% PS20 dramatically increased the phenol concentration required for precipitation, while the lower concentration of PS20 produced only a minimal influence. This observation indicated that within the tested concentration, only when the concentration was higher than 0.1%, PS20 provided a protective effect on hGH.

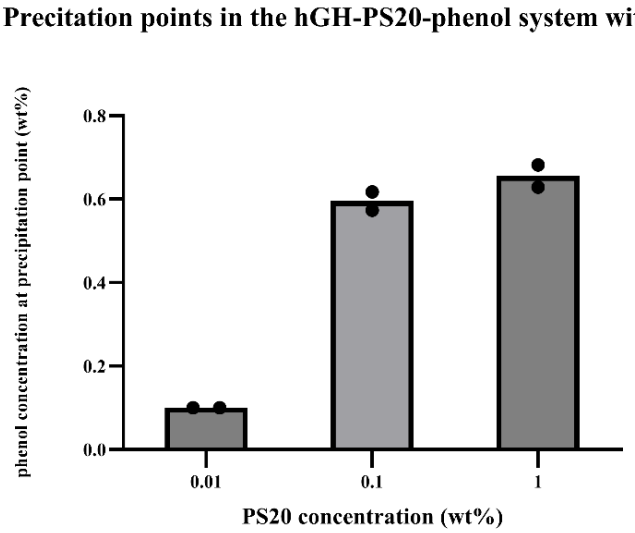

Figure 2.5. Phenol-induced precipitation points in the hGH (10 mg/mL) system without CD

When compared to the individual precipitation/clouding point of two components induced by phenol, the precipitation points in the hGH-PS20-phenol ternary system were higher than both PS20 clouding points and hGH precipitation point at 1% and 0.1% PS20, while the precipitation point of the ternary system at 0.01% PS20 was closer to the hGH precipitation point. This difference indicated that the predominant factors for precipitation were different in the three systems, where co-precipitation complex dominated the incompatibility at 1% and 0.1% PS20, and hGH precipitation dominated at 0.01% PS20.

Similarly, at these three PS20 concentrations, the fluorescence spectra of the ternary systems also possessed some differences. For the hGH ternary systems without cyclodextrin, the samples containing 1% and 0.1% PS20 showed a similar blue shifting (Figure A.2.22 and Figure

A.2.23) upon phenol titration to the results observed for hGH alone and hGH with cyclodextrin, which was induced by phenol interaction. In contrast, at 0.01% PS20, only intensity quenching at 260 nm was observed (Figure A.2.21), without an accompanying wavelength shift. This result suggested that at 0.01% PS20 concentration, phenol still interacted with the hydrophobic patches on the hGH surface, but these interactions did not alter the microenvironment around tryptophan (Trp) to cause shifting.

Based on the performance in the hGH ternary system described above, addition of 10 mg/mL, 50 mg/mL, and 100mg/mL of CD was employed to investigate the effect of CD in the hGH system. Results of light scattering obtained from the hGH-PS20-phenol system at these four CD concentrations are presented in Figure 2.6.

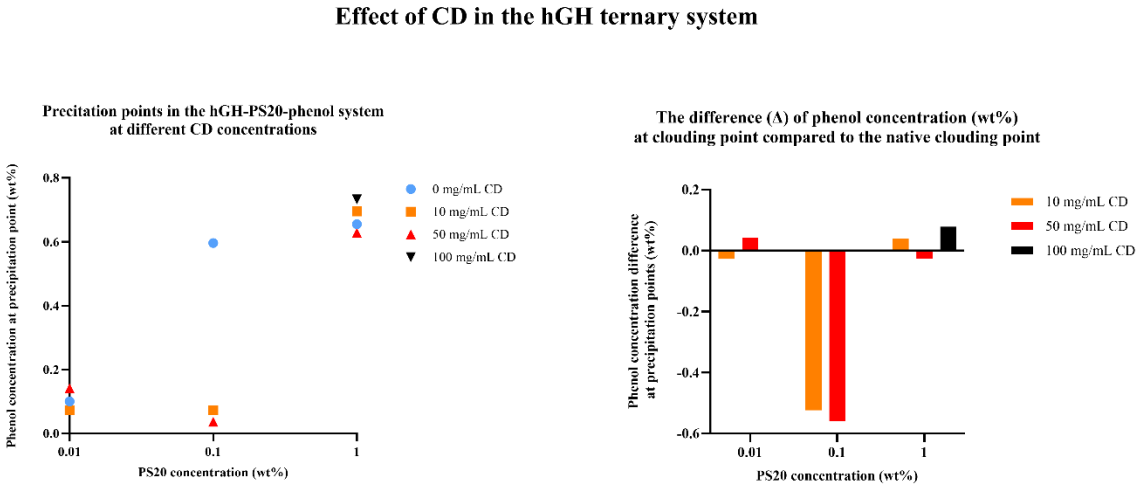

Figure 2.6. Influence of different CD on the phenol-induced precipitation points in the hGH (10 mg/mL) ternary system. (The left panel shows the absolute phenol concentration at precipitation point across different PS20 and CD concentration, and the right panel shows the differences in phenol concentration relative to the control (0 mg/mL CD), where colors represent different CD levels: blue – 0 mg/mL, orange – 10 mg/mL, red – 50 mg/mL, and black – 100 mg/mL in both panels.)

When comparing across various CD concentrations (0, 10, and 50 mg/mL), no notable difference in the precipitation point was observed at 0.01% and 1% of PS20 among the three CD concentrations. In contrast, at 0.1% PS20, the addition of CD dramatically lowered the phenol concentration required to trigger the precipitation, indicating that the presence of CD did not provide an obviously protective effect. On the contrary, under certain conditions, CD even possessed a destabilizing effect on the hGH-PS20-phenol system, especially weakening the protective effect of PS20.

To further understand the relationship between the destabilizing effect on PS20 and the CD: PS20 molar ratio, an additional experiment was performed in which the molar ratio applied at 10 mg/mL CD-0.1% PS20 (CD: PS20 = 8.7:1) was replicated under 1% PS20 condition. Therefore, 100mg/mL CD was tested only at 1%PS20. Similar to the performance of the other CD concentrations at 1% PS20, but different from the behavior at the same CD: PS20 ratio in

the 0.1% PS20 condition, addition of 100 mg/mL also produced little influence on the hGH ternary system. This observation suggested that the destabilizing effect of CD on the hGH-PS20-phenol system depends on the absolute concentration of PS20 rather than the CD: PS20 molar ratio.

Moreover, fluorescence spectra were also collected to provide supplementary evidence for the combination between hGH and the hydrophobic components in the system. After adding different concentrations of cyclodextrin, the fluorescence responses at all three PS20 concentrations performed the same trend: the wavelength of maximum emission peak shifted from the initial region (around 320 – 350 nm) to 326 nm, and subsequently to 314 nm (Figure A.2.24 to Figure A.2.30). When compared with the fluorescence performances in the absence of cyclodextrin, the blue shift phenomenon at 0.01% PS20 concentration reappeared after the addition of CD, illustrating that cyclodextrin affected the PS20-hGH interaction in some cases (at 0.01% PS20).

Salt induced precipitation

Based on the precipitation thresholds identified from phenol-induced results, a phenol-stable condition was applied for further evaluation. Salt-induced precipitation was therefore introduced as an independent stress model to provide a complementary validation of CD effects on the stability of the hGH-PS20-phenol ternary system.

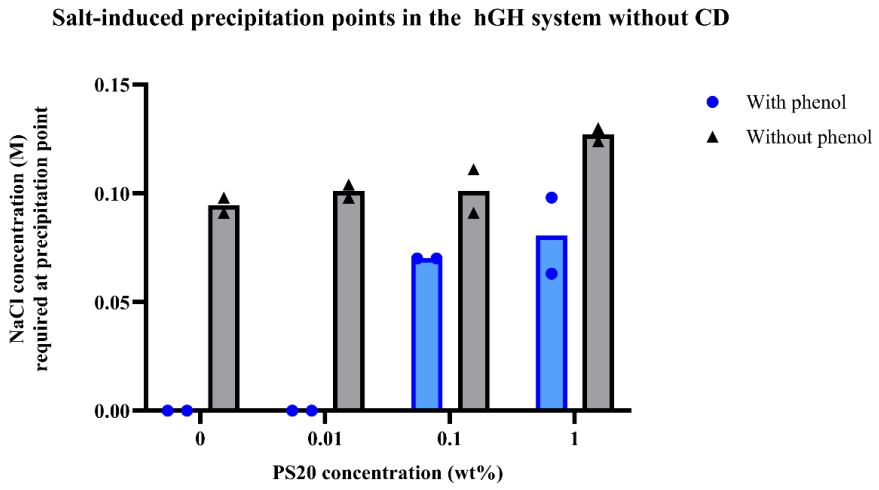

Figure 2.7. Salt-induced precipitation points of hGH (10 mg/mL) at various concentrations of PS20 and phenol in the absence of cyclodextrin. (Blue columns with circle represent the presence of phenol in the system, while black columns with triangle represent the absence of phenol in the system.)

The results of salt-induced precipitation point (from light scattering signals) of hGH with different PS20 concentrations in the absence of cyclodextrin are presented in Figure 2.7. Without phenol in the system, the addition of 1% PS20 obviously increased the concentration of NaCl required for precipitation and lowered the intensity of final light scattering (Figure A.1.50), whereas 0.1% and 0.01% PS20 caused only minor shifts in the NaCl concentration. Such an observation reflected that only 1% PS20 enhanced the stability of the hGH system

under ionic stress, while lower concentrations did not work. In the case when phenol is not present the increase seen in scattering with Probe Drum was not followed by a visual precipitation, indicating that this could be formation of aggregates rather than large visual precipitation.

Additionally, for both 1% and 0.1% PS20, the presence of phenol reduced the NaCl concentration needed for precipitation and increased light scattering intensity compared to their phenol-free counterparts, indicating that phenol shifted the system toward more extensive aggregation under the ionic stress (Figure A.1.49 to Figure A.1.52). Consistent with observation under individual salt and phenol stress, the 1% PS20 system required a slightly higher NaCl volume to precipitate than the 0.1% PS20 system.

Figure 2.8 summarizes the salt-induced precipitation behavior of the 1% PS20 system at different CD concentrations. Comparing across different concentrations of CD in the absence of phenol, addition of CD decreased the NaCl concentration required for precipitation, while decreasing level dropped with the higher CD concentrations. Additionally, the light scattering intensity in the system with different CD concentrations was higher than that of the system without CD (Figure A.1.50, and Figure A.1.53 to Figure A.1.55). This trend suggested that the presence of CD provided a concentration relevant destabilizing effect on the hGH-PS20 system at high PS20 concentration against the ionic stress. However, once the phenol was included in the systems, the NaCl concentration required to precipitate dropped, all of which remained similar with minimal differences at four CD concentrations. At the same time, the light scattering intensity of four systems sharply increased to around 600000 (Figure A.1.56 to Figure A.1.58). These results indicated that when phenol was present in the system containing high PS20 concentration, the effect of CD was not observed, which was consistent with the results obtained from the phenol-induced precipitation experiment.

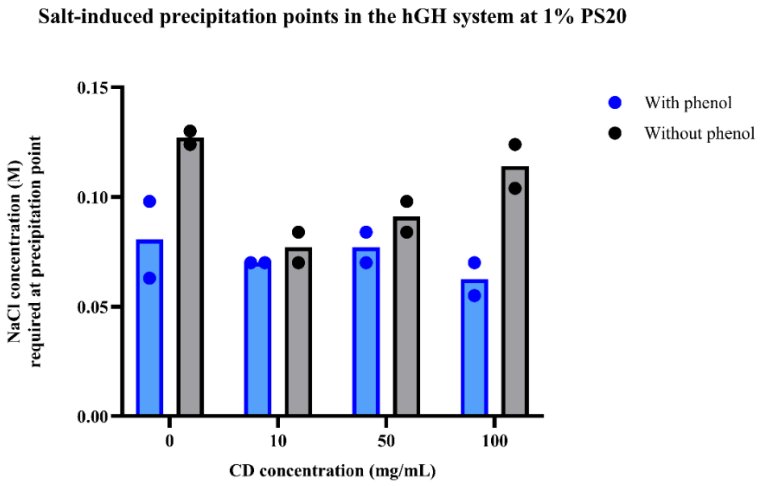

Figure 2.8. Salt-induced precipitation points of hGH (10 mg/mL) at 1% PS20 with different CD concentrations. (Blue columns with circle represent the presence of phenol in the system, while black columns with triangle represent the absence of phenol in the system.)

Under the condition with salt stress, the fluorescence spectra did not change with the addition of 1M NaCl solution (Figure A.2.31 and Figure A.2.32), representing that this stress did not induce huge structural change of the hGH. When phenol was present in the hGH system, the maximum wavelength of the emission peak was blue shifted from a range between 320-350 nm to 326 nm and 314 nm (Figure A.2.33 to Figure A.2.37), which showed a consistent with the performance in the hHG ternary system during the phenol addition experiments.

6 Discussion

In this project, we systematically investigated how HP-β-CD modulates the behavior of a protein-surfactant-preservative (BSA/hGH-PS20-phenol) system by first characterizing its influence on individual molecular interactions and then integrating these results to clarify the collective behavior of the full formulation.

The effect of CD on the PS20-phenol interaction was first determined. However, a comprehensive interpretation of this effect requires a fundamental understanding of the underlying PS20-phenol interaction mechanism as a basis. Distinct from the conventional thermal-induced PS20 clouding phenomenon driven by heating, clouding behaviors triggered by phenol addition at a constant temperature are caused by local and non-covalent interactions on the micellar surface rather than loss of POE segments[90]. Prior to phenol exposure, the POE segments on the surface of PS20 micelle are stabilized by a hydration layer. With the phenol addition, the phenolic hydroxyl group combines with the POE surface through a hydrogen bond. Based on observations in structurally analogous surfactant-aromatic compound systems[91], the connected and exposed benzene rings subsequently displace the surrounding water molecules through hydrophobic repulsion, thereby enhancing the dehydration and increasing the probability of micellar aggregation. As shown in the result, the U-shape PS20 clouding point diagram induced by phenol can be categorized into three regions, each governed by a different molecular mechanism. In the left decreasing part, where PS20 concentration is very close to its CMC[83], the structure of the surfactant system consists of monomers as the majority and micelles as a minority. Here, the fewer micelles there are, the more phenol is required to provide the dehydration effect and collision driving force. And with increasing PS20 concentration, micelle density and collision opportunity increase; consequently, the need for phenol reduces a lot. Conversely, in the right increasing part, micelle number and size dramatically increase, yielding a larger POE area and the diluted coverage of phenol on the surface of each micelle, demanding a higher phenol concentration to induce clouding. While within the intermediate plateau region, the decreasing coverage proportion and increasing collision probability counteract, stabilizing the phenol concentrations at the clouding point. Such a curve with comparable shape and trend has appeared in other research as well[66], but the specific phenol concentration values are different, which might be caused by the difference in ionic strength.

Then, when discussing the CD effect on the PS20-phenol interaction, we found that high concentrations of CD possessed a protective effect against phenol-induced PS20 clouding, which could not be fully explained by phenol inclusion in the hydrophobic cavity of the CD, because the phenol concentration difference was not consistent at a constant CD concentration. This supports additional contributions from the CD-PS20 interactions. CD-phenol inclusion reduces the free phenol concentration[78], thereby lowering its ability to disrupt and aggregate PS20 micelles. And CD can be selectively strung onto the PEO fragments of surfactants to block the formation of phenol complexes on the micelle surface, which are more thermodynamically stable than CD complexes with hydrophobic tails[92]. Together with these two interactions, CD's protection can be explained. However, CD could also encapsulate the hydrophobic tail of PS20 monomer into the cavity[93], subsequently forming a self-assembly

complex through hydrogen bonds, which modulates the PS20 micelle-monomer equilibrium. This results in the loose micelles, which are more susceptible to attack by phenol. When this destabilizing effect counteracts the protection, the performance of CD shows almost no protective effect and even a destabilizing trend. This might be a reason for the effect of the low CD concentration. The observation that high CD concentrations still exhibited a protective effect suggests that the destabilizing contribution is weaker than the protection under these conditions.

When the concentration of CD is further increased, more PS20 monomers are dragged out of the micelles, and the micelles change from a loosely structured state to a new stable balance state (but with fewer and smaller micelles). This situation can be regarded as a parallel rightward shift on the clouding curve. Therefore, for low PS20 concentrations located in the left decreasing region, it is actually a positive effect, while for high concentrations of PS20, it shows no effect or a slightly negative effect, because the slope of the decreasing region on the left is greater than that on the right. At the same time, for high concentrations of PS20, the huge density makes the CD molecules that can be bound to polar headgroups on the micellar surface easily reach the "saturation" state due to spatial hindrance. We speculate that these may be the reasons for the lower sensitivity of high concentration PS20 to the protective effect of CD.

Subsequently, the effect of CD on the protein-phenol interaction was detected. For two proteins, BSA and hGH, the phenol interaction is different. This different sensitivity to the phenol is caused by the different area of hydrophobic patches and accessibility on the surface, as shown in Figure 1.4. The hydrophobic interaction or π-π interaction between phenol and hydrophobic/aromatic residues disturbs the structure of the protein, increasing protein aggregation tendency. Protein hGH obtains a higher exposure of hydrophobic patches and a lower structural stability. On this basis, the presence of a disulfide bond in BSA makes it more resistant to phenol disturbance and structural looseness.

As for different performances of hGH at 4.40% and 6.13% phenol, we speculated that the 6% phenol provided an excessively strong local aggregation stress, making the hGH-phenol interaction more easily cross the reversible range of the aggregation pre-stage and enter the irreversible aggregation state. Compared to this, 4.40% phenol causes relatively mild changes to the environment. Some aggregates still obtained the possibility of dynamic dissociation, thus resulting in a relatively slower increase in signal intensity.

Not only do the two proteins exhibit different sensitivities in their interaction with phenol, but the effects of CD on their protein-phenol interactions also differed. For BSA, the quenching in the fluorescence signal without wavelength shifting reflects that within our experimental range, phenol interacts with the hydrophobic residue (including Trp) on the BSA surface, but does not cause BSA structural disturbance. However, adding a small concentration of CD to the system promotes BSA unfolding[94] through hydrophobic interaction, exposing more internal Trp, consequently leading to an initial surge in intensity and subsequent blue shifting. While as the CD concentration increases further, this destabilizing effect is suppressed. We speculate that this is because too high CD concentrations lead to a significant increase in liquid density, resulting in "crowding" between molecules and thus reducing the space for BSA unfolding. But

as for hGH, addition of CD was defined as having almost no impact. This "no effect" is inconsistent with our initial expectation regarding CD's ability to combine phenol and proteins (as described in the theoretical background section). We propose that the order of magnitude of the protein-phenol binding constant is much higher than that of CD-phenol[95–99], suggesting that in our phenol titration experiments, the destination of phenol is primarily determined by the thermodynamic binding constant rather than the number of binding sites, therefore the effect of CD in preventing phenol from approaching the protein surface is insufficient to counteract the spontaneity of their binding. Whereas, CD's unfolding effect on hGH was not observed, based on the initial flat peak. Consequently, phenol preferentially binds to the protein, resulting in CD's no influence on the hGH-phenol interaction. Bringing the discussion back to BSA and taking both factors into account, we predict that when the phenol concentration continues to increase to a level that can cause BSA to aggregate and precipitate, the presence of CD should have a slight destabilizing effect.

Finally, the effect of CD on the protein-surfactant-preservative ternary system was investigated on the basis of the influence of CD on two individual interactions. In the two ternary systems containing BSA and hGH, the mechanisms causing system incompatibility are different, so the effects presented by CD are also distinct.

In the BSA ternary system, the PS20 clouding dominates the precipitation throughout the entire system. Therefore, the performance of the CD effect here and the CD effect on PS20-phenol interaction is similar. In addition to the aforementioned interactions observed among protein, phenol, PS20, and CD, the PS20-BSA interaction was also observed in the fluorescence signals of the ternary system (which only happened at 1% PS20). The interaction between PS20 and BSA involves hydrophobic binding of the fatty acid tails and the binding between hydrophilic residues on the BSA surface and the POE heads, with the later "hydriphilic" binding showing a higher contribution[100]. The PS20 headgroup, combined with the unspecific polar residues on the BSA surface, triggers the self-assembly of micelles. Subsequently, the abundance of surrounding micelles further increases the probability that hydrophobic plaques are encapsulated by the hydrophobic core of the micelle, resulting in a more hydrophobic microenvironment for the Trp within the hydrophobic patches, therefore the fluorescence signal exhibited a blue shift under high concentrations of PS20, which has also been observed in other studies[101]. Then, as the CD was added, this blue shift phenomenon gradually disappeared because the CD decrease the size and amount of micelle as described above.

When it comes to the hGH ternary system, an interesting finding is that only high concentrations of PS20 can provide protection for hGH. When the concentration of PS20 is high enough, a large number of micelles exist in the system and interact with the hydrophilic amino acid residues on the surface of hGH, which follows the same trend as that of BSA and all proteins. The presence of micelle promotes protein more folded[14] through covering hydrophobic patches, the complex formed between micelles and hGH inhibits the formation of aggregated dimers during this process[102]. Therefore, PS20 shows a protective effect at high concentrations. And with the formation of this complex, once the concentration of phenol exceeds the threshold, the denatured protein will adhere to the micelles and form a co-precipitate. Whereas, at low concentrations, PS20 does not offer any protective effect, where the system incompatibility is

dominated by hGH precipitation. The possible reason for this phenomenon is in this system, most of the PS20s exist in a monomer form, although the PS20 monomers would bind to the hydrophobic patches on the surface of hGH, preventing collisions through these hydrophobic patches[103], the binding strength between the hydrophobic patches and the monomers is not as strong as that between them and phenol. As a result, in the presence of phenol, the PS20 monomers do not provide protection.

On the other hand, for the different changes of the fluorescence signals in the hGH ternary system at different PS20 concentrations, the explanation is distinct. Since the only amino acid Trp in hGH that can trigger the intrinsic fluorescence spectra is located within the hydrophobic core of the protein rather than on the surface hydrophobic patches[104], and in the case that high-concentration micelles cannot prevent the hGH unfolding, the binding of phenol to the internal Trp is not affected, resulting in the same shifting as when PS20 is absent. At low concentrations, it is hypothesized that the PS20 monomers affect the microenvironment for the binding of phenol to Trp, leading to only quenching occurring.

Then, switching focus to how CD affects this hGH ternary system, CD does not provide protective effects. Instead, it exhibits destabilizing effects by weakening the protection of PS20. Regardless of concentration, the addition of CD completely weakened the protective effect of 0.1% PS20. This was because the hydrophobic interaction between CD and PS20 reduced the number of micelles, causing them to fall below the threshold at which PS20 micelles could function. And because 1% contains an adequate number of micelles, even though some are bound by CD, the remaining total amount of micelles still plays a protective role. Furthermore, the binding constant of CD-phenol is also smaller than that of CD-PS20[105]. In this case, CD preferentially binds to PS20, while phenol preferentially binds to hGH. The combination of the two interactions led to the inability of PS20 to continue providing protection. Meanwhile, the strong binding between the CD and the PS20 monomer can also explain why the blue shift phenomenon in the fluorescence spectra reappeared at a concentration of 0.01% of PS20 after the addition of CD.

Although the protective effect of PS20 was not observed in the BSA system, the underlying logic of PS20's protective effect on various proteins is the same, so it also promotes BSA folded at high concentrations. However, at the same time, we know that the presence of CD slightly induces BSA structure unfolding. The counteraction between these two effects results in significant differences in the binding amounts of phenol to BSA at different PS concentrations, shown in Figure 2.4.

Apart from increasing the inherent incompatible hydrophobic stress within the system, we also considered incorporating a new stress, ionic strength, to observe the effect of CD. However, the experiments that increased the ionic concentration were only conducted for the hGH ternary system, because the two proteins have different sensitivities to salting out. As described earlier, salting out is achieved by removing the hydration layer, reducing electrostatic repulsion, and enhancing hydrophobic interactions. The BSA surface is covered with thick hydration layers, which make it resistant to ion attacks and enable it to maintain a stable state even under high ionic concentration conditions[106,107]. However, hGH does not benefit from the same level of

hydration shielding protection as BSA and is therefore more susceptible to hydrophobic collisions. As a result, it exhibits high sensitivity to ionic strength[72,108]. It is precisely for this reason that in different ionic strength environments, the s resistance to aggregation of hGH varies, and the level of hydrophobic attraction needed to precipitate also differs, leading to the phenol concentration required for hGH precipitation as measured in our project being different from the results of other researchers[72].

Moreover, high concentrations of PS20 also exhibit the same protective effects under the ionic stress conditions to hGH as under the phenol stress. However, unlike phenol stress, the presence and integrity of the hydration layer are crucial for ionic strength stress[109]. With increased ionic strength, the hydration layer of the micelle is also weakened, and the inhibition effect for phenol interaction of the micelle bound to the hGH surface, which acts as a cushion barrier, also reduces. Therefore, the protective effect of PS20 under ionic strength stress is not as strong as that under phenol stress. Under ionic strength stress, the presence of CD leads to looser, smaller, and fewer micelles, thus reducing their protective effect. As the CD concentration increases, the micelles reach a new equilibrium, and the solution density increases, further decreasing the extent of this reduction. Simultaneously, the addition of CD weakens the coverage of the PS20 micelles on the hydrophobic patches of hGH, resulting in the higher phenol accessibility. Therefore, in the initial fluorescence spectra before salt addition, the sample with CD shifted to a shorter wavelength.

We speculate that the difference in CD performance under the two stresses may be due to the different dominant controlling factors in the protein aggregation pathway between the two stresses. Generally, these controlling factors are considered to include conformational stability, colloidal stability, and nucleation-dependent aggregation[110,111]. Ionic strength contributes more to colloidal stability, while phenol stress affects the entire aggregation pathway mainly by influencing conformational stability. PS20 micelles function primarily through inhibiting dimer formation to provide protection, and their anti-unfolding effect is slight for phenol approaching, so it is regarded as primarily functioning at the colloidal stability level. Therefore, CDs' modulation on PS20 micelles more significantly affects aggregation under ionic strength stress, whose dominant controlling factor is colloidal stability.

When both phenol and salt stress are present in the solution, phenol will penetrate the hydration layer and cause protein denaturation, greatly promoting aggregation and making the slight modulation of CD on the micelle negligible. But when considering these two types of stress individually, the salt stress does not cause hGH unfolding to the same extent as the phenol stress does, reflected by fluorescence spectra change. As a consequence, the hydrophobic aggregation tendency induced by ionic strength is much lower than that of phenol stress. Therefore, when applying salt to the hGH system that has been exposed to phenol in advance, the two stresses have a synergistic effect, resulting in an enhanced structural disturbance and aggregation tendency.

Otherwise, although this project made every effort to investigate the effect of CD on the complex protein-PS20-phenol system, there were still some limitations in the experiments, which will be elaborated in the future work section.

7 Conclusion

This project investigated the effect of cyclodextrin (represented by HP-β-CD) on the stability of a protein-surfactant-preservative system (BSA/hGH-PS20-phenol) through a stepwise experimental approach, from binary interactions to full ternary formulation-like systems.

For the PS20-phenol interaction, high concentrations of CD (50 and 100 mg/mL) provided a protective effect against phenol-induced clouding through a combination of phenol inclusion in the CD cavity and CD's interaction onto the PS20 POE headgroups, thereby reducing phenol's dehydration impact on micelles. However, low CD concentration (10 mg/mL) showed a tendency toward destabilization, likely due to CD encapsulation of the hydrophobic tail of PS20 monomers, which loosened micellar structure. The sensitivity of PS20 systems to CD protection was greater at lower PS20 concentrations, near or slightly above the CMC.

For the protein-phenol interaction, two proteins showed different sensitivity to phenol, and the effects of CD on them also varied. BSA exhibited resistance to phenol-induced precipitation within the tested range, and CD at low concentrations slightly promoted BSA unfolding through hydrophobic interaction. For hGH, which is more sensitive to phenol, CD provided no effect at any concentration tested, as the binding affinity of phenol for protein exceeded that of CD-pheno interaction.

In the BSA ternary system, precipitation was dominated by PS20 clouding, and CD's effect was consistent with its influence on the binary PS20-phenol system. CD also modulated the PS20-BSA interaction, progressively reducing hydrophobic binding between PS20 micelles and BSA at increasing CD concentrations. In the hGH ternary system, when PS20 protected hGH from precipitation, system incompatibility was dominated by PS20 micelle-hGH co-precipitation, whereas, on the other hand, when PS20 could not protect, the incompatibility was dominated by hGH precipitation. CD failed to provide protection and, at certain PS20 concentrations (particularly 0.1%), actively destabilized the system by disrupting PS20 micelles' protective effect on hGH. This effect depended on the absolute PS20 concentration rather than on the CD: PS20 molar ratio. Salt-induced precipitation experiments confirmed these findings, showing that CD's destabilizing influence on the hGH-PS20 system was observable under ionic stress, but was shielded in the presence of phenol. Consequently, in ternary systems, CD expressed its effect on formulation stability primarily through modulation of PS20 behavior.

Overall, these findings demonstrate that the effect of CD on formulation stability is highly condition-dependent, governed by the interplay of CD concentration, protein type, and surfactant concentration. CD cannot be considered a universally beneficial stabilizer for complex protein formulations containing surfactants and preservatives. Its incorporation requires case-by-case evaluation, with particular attention to the potential reduction of PS20's protective role.

8 Future work

As described in the discussion section, some limitations are present in this project. For example, the stability assessed in this project mainly reflects immediately incompatible trigger points rather than traditional long-term stability. This focus on short-term thresholds may lead to observed phenomena that do not fully align with long-term performance in actual formulation systems. Therefore, long-term stability can be selected as the future work to further investigate the performance of CD in the practical formulation. Under actual formulation and different storage conditions (refrigerator, freezer, or room temperature), the same system was monitored over a long period to observe whether CD still exhibited the same protective or destabilizing trend over the extended timeframe, and whether time-dependent aggregations occurred. Moreover, in terms of long-term stability, one important point to note is that, as described in the theoretical background section, surfactants would undergo hydrolysis to produce fatty acids, which have an adverse effect on protein stability. And these hydrophobic fatty acids have the potential to bind to the hydrophobic cavity of CD. Therefore, CD may exhibit additional functions.

Besides, we employed a direct macroscopic characterization method accompanied by an indirect molecular-level characterization, without covering direct molecular-level observations. Therefore, inferences about interactions and binding mechanisms rely more on the trends in macroscopic cluster formation and fluorescence change than on explicit structural or molecular evidence. Macroscopic light scattering signals themselves also possess a degree of ambiguity: we considered the titrant (phenol or NaCl solution) concentration at the precipitation point as the evaluation and comparison criteria, but the determination of this critical precipitation point is subject to some extent, especially when fluctuation occurs around the points and when the signal intensity increases progressively. And for the precipitation in the ternary system, we cannot distinguish between protein precipitation and PS20 clouding within the same signal to determine how CD affected them individually. Additionally, all experiments were performed in duplicate. While the measurements showed general consistency in trend, the limited number of replications blocks robust statistical analysis and makes it difficult to fully assess experimental variability, particularly in cases where slight differences between conditions were observed. Considering all the mentioned limitations, future work should include expanding the type of detected signals (such as DLS, ITC, T_{agg}, $T_{melting}$, and NMRH), increasing the number of replications, separating the precipitation in the ternary system, and trying to define the precipitation point as the moment when the first derivative of a signal exceeds a certain value.

The ionic strength and protein concentration used in the experiments are not entirely identical to those of actual formulations. As observed in the project, both types of precipitation are affected by ionic strength. This means that the threshold may shift in a real formulation environment. But it is unclear whether the precipitation threshold would be affected by protein concentration. What's more, in some systems, a gradual increase in scattering signal was observed before reaching the precipitation point, indicating that invisible particles began forming at an earlier stage. According to pharmacopoeia requirements, the number and size of these invisible or subvisible particles also fall within the controllable range. However, our

project did not include the formation of these invisible particles in the threshold assessment. Therefore, the "threshold" obtained in this project cannot be directly applied to actual formulation development or manufacturing standards.

9 References

1. United States Pharmacopeia. USP <1> Injections and Implanted Drug Products (Parenterals)—Product Quality Tests. In: United States Pharmacopeia and National Formulary (USP-NF). Rockville (MD): United States Pharmacopeia Convention; 2026.

2. European Pharmacopoeia. Parenteral Preparations. In: European Pharmacopoeia (EP 7.0). Strasbourg (FR): Council of Europe; 2010.

3. Banjade P, Beltran C, Itani A, Sharma M. Pulmonary Foreign Body Granulomatosis Following Intravenous Injection of Oral Medication: A Rare Case Report. *Cureus*. 2024;16(7):e65429. doi:10.7759/cureus.65429

4. Doessegger L, Mahler HC, Szczesny P, et al. The potential clinical relevance of visible particles in parenteral drugs. *Journal of Pharmaceutical Sciences*. 2012;101(8):2635-2644. doi:10.1002/jps.23217

5. Bukofzer S, Ayres J, Chavez A, et al. Industry Perspective on the Medical Risk of Visible Particles in Injectable Drug Products. *PDA Journal of Pharmaceutical Science and Technology*. 2015;69(1):123-139. doi:10.5731/pdajpst.2015.01037

6. Dettmeyer RB, Verhoff MA, Brückel B, Walter D. Widespread pulmonary granulomatosis following long time intravenous drug abuse—A case report. *Forensic Science International*. 2010;197(1-3):e27-e30. doi:10.1016/j.forsciint.2009.12.066

7. Nagarajan K, Preethi J, A S, M R, Selvaraj C. Pulmonary Arterial Hypertension Due to Talc Granulomatosis Following Intravenous Use of Oral Medications: A Report of a Rare Case. *Cureus*. 17(7):e88887. doi:10.7759/cureus.88887

8. Liu F, Hutchinson R. Visible particles in parenteral drug products: A review of current safety assessment practice. *Current Research in Toxicology*. 2024;7:100175. doi:10.1016/j.crtox.2024.100175

9. Particles in Parenterals: 2019 Update. Packaging World. October 4, 2019. Accessed April 28, 2026. https://www.packworld.com/leaders-new/materials/containers/article/15693473/particles-in-parenterals-2019-update

10. Stroppel L, Schultz-Fademrecht T, Cebulla M, et al. Antimicrobial Preservatives for Protein and Peptide Formulations: An Overview. *Pharmaceutics*. 2023;15(2):563. doi:10.3390/pharmaceutics15020563

11. Lee BY, Norman BA, Assi TM, et al. Single versus multi-dose vaccine vials: An economic computational model. *Vaccine*. 2010;28(32):5292-5300. doi:10.1016/j.vaccine.2010.05.048

12. United States Pharmacopeia. USP <51> Antimicrobial Effectiveness Testing. In: United

States Pharmacopeia and National Formulary (USP 29-NF 24). Rockville (MD): United States Pharmacopeia Convention; 2006.

13. Mattner F, Gastmeier P. Bacterial contamination of multiple-dose vials: a prevalence study. *American Journal of Infection Control*. 2004;32(1):12-16. doi:10.1016/j.ajic.2003.06.004

14. Arsiccio A, Pisano R. Surfactants as stabilizers for biopharmaceuticals: An insight into the molecular mechanisms for inhibition of protein aggregation. *European Journal of Pharmaceutics and Biopharmaceutics*. 2018;128:98-106. doi:10.1016/j.ejpb.2018.04.005

15. Li J, Krause ME, Chen X, et al. Interfacial Stress in the Development of Biologics: Fundamental Understanding, Current Practice, and Future Perspective. *AAPS J*. 2019;21(3):44. doi:10.1208/s12248-019-0312-3

16. Gilbert PH, Zhang Z, Qian KK, Allen DP, Wagner NJ, Liu Y. Preservative Induced Polysorbate 80 Micelle Aggregation. *J Pharm Sci*. 2021;110(6):2395-2404. doi:10.1016/j.xphs.2020.12.030

17. Bis RL, Singh SM, Cabello-Villegas J, Mallela KMG. ROLE OF BENZYL ALCOHOL IN THE UNFOLDING AND AGGREGATION OF INTERFERON α-2A. *J Pharm Sci*. 2015;104(2):407-415. doi:10.1002/jps.24105

18. E. Lundahl ML, Fogli S, E. Colavita P, M. Scanlan E. Aggregation of protein therapeutics enhances their immunogenicity: causes and mitigation strategies. *RSC Chemical Biology*. 2021;2(4):1004-1020. doi:10.1039/D1CB00067E

19. Moussa EM, Panchal JP, Moorthy BS, et al. Immunogenicity of Therapeutic Protein Aggregates. *JPharmSci*. 2016;105(2):417-430. doi:10.1016/j.xphs.2015.11.002

20. United States Pharmacopeia. USP <1041> Biologics. In: United States Pharmacopeia and National Formulary (USP 29-NF 24). Rockville (MD): United States Pharmacopeia Convention; 2006.

21. Rospiccio M, Arsiccio A, Winter G, Pisano R. The Role of Cyclodextrins against Interface-Induced Denaturation in Pharmaceutical Formulations: A Molecular Dynamics Approach. *Mol Pharmaceutics*. 2021;18(6):2322-2333. doi:10.1021/acs.molpharmaceut.1c00135

22. Li J, Wang H, Wang L, Yu D, Zhang X. Stabilization effects of saccharides in protein formulations: A review of sucrose, trehalose, cyclodextrins and dextrans. *European Journal of Pharmaceutical Sciences*. 2024;192:106625. doi:10.1016/j.ejps.2023.106625

23. United States Pharmacopeia. USP <788> Particulate Matter in Injections. In: United States Pharmacopeia and National Formulary (USP 29-NF 24). Rockville (MD): United States Pharmacopeia Convention; 2006

24. European Pharmacopoeia. 2.9.20. Particulate Contamination: Visible Particles. In:

European Pharmacopoeia (EP 6.0). Strasbourg (FR): Council of Europe; 2007.

25. United States Pharmacopeia. USP <790> Visible Particulates in Injections. In: United States Pharmacopeia and National Formulary (USP 37-NF 32). Rockville (MD): United States Pharmacopeia Convention; 2014.

26. Langille SE. Particulate Matter in Injectable Drug Products. *PDA Journal of Pharmaceutical Science and Technology*. 2013;67(3):186-200. doi:10.5731/pdajpst.2013.00922

27. Wang W, Nema S, Teagarden D. Protein aggregation—Pathways and influencing factors. *International Journal of Pharmaceutics*. 2010;390(2):89-99. doi:10.1016/j.ijpharm.2010.02.025

28. Wang W, Roberts CJ. Protein aggregation – Mechanisms, detection, and control. *International Journal of Pharmaceutics*. 2018;550(1-2):251-268. doi:10.1016/j.ijpharm.2018.08.043

29. Roberts CJ. Therapeutic Protein Aggregation: Mechanisms, Design, and Control. *Trends Biotechnol*. 2014;32(7):372-380. doi:10.1016/j.tibtech.2014.05.005

30. Caflisch A. Computational models for the prediction of polypeptide aggregation propensity. *Current Opinion in Chemical Biology*. 2006;10(5):437-444. doi:10.1016/j.cbpa.2006.07.009

31. Rodrigues MÂ, Duarte A, Neves R, et al. Deciphering protein aggregation in freeze-thaw process: the roles of cold denaturation and shear stress. *European Journal of Pharmaceutics and Biopharmaceutics*. 2025;217:114905. doi:10.1016/j.ejpb.2025.114905

32. Dao HM, Sandoval MA, Cui Z, Williams Iii RO. Reconsidering freeze-induced protein aggregation: Air bubbles as the root cause of ice-water interface stress. *International Journal of Pharmaceutics*. 2024;665:124723. doi:10.1016/j.ijpharm.2024.124723

33. Aggregation from Shear Stress and Surface Interaction: Molecule-Specific or Universal Phenomenon? BioProcess International. Accessed April 28, 2026. https://www.bioprocessintl.com/formulation/aggregation-from-shear-stress-and-surface-interaction-molecule-specific-or-universal-phenomenon-

34. Fedurkina NV, Belousova LV, Mitskevich LG, Zhou HM, Chang Z, Kurganov BI. Change in kinetic regime of protein aggregation with temperature increase. Thermal aggregation of rabbit muscle creatine kinase. *Biochemistry (Moscow)*. 2006;71(3):325-331. doi:10.1134/S000629790603014X

35. Meersman F, Heremans K. Temperature-Induced Dissociation of Protein Aggregates: Accessing the Denatured State. *Biochemistry*. 2003;42(48):14234-14241. doi:10.1021/bi035623e

36. Bergfreund J, Bertsch P, Fischer P. Adsorption of proteins to fluid interfaces: Role of the hydrophobic subphase. *Journal of Colloid and Interface Science*. 2021;584:411-417. doi:10.1016/j.jcis.2020.09.118

37. Beverung CJ, Radke CJ, Blanch HW. Protein adsorption at the oilrwater interface: characterization of adsorption kinetics by dynamic interfacial tension measurements.

38. Fang F, Szleifer I. Kinetics and Thermodynamics of Protein Adsorption: A Generalized Molecular Theoretical Approach. *Biophysical Journal*. 2001;80(6):2568-2589. doi:10.1016/S0006-3495(01)76228-5

39. Koepf E, Eisele S, Schroeder R, Brezesinski G, Friess W. Notorious but not understood: How liquid-air interfacial stress triggers protein aggregation. *International Journal of Pharmaceutics*. 2018;537(1-2):202-212. doi:10.1016/j.ijpharm.2017.12.043

40. Yano YF, Arakawa E, Voegeli W, Matsushita T. Real-time investigation of protein unfolding at an air–water interface at the 1 s time scale. *J Synchrotron Rad*. 2013;20(6):980-983. doi:10.1107/S0909049513023741

41. Perevozchikova T, Nanda H, Nesta DP, Roberts CJ. Protein Adsorption, Desorption, and Aggregation Mediated by Solid-Liquid Interfaces. *Journal of Pharmaceutical Sciences*. 2015;104(6):1946-1959. doi:10.1002/jps.24429

42. Rosenfeld MA, Leonova VB, Konstantinova ML, Razumovskii SD. Self-assembly of fibrin monomers and fibrinogen aggregation during ozone oxidation. *Biochemistry Moscow*. 2009;74(1):41-46. doi:10.1134/S0006297909010064

43. Wei Y, Chen L, Chen J, Ge L, He RQ. Rapid glycation with D-ribose induces globular amyloid-like aggregations of BSA with high cytotoxicity to SH-SY5Y cells. *BMC Cell Biol*. 2009;10(1):10. doi:10.1186/1471-2121-10-10

44. Cabra V, Vázquez-Contreras E, Moreno A, Arreguin-Espinosa R. The effect of sulfhydryl groups and disulphide linkage in the thermal aggregation of Z19 α-zein. *Biochimica et Biophysica Acta (BBA) - Proteins and Proteomics*. 2008;1784(7-8):1028-1036. doi:10.1016/j.bbapap.2008.04.002

45. Buren NV, Rehder D, Gadgil H, Matsumura M, Jacob J. Elucidation of Two Major Aggregation Pathways in an IgG2 Antibody. *JPharmSci*. 2009;98(9):3013-3030. doi:10.1002/jps.21514

46. King TE, Humphrey JR, Laughton CA, Thomas NR, Hirst JD. Optimizing Excipient Properties to Prevent Aggregation in Biopharmaceutical Formulations. *J Chem Inf Model*. 2023;64(1):265-275. doi:10.1021/acs.jcim.3c01898

47. Thompson RW Jr, Latypov RF, Wang Y, et al. Evaluation of effects of pH and ionic strength on colloidal stability of IgG solutions by PEG-induced liquid-liquid phase separation. *J Chem Phys*. 2016;145(18):185101. doi:10.1063/1.4966708

48. Pham NB, Meng WS. Protein Aggregation and Immunogenicity of Biotherapeutics. *Int J Pharm*. 2020;585:119523. doi:10.1016/j.ijpharm.2020.119523

49. De Simone A, Kitchen C, Kwan AH, Sunde M, Dobson CM, Frenkel D. Intrinsic disorder modulates protein self-assembly and aggregation. *Proc Natl Acad Sci U S A*. 2012;109(18):6951-6956. doi:10.1073/pnas.1118048109

50. Dobson CM. Protein folding and misfolding. *Nature*. 2003;426(6968):884-890. doi:10.1038/nature02261

51. Chiti F. Relative Importance of Hydrophobicity, Net Charge, and Secondary Structure Propensities in Protein Aggregation. In: Uversky VN, Fink AL, eds. *Protein Misfolding, Aggregation, and Conformational Diseases: Part A: Protein Aggregation and Conformational Diseases*. Springer US; 2006:43-59. doi:10.1007/0-387-25919-8_3

52. Khan TA, Mahler HC, Kishore RSK. Key interactions of surfactants in therapeutic protein formulations: A review. *European Journal of Pharmaceutics and Biopharmaceutics*. 2015;97:60-67. doi:10.1016/j.ejpb.2015.09.016

53. Parshad B, Prasad S, Bhatia S, et al. Non-ionic small amphiphile based nanostructures for biomedical applications. *RSC Adv*. 2020;10(69):42098-42115. doi:10.1039/D0RA08092F

54. Cárdenas H, Kamrul-Bahrin MAH, Seddon D, et al. Determining interfacial tension and critical micelle concentrations of surfactants from atomistic molecular simulations. *Journal of Colloid and Interface Science*. 2024;674:1071-1082. doi:10.1016/j.jcis.2024.07.002

55. Vargo KB, Stahl P, Hwang B, et al. Surfactant Impact on Interfacial Protein Aggregation and Utilization of Surface Tension to Predict Surfactant Requirements for Biological Formulations. *Mol Pharmaceutics*. 2021;18(1):148-157. doi:10.1021/acs.molpharmaceut.0c00743

56. Bam NB, Cleland JL, Yang J, et al. Tween protects recombinant human growth hormone against agitation-induced damage via hydrophobic interactions. *Journal of Pharmaceutical Sciences*. 1998;87(12):1554-1559. doi:10.1021/js980175v

57. Charman SA, Mason KL, Charman WN. Techniques for Assessing the Effects of Pharmaceutical Excipients on the Aggregation of Porcine Growth Hormone. *Pharm Res*. 1993;10(7):954-962. doi:10.1023/A:1018994102218

58. Ruiz-Peña M, Oropesa-Nuñez R, Pons T, Louro SRW, Pérez-Gramatges A. Physico-chemical studies of molecular interactions between non-ionic surfactants and bovine serum albumin. *Colloids and Surfaces B: Biointerfaces*. 2010;75(1):282-289. doi:10.1016/j.colsurfb.2009.08.046

59. Whiteley J, Waters LJ, Humphrey J, Mellor S. A thermodynamic investigation into protein–excipient interactions involving different grades of polysorbate 20 and 80. *J*

Therm Anal Calorim. 2024;149(23):13941-13951. doi:10.1007/s10973-024-13533-6

60. Hoffmann C, Blume A, Miller I, Garidel P. Insights into protein–polysorbate interactions analysed by means of isothermal titration and differential scanning calorimetry. *Eur Biophys J*. 2009;38(5):557-568. doi:10.1007/s00249-009-0404-6

61. SINGH SM, BANDI S, JONES DNM, MALLELA KMG. Effect of Polysorbate 20 and Polysorbate 80 on the Higher Order Structure of a Monoclonal Antibody and its Fab and Fc Fragments Probed Using 2D NMR Spectroscopy. *J Pharm Sci*. 2017;106(12):3486-3498. doi:10.1016/j.xphs.2017.08.011

62. Whiteley J, Abrahmsén-Alami S, Booth J, Mellor S, Humphrey J, Waters LJ. Pharmaceutical Analysis of Protein–Peptide Coformulations and the Influence of Polysorbates. *Mol Pharmaceutics*. 2025;22(6):3189-3197. doi:10.1021/acs.molpharmaceut.5c00119

63. Markus T, Lumer J, Stasavage R, Ruffner DB, Philips LA, Cheong FC. Monitoring polysorbate 80 degradation in protein solutions using Total Holographic Characterization. *International Journal of Pharmaceutics*. 2024;652:123843. doi:10.1016/j.ijpharm.2024.123843

64. Larson NR, Wei Y, Prajapati I, et al. Comparison of Polysorbate 80 Hydrolysis and Oxidation on the Aggregation of a Monoclonal Antibody. *JPharmSci*. 2020;109(1):633-639. doi:10.1016/j.xphs.2019.10.069

65. Mukherjee P, Padhan SK, Dash S, Patel S, Mishra BK. Clouding behaviour in surfactant systems. *Advances in Colloid and Interface Science*. 2011;162(1-2):59-79. doi:10.1016/j.cis.2010.12.005

66. Wahlgren M, Börjesdotter AM, Hjalte J, et al. Interactions between polysorbate and antimicrobial preservatives in aqueous parenteral products. *Journal of Drug Delivery Science and Technology*. 2025;107:106765. doi:10.1016/j.jddst.2025.106765

67. Kumar S, Alam MdS, Parveen N, Kabir-ud-Din. Influence of additives on the clouding behavior of amphiphilic drug solutions. *Colloid Polym Sci*. 2006;284(12):1459-1463. doi:10.1007/s00396-006-1506-7

68. Ecevit K, Barros AA, Silva JM, Reis RL. Preventing Microbial Infections with Natural Phenolic Compounds. *Future Pharmacology*. 2022;2(4):460-498. doi:10.3390/futurepharmacol2040030

69. Wang Z, Zhao F, Li D. Determination of solubilization of phenol at coacervate phase of cloud point extraction. *Colloids and Surfaces A: Physicochemical and Engineering Aspects*. Published online 2003. doi:10.1016/s0927-7757(02)00560-5

70. Hutchings RL, Singh SM, Cabello-Villegas J, Mallela KMG. Effect of antimicrobial preservatives on partial protein unfolding and aggregation. *J Pharm Sci*. 2013;102(2):365-

376. doi:10.1002/jps.23362

71. Bis RL, Mallela KMG. Antimicrobial preservatives induce aggregation of interferon alpha-2a: The order in which preservatives induce protein aggregation is independent of the protein. *Int J Pharm*. 2014;472(0):356-361. doi:10.1016/j.ijpharm.2014.06.044

72. Hjalte J, Börjesdotter AM, Diehl C, Ulvenlund S, Wahlgren M, Sjögren H. Excipient effect on phenol-induced precipitation of human growth hormone and bovine serum albumin. *International Journal of Pharmaceutics*. 2025;676:125624. doi:10.1016/j.ijpharm.2025.125624

73. Poulson BG, Alsulami QA, Sharfalddin A, et al. Cyclodextrins: Structural, Chemical, and Physical Properties, and Applications. *Polysaccharides*. 2022;3(1):1-31. doi:10.3390/polysaccharides3010001

74. Ferreira L, Campos J, Veiga F, Cardoso C, Paiva-Santos AC. Cyclodextrin-based delivery systems in parenteral formulations: A critical update review. *European Journal of Pharmaceutics and Biopharmaceutics*. 2022;178:35-52. doi:10.1016/j.ejpb.2022.07.007

75. European Medicines Agency. Cyclodextrins used as excipients: Report published in support of the 'Questions and answers on cyclodextrins used as excipients in medicinal products for human use' (EMA/CHMP/495747/2013). Amsterdam (NL): European Medicines Agency; 2017.

76. Van De Manakker F, Vermonden T, Van Nostrum CF, Hennink WE. Cyclodextrin-Based Polymeric Materials: Synthesis, Properties, and Pharmaceutical/Biomedical Applications. *Biomacromolecules*. 2009;10(12):3157-3175. doi:10.1021/bm901065f

77. Niccoli M, Oliva R, Castronuovo G. Cyclodextrin–protein interaction as inhibiting factor against aggregation. *J Therm Anal Calorim*. 2017;127(2):1491-1499. doi:10.1007/s10973-016-5736-8

78. Holm R, Olesen NE, Alexandersen SD, Dahlgaard BN, Westh P, Mu H. Thermodynamic investigation of the interaction between cyclodextrins and preservatives — Application and verification in a mathematical model to determine the needed preservative surplus in aqueous cyclodextrin formulations. *European Journal of Pharmaceutical Sciences*. 2016;87:22-29. doi:10.1016/j.ejps.2015.09.011

79. Serno T, Geidobler R, Winter G. Protein stabilization by cyclodextrins in the liquid and dried state. *Advanced Drug Delivery Reviews*. 2011;63(13):1086-1106. doi:10.1016/j.addr.2011.08.003

80. Härtl E, Winter G, Besheer A. Influence of Hydroxypropyl-Beta-Cyclodextrin on the Stability of Dilute and Highly Concentrated Immunoglobulin G Formulations. *JPharmSci*. 2013;102(11):4121-4131. doi:10.1002/jps.23729

81. Meyer BK, Ni A, Hu B, Shi L. Antimicrobial preservative use in parenteral products: Past

and present. *Journal of Pharmaceutical Sciences*. 2007;96(12):3155-3167. doi:10.1002/jps.20976

82. Kriegel C, Festag M, Kishore RSK, Roethlisberger D, Schmitt G. Pediatric Safety of Polysorbates in Drug Formulations. *Children*. 2020;7(1):1. doi:10.3390/children7010001

83. Wuchner K, Yi L, Chery C, et al. Industry Perspective on the use and Characterization of Polysorbates for Biopharmaceutical Products Part 1: Survey Report on Current State and Common Practices for Handling and Control of Polysorbates. *Journal of Pharmaceutical Sciences*. 2022;111(5):1280-1291. doi:10.1016/j.xphs.2022.02.009

84. Bujacz A. Structures of bovine, equine and leporine serum albumin. *Acta Cryst D*. 2012;68(10):1278-1289. doi:10.1107/S0907444912027047

85. Drug Enforcement Administration, Diversion Control Division. Human Growth Hormone (Trade Names: Genotropin®, Humatrope®, Norditropin®, Nutropin®, Saizen®, Serostim®). Washington (DC): Drug & Chemical Evaluation Section, US Department of Justice; 2023.

86. Chura-Chambi RM, Farah CS, Morganti L. Human growth hormone inclusion bodies present native-like secondary and tertiary structures which can be preserved by mild solubilization for refolding. *Microb Cell Fact*. 2022;21:164. doi:10.1186/s12934-022-01887-1

87. Duong-Ly KC, Gabelli SB. Salting out of Proteins Using Ammonium Sulfate Precipitation. In: *Methods in Enzymology*. Vol 541. Elsevier; 2014:85-94. doi:10.1016/B978-0-12-420119-4.00007-0

88. Eftink MR. Intrinsic Fluorescence of Proteins. In: Lakowicz JR, ed. *Topics in Fluorescence Spectroscopy: Volume 6: Protein Fluorescence*. Springer US; 2000:1-15. doi:10.1007/0-306-47102-7_1

89. Brar SK, Verma M. Measurement of nanoparticles by light-scattering techniques. *TrAC Trends in Analytical Chemistry*. 2011;30(1):4-17. doi:10.1016/j.trac.2010.08.008

90. Duarte LJN, Canselier JP. Oxo-Alcohol Ethoxylates: Surface and Thermodynamic Properties and Effect of Various Additives on the Cloud Point. *Tenside Surfactants Detergents*. 2005;42(5):299-306. doi:10.3139/113.100272

91. Parekh P, Ganguly R, Aswal VK, Bahadur P. Room temperature sphere-to-rod growth of Pluronic® P85 micelles induced by salicylic acid. *Soft Matter*. Published online 2012. doi:10.1039/C2SM25517K

92. Topchieva I, Karezin K. Self-Assembled Supramolecular Micellar Structures Based on Non-ionic Surfactants and Cyclodextrins. *Journal of Colloid and Interface Science*. 1999;213(1):29-35. doi:10.1006/jcis.1998.6065

93. Zhou C, Cheng X, Zhao Q, Yan Y, Et. A. Self-Assembly of Nonionic Surfactant Tween 20@2β-CD Inclusion Complexes in Dilute Solution. *Langmuir*. Published online 2013. doi:10.1021/la403257v

94. Cooper A, Lovatt M, Nutley MA. Energetics of protein-cyclodextrin interactions. *Journal of Inclusion Phenomena and Molecular Recognition in Chemistry*. Published online 1996. doi:10.1007/BF01041542

95. Rawel HM, Meidtner K, Kroll J. Binding of Selected Phenolic Compounds to Proteins. *Journal of Agricultural and Food Chemistry*. Published online 2005. doi:10.1021/jf0480290

96. Rekharsky MV, Inoue Y. Complexation Thermodynamics of Cyclodextrins. *Chemical Reviews*. Published online 1998. doi:10.1021/cr970015o

97. Le Saux T, Hisamoto H, Terabe S. Measurement of monomolecular binding constants of neutral phenols into the β-cyclodextrin by continuous frontal analysis in capillary and microchip electrophoresis via a competitive assay. *Journal of Chromatography A*. 2006;1104(1-2):352-358. doi:10.1016/j.chroma.2005.11.125

98. Wada S, Tomioka S, Moriguchi I. Protein Bindings. VI. Binding of Phenols to Bovine Serum Albumin. *Chemical and Pharmaceutical Bulletin*. Published online 1969. doi:10.1248/cpb.17.320

99. Aachmann FL, Otzen DE, Larsen KL, Wimmer R. Structural background of cyclodextrin-protein interactions. *Protein Engineering Design and Selection*. Published online 2003. doi:10.1093/protein/gzg137

100. Delgado-Magnero KH, Valiente PA, Ruiz-Peña M, Pérez-Gramatges A, Pons T. Unraveling the binding mechanism of polyoxyethylene sorbitan esters with bovine serum albumin: A novel theoretical model based on molecular dynamic simulations. *Colloids and Surfaces B: Biointerfaces*. 2014;116:720-726. doi:10.1016/j.colsurfb.2013.11.018

101. Ruiz-Peña M, Oropesa-Nuñez R, Pons T, Louro SRW, Pérez-Gramatges A. Physico-chemical studies of molecular interactions between non-ionic surfactants and bovine serum albumin. *Colloids and Surfaces B: Biointerfaces*. 2010;75(1):282-289. doi:10.1016/j.colsurfb.2009.08.046

102. Katakam M, Bell LN, Banga AK. Effect of Surfactants on the Physical Stability of Recombinant Human Growth Hormone. *Journal of Pharmaceutical Sciences*. 1995;84(6):713-716. doi:10.1002/jps.2600840609

103. Bam NB, Cleland JL, Yang J, Manning MC, Et. A. Tween protects recombinant human growth hormone against agitation-induced damage via hydrophobic interactions. *Journal of Pharmaceutical Sciences*. Published online 1998. doi:10.1021/js980175v

104. de Vos AM, Ultsch M, Kossiakoff AA. Human Growth Hormone and Extracellular

Domain of Its Receptor: Crystal Structure of the Complex. *Science*. Published online 1992. doi:10.1126/science.1549776

105. Eli W, Chen W, Xue Q. The Association of Triton X Surfactants with β-Cyclodextrin. An Isothermal Titration Calorimetry Study. *Journal of Inclusion Phenomena*. 2000;36(4):439-445. doi:10.1023/A:1008105200081

106. Bye JW, Meliga S, Ferachou D, Cinque G, Et. A. Analysis of the Hydration Water around Bovine Serum Albumin Using Terahertz Coherent Synchrotron Radiation. *The Journal of Physical Chemistry A*. Published online 2013. doi:10.1021/jp407410g

107. Dumetz AC, Snellinger-O'Brien AM, Kaler EW, Lenhoff AM. Patterns of protein–protein interactions in salt solutions and implications for protein crystallization. *Protein Science*. Published online 2007. doi:10.1110/ps.072957907

108. Kim MJ, Park HS, Seo KH, Yang HJ, Kim SK, Choi JH. Complete Solubilization and Purification of Recombinant Human Growth Hormone Produced in Escherichia coli. *PLoS One*. 2013;8(2):e56168. doi:10.1371/journal.pone.0056168

109. van Oss CJ, Good RJ, Chaudhury MK. Solubility of proteins. *J Protein Chem*. 1986;5(6):385-405. doi:10.1007/BF01025572

110. Chi EY, Krishnan S, Randolph TW, Carpenter JF. Physical Stability of Proteins in Aqueous Solution: Mechanism and Driving Forces in Nonnative Protein Aggregation. *Pharm Res*. 2003;20(9):1325-1336. doi:10.1023/A:1025771421906

111. Chaudhuri R, Cheng Y, Middaugh CR, Volkin DB. High-Throughput Biophysical Analysis of Protein Therapeutics to Examine Interrelationships Between Aggregate Formation and Conformational Stability. *AAPS J*. 2013;16(1):48-64. doi:10.1208/s12248-013-9539-6

10 Appendices

10.1 Appendix A: Raw data and results of light scattering signals

Table A.1.1 The phenol concentration at clouding points of PS20 induced by phenol

PS20 (%)	0.0025		0.01		0.05		0.1		0.5		1		2		5
	1	2	1	2	1	2	1	2	1	2	1	2	1	2	1
Volume of Phenol (mL)	90	95	120	125	115	115	115	115	120	110	130	145	160	150	130
Conc. of Phenol (wt%)	0.800	0.838	0.574	0.595	0.553	0.553	0.553	0.553	0.574	0.532	0.615	0.675	0.733	0.695	1.504
Average conc. of Phenol (wt%)	0.819		0.584		0.553		0.553		0.553		0.645		0.714		1.504

Table A.1.2 The phenol concentration at clouding points of PS20 induced by phenol with different concentrations of CD

PS20 (%)	0.0025						0.01						0.1						1					
Conc. of CD (mg/mL)	10		50		100		10		50		100		10		50		100		10		50		100	
	1	2	1	2	1	2	1	2	1	2	1	2	1	2	1	2	1	2	1	2	1	2	1	2
Volume of Phenol (mL)	65	75	105	95	145	155	70	75	70	65	95	105	60	55	70	75	85	90	60	65	95	90	100	90
Conc. of Phenol (wt%)	0.599	0.681	0.913	0.838	1.193	1.258	0.640	0.681	0.640	0.599	0.838	0.913	0.557	0.515	0.640	0.681	0.761	0.800	0.557	0.599	0.838	0.800	0.876	0.800
Average conc. of Phenol (wt%)	0.640		0.875		1.226		0.661		0.620		0.875		0.536		0.661		0.780		0.578		0.819		0.838	
ΔConc. of Phenol compared to without CD (wt%)	-0.179		0.057		0.407		0.077		0.036		0.291		-0.017		0.108		0.227		-0.067		0.174		0.193	

Table A.1.3 The phenol concentration at precipitation points of BSA ternary systems induced by phenol with different concentrations of CD

PS20 (%)	0.01								0.1								1							
Conc. of BSA (mg/mL)	10								10								10							
Conc. of CD (mg/mL)	0		10		50		100		0		10		50		100		0		10		50		100	
	1	2	1	2	1	2	1	2	1	2	1	2	1	2	1	2	1	2	1	2	1	2	1	2
Volume of Phenol (mL)	65	65	60	65	80	80	110	115	65	55	60	60	80	80	85	90	75	65	80	70	95	105	125	110
Conc. of Phenol (wt%)	0.599	0.599	0.557	0.599	0.721	0.721	0.950	0.986	0.599	0.515	0.557	0.557	0.721	0.721	0.761	0.800	0.681	0.599	0.721	0.640	0.838	0.913	1.057	0.950
Average conc. of Phenol (wt%)	0.599		0.578		0.721		0.968		0.557		0.557		0.721		0.780		0.640		0.681		0.875		1.003	
ΔConc. of Phenol compared to without CD (wt%)	-		-0.021		0.122		0.369		-		0.000		0.164		0.223		-		0.041		0.235		0.363	
ΔConc. of Phenol compared to without BSA (wt%)	0.015		-0.083		0.101		0.092		0.004		0.574		0.613		0.553		-0.005		0.103		0.057		0.166	

Table A.1.4 The phenol concentration at precipitation points of hGH induced by phenol with different concentrations of CD

Conc. of hGH (mg/mL)	10							
Conc. of CD (mg/mL)	0		10		50		100	
	1	2	1	2	1	2	1	2
Volume of Phenol (mL)	15	15	15	15	15	15	15	10
Conc. of Phenol (wt%)	0.107	0.107	0.107	0.107	0.107	0.107	0.107	0.072
Average conc. of Phenol (wt%)	0.107		0.107		0.107		0.090	
ΔConc. of Phenol compared to without CD (wt%)	-		0.000		0.000		-0.018	

Table A.1.5 The phenol concentration at precipitation points of hGH ternary systems induced by phenol with different concentrations of CD

PS20 (%)	0.01						0.1						1							
Conc. of hGH (mg/mL)	10						10						10							
Conc. of CD (mg/mL)	0		10		50		0		10		50		0		10		50		100	
	1	2	1	2	1	2	1	2	1	2	1	2	1	2	1	2	1	2	1	2
Volume of Phenol (mL)	14	14	10	10	25	15	98	90	10	10	10	0	110	100	110	115	95	105	120	120
Conc. of Phenol (wt%)	0.100	0.100	0.072	0.072	0.176	0.107	0.618	0.574	0.072	0.072	0.072	0.000	0.682	0.629	0.682	0.708	0.601	0.655	0.733	0.733
Average conc. of Phenol (wt%)	0.100		0.072		0.142		0.596		0.072		0.036		0.655		0.695		0.628		0.733	
ΔConc. of Phenol compared to without CD (wt%)	-		-0.028		0.041		-		-0.524		-0.560		-		0.040		-0.027		0.078	

Table A.1.6 The phenol concentration at precipitation points of hGH systems containing different concentrations of PS20 and CD induced by salt without phenol

PS20 (%)	0		0.01		0.1		1							
Conc. of hGH (mg/mL)	10		10		10		10							
Conc. of CD (mg/mL)	0		0		0		0		10		50		100	
	1	2	1	2	1	2	1	2	1	2	1	2	1	2
Volume of NaCl solution (mL)	65	60	65	70	75	60	85	90	45	55	65	55	85	70
Conc. of NaCl (M)	0.098	0.091	0.098	0.104	0.111	0.091	0.124	0.130	0.070	0.084	0.098	0.084	0.124	0.104
Average conc. of NaCl (M)	0.094		0.101		0.101		0.127		0.077		0.091		0.114	
ΔConc. of NaCl compared to without CD (M)	-		-		-		-		-0.050		-0.036		-0.013	

Table A.1.6 The phenol concentration at precipitation points of systems containing 10 mg/mL hGH, and different concentrations of PS20, phenol, and CD induced by salt (where the concentration of phenol was at half of precipitation threshold)

PS20 (%)	0.1		1							
Conc. of hGH (mg/mL)	10		10							
Conc. of CD (mg/mL)	0		0		10		50		100	
	1	2	1	2	1	2	1	2	1	2
Volume of NaCl solution (mL)	45	45	40	65	45	45	45	55	45	35
Conc. of NaCl (M)	0.070	0.070	0.063	0.098	0.070	0.070	0.070	0.084	0.070	0.055
Average conc. of NaCl (M)	0.070		0.080		0.070		0.077		0.062	
ΔConc. of NaCl compared to without CD (M)	-		-		-0.010		-0.003		-0.018	
ΔConc. of NaCl compared to without phenol (M)	-0.031		-0.047		-0.007		-0.014		-0.052	

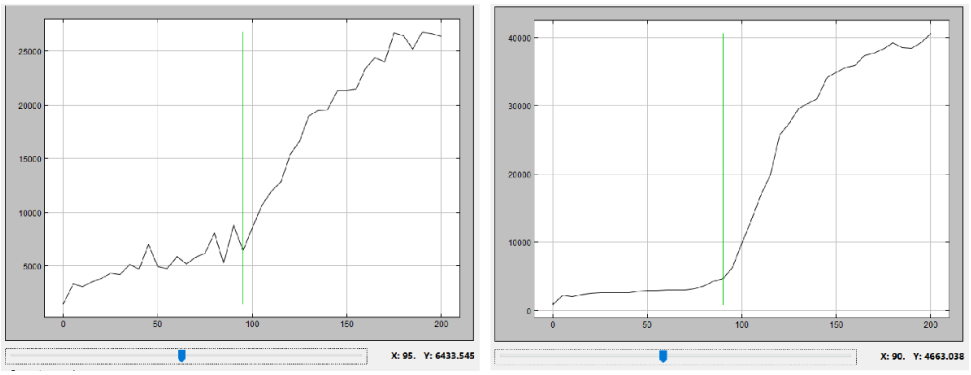

Figure A.1.1. Light scattering intensity changes with the addition of phenol in the system containing 0.0025% PS20. (X: the added volume of phenol, Y: the intensity of light scattering signal; data shown are two independent replicates)

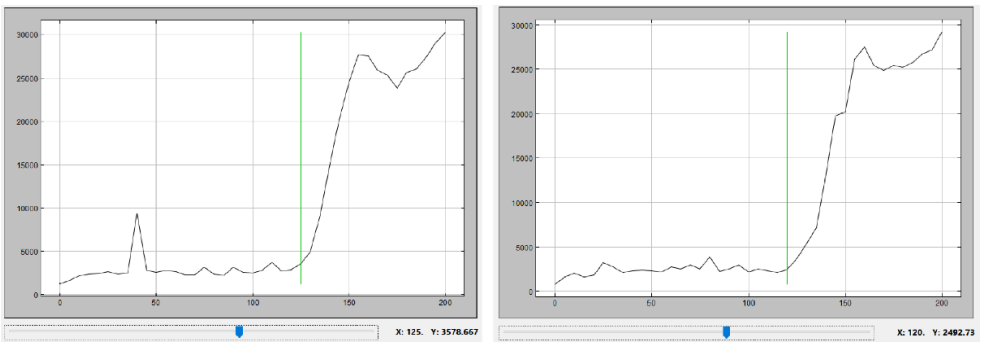

Figure A.1.2. Light scattering intensity changes with the addition of phenol in the system containing 0.01% PS20. (X: the added volume of phenol, Y: the intensity of light scattering signal; data shown are two independent replicates)

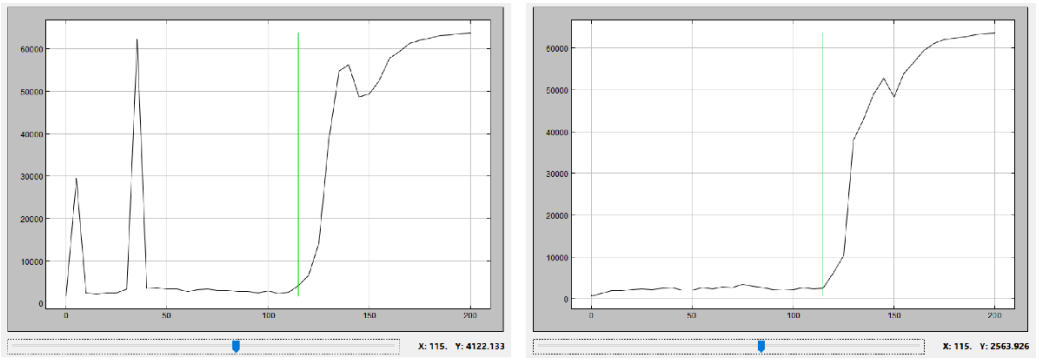

Figure A.1.3. Light scattering intensity changes with the addition of phenol in the system containing 0.05% PS20. (X: the added volume of phenol, Y: the intensity of light scattering signal; data shown are two independent replicates)

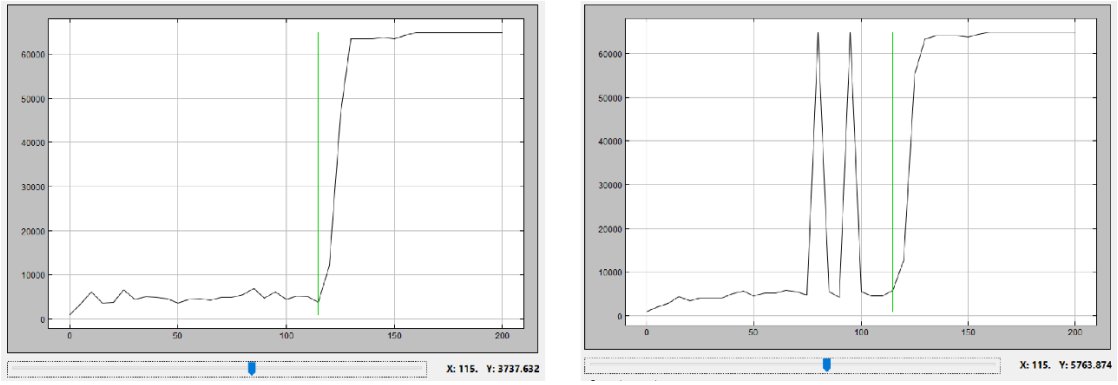

Figure A.1.4. Light scattering intensity changes with the addition of phenol in the system containing 0.1% PS20. (X: the added volume of phenol, Y: the intensity of light scattering signal; data shown are two independent replicates)

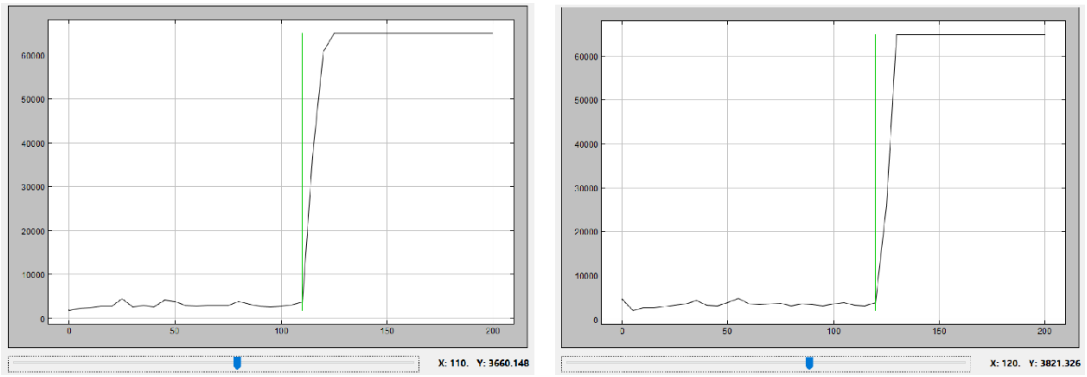

Figure A.1.5. Light scattering intensity changes with the addition of phenol in the system containing 0.5% PS20. (X: the added volume of phenol, Y: the intensity of light scattering signal; data shown are two independent replicates)

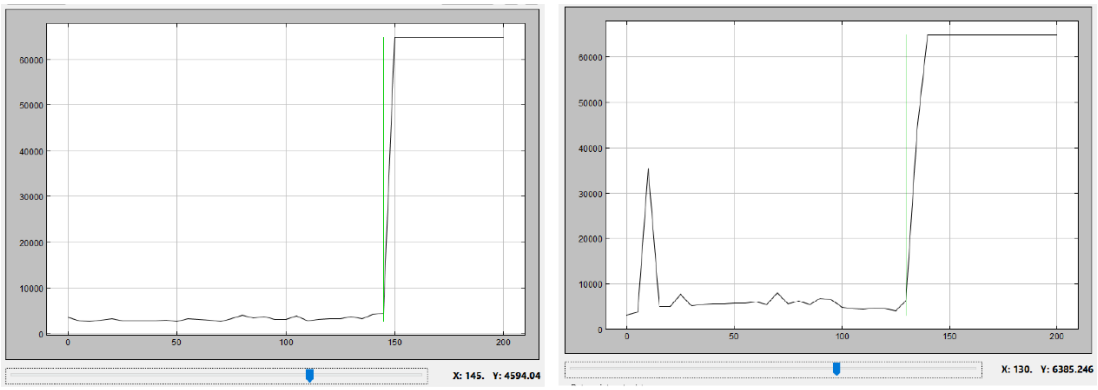

Figure A.1.6. Light scattering intensity changes with the addition of phenol in the system containing 1% PS20. (X: the added volume of phenol, Y: the intensity of light scattering signal; data shown are two independent replicates)

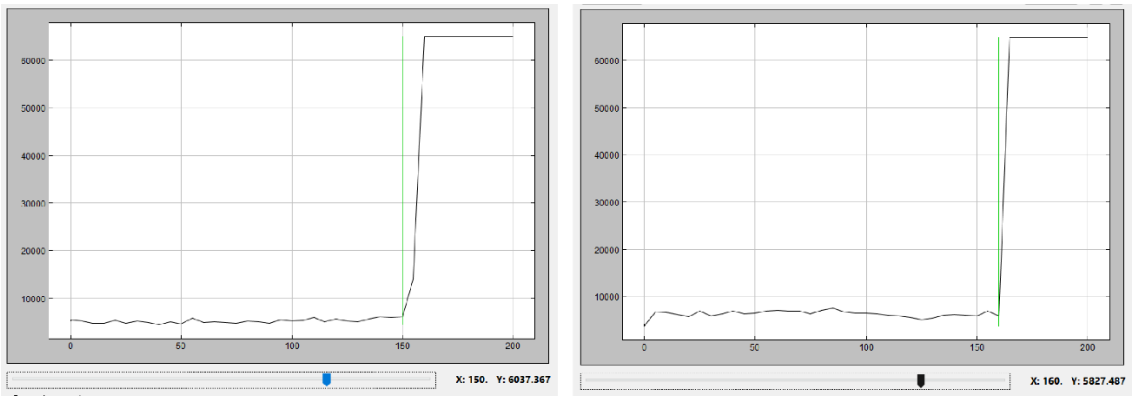

Figure A.1.7. Light scattering intensity changes with the addition of phenol in the system containing 2% PS20. (X: the added volume of phenol, Y: the intensity of light scattering signal; data shown are two independent replicates)

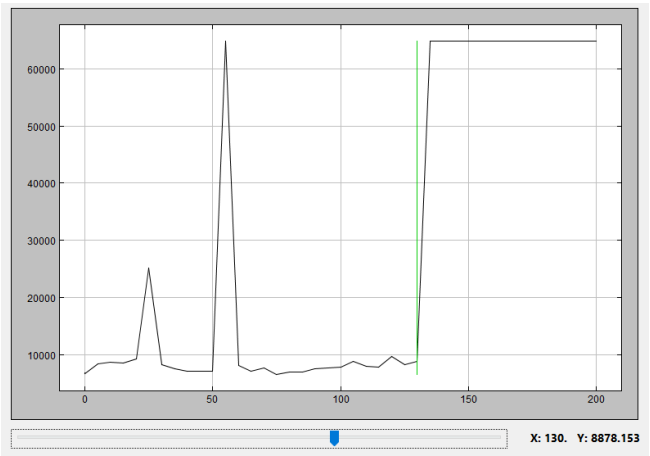

Figure A.1.8. Light scattering intensity changes with the addition of phenol in the system containing 5% PS20. (X: the added volume of phenol, Y: the intensity of light scattering signal)

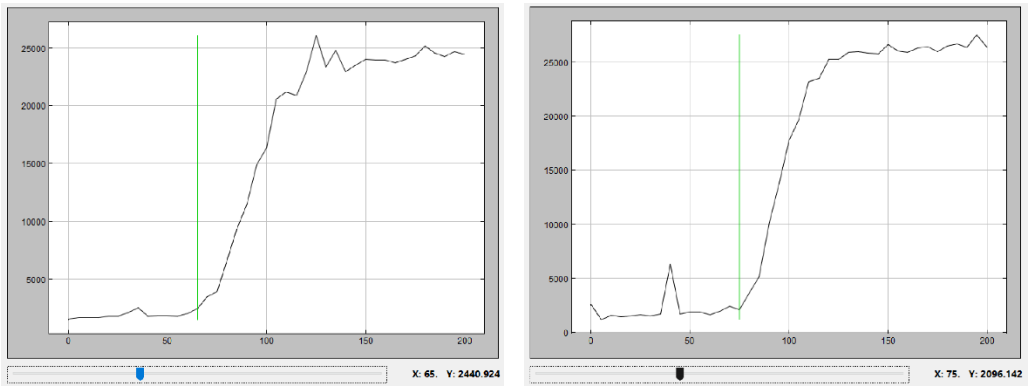

Figure A.1.9. Light scattering intensity changes with the addition of phenol in the system containing 0.0025% PS20 and 10 mg/mL CD. (X: the added volume of phenol, Y: the intensity of light scattering signal; data shown are two independent replicates)

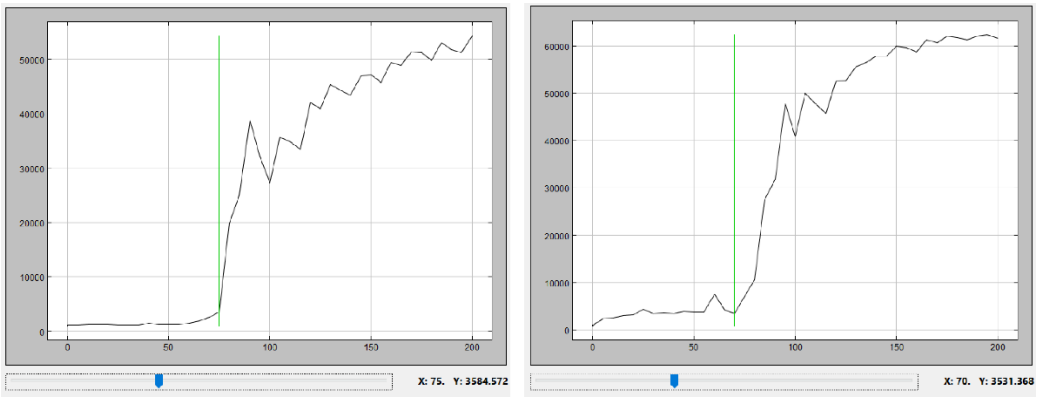

Figure A.1.10. Light scattering intensity changes with the addition of phenol in the system containing 0.01% PS20 and 10 mg/mL CD. (X: the added volume of phenol, Y: the intensity of light scattering signal)

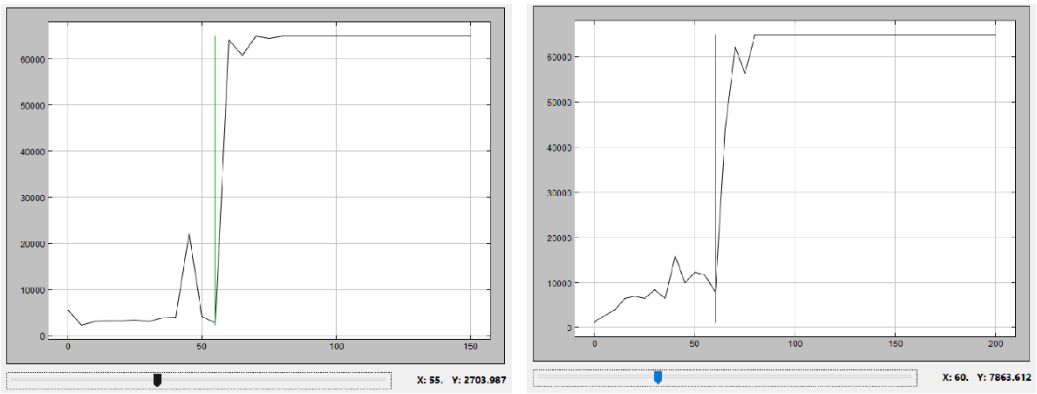

Figure A.1.11. Light scattering intensity changes with the addition of phenol in the system containing 0.1% PS20 and 10 mg/mL CD. (X: the added volume of phenol, Y: the intensity of light scattering signal; data shown are two independent replicates)

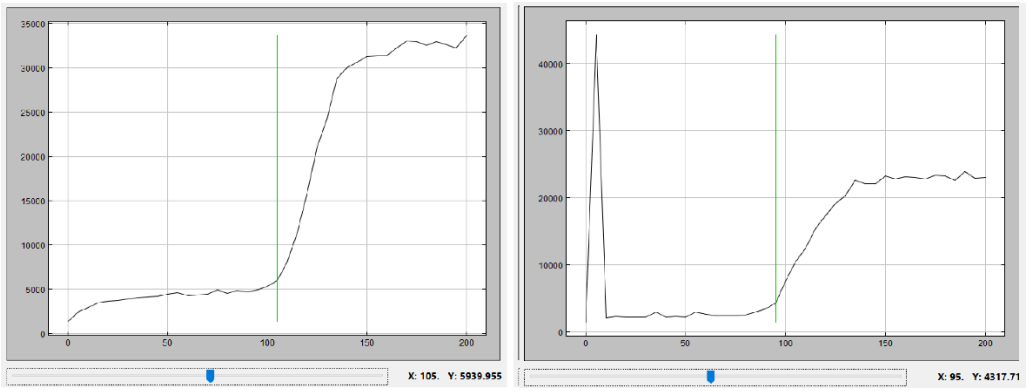

Figure A.1.12. Light scattering intensity changes with the addition of phenol in the system containing 0.0025% PS20 and 50 mg/mL CD. (X: the added volume of phenol, Y: the intensity of light scattering signal; data shown are two independent replicates)

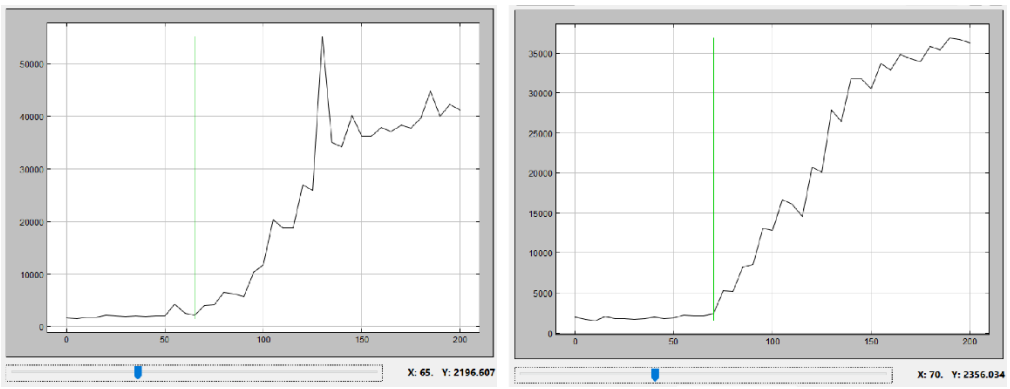

Figure A.1.13. Light scattering intensity changes with the addition of phenol in the system containing 0.01% PS20 and 50 mg/mL CD. (X: the added volume of phenol, Y: the intensity of light scattering signal; data shown are two independent replicates)

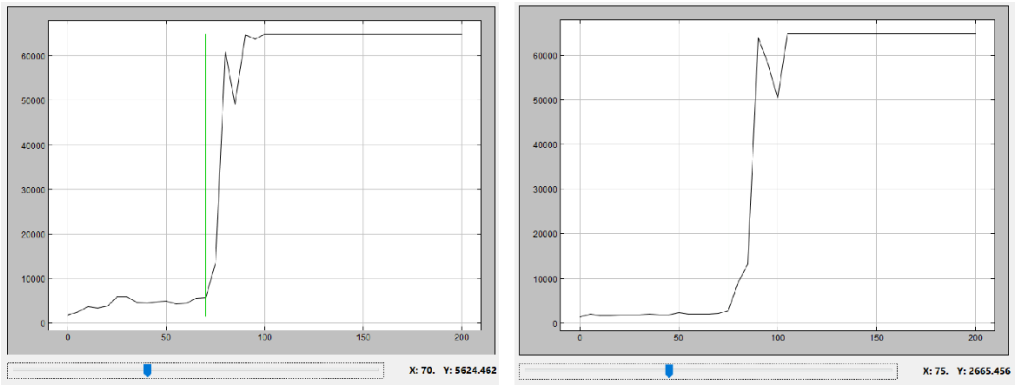

Figure A.1.14. Light scattering intensity changes with the addition of phenol in the system containing 0.1% PS20 and 50 mg/mL CD. (X: the added volume of phenol, Y: the intensity of light scattering signal; data shown are two independent replicates)

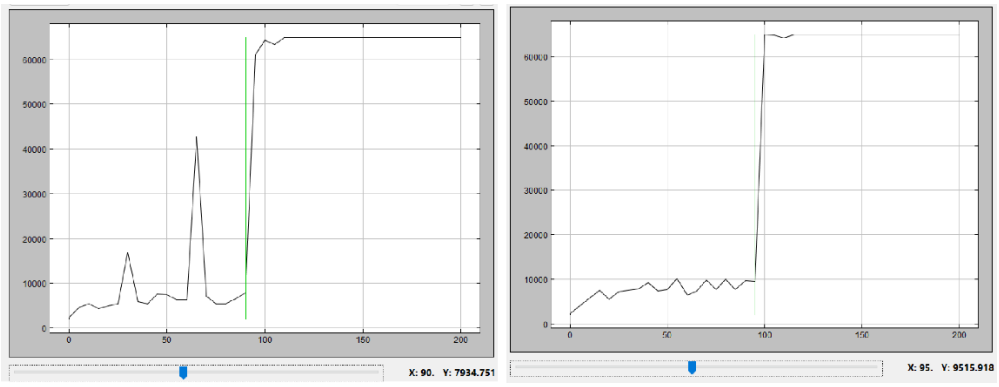

Figure A.1.15. Light scattering intensity changes with the addition of phenol in the system containing 1% PS20 and 50 mg/mL CD. (X: the added volume of phenol, Y: the intensity of light scattering signal; data shown are two independent replicates)

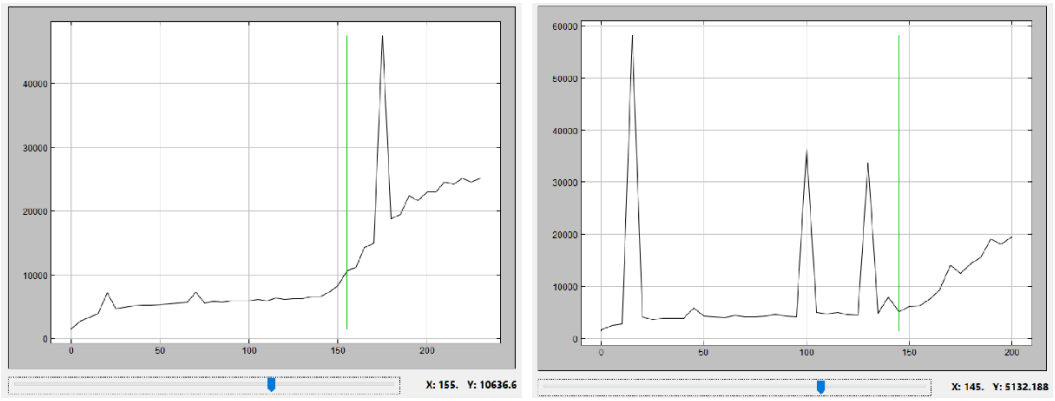

Figure A.1.16. Light scattering intensity changes with the addition of phenol in the system containing 0.0025% PS20 and 100 mg/mL CD. (X: the added volume of phenol, Y: the intensity of light scattering signal; data shown are two independent replicates)

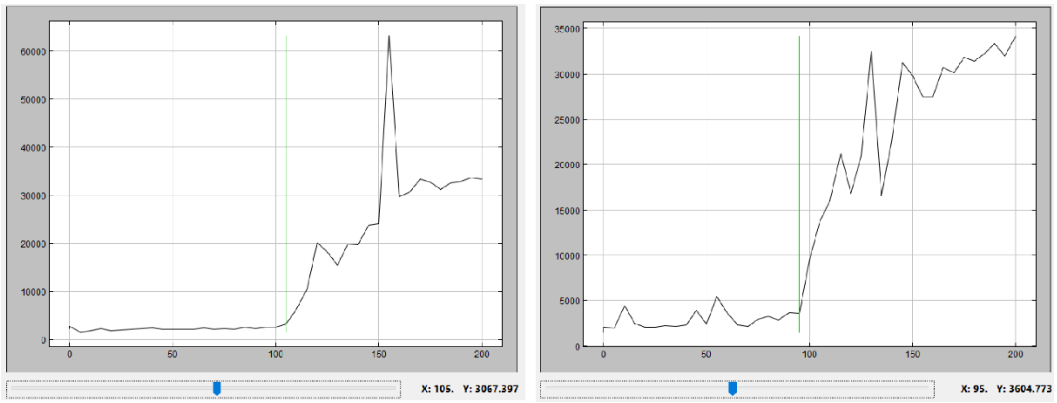

Figure A.1.17. Light scattering intensity changes with the addition of phenol in the system containing 0.01% PS20 and 100 mg/mL CD. (X: the added volume of phenol, Y: the intensity of light scattering signal; data shown are two independent replicates)

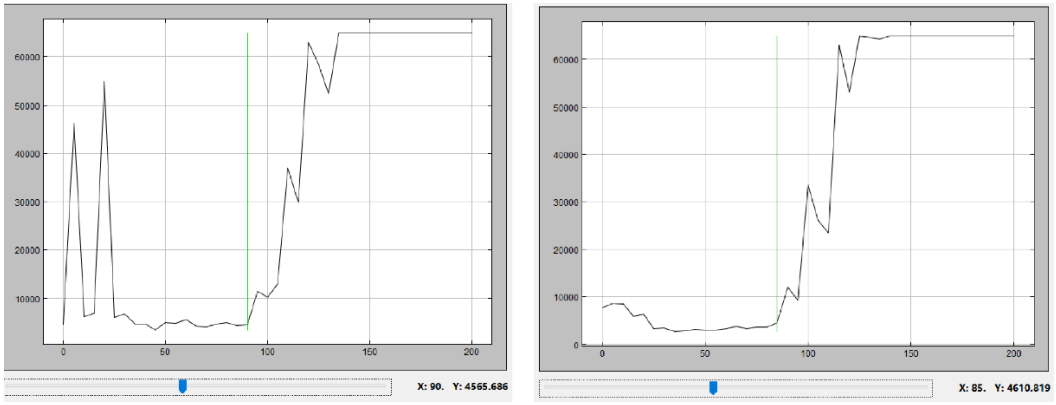

Figure A.1.18. Light scattering intensity changes with the addition of phenol in the system containing 0.1% PS20 and 100 mg/mL CD. (X: the added volume of phenol, Y: the intensity of light scattering signal; data shown are two independent replicates)

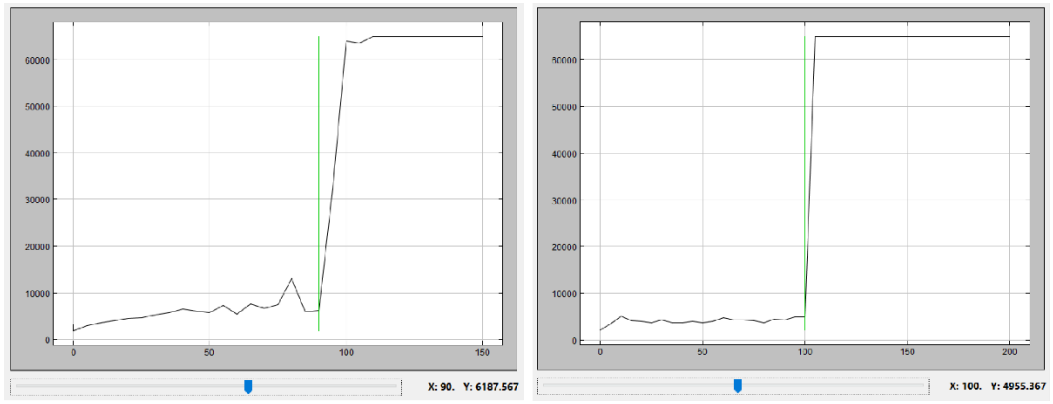

Figure A.1.19. Light scattering intensity changes with the addition of phenol in the system containing 1% PS20 and 100 mg/mL CD. (X: the added volume of phenol, Y: the intensity of light scattering signal; data shown are two independent replicates)

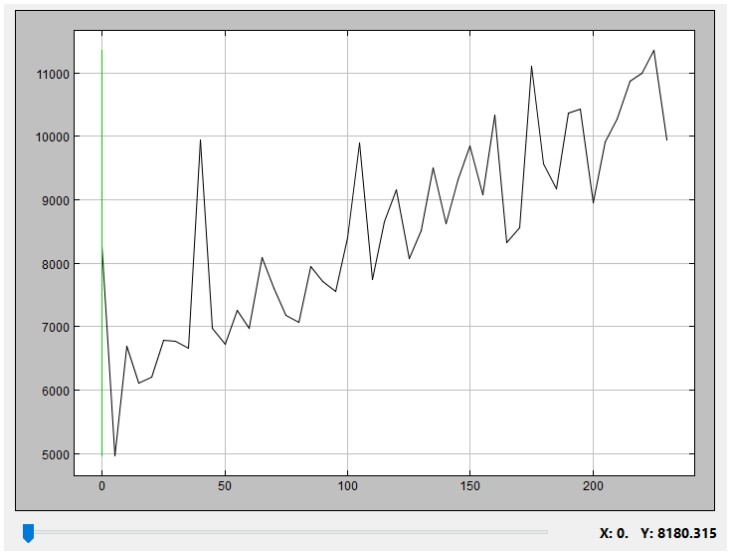

Figure A.1.20. Light scattering intensity changes with the addition of phenol in the system containing 10mg/mL BSA. (X: the added volume of phenol, Y: the intensity of light scattering signal)

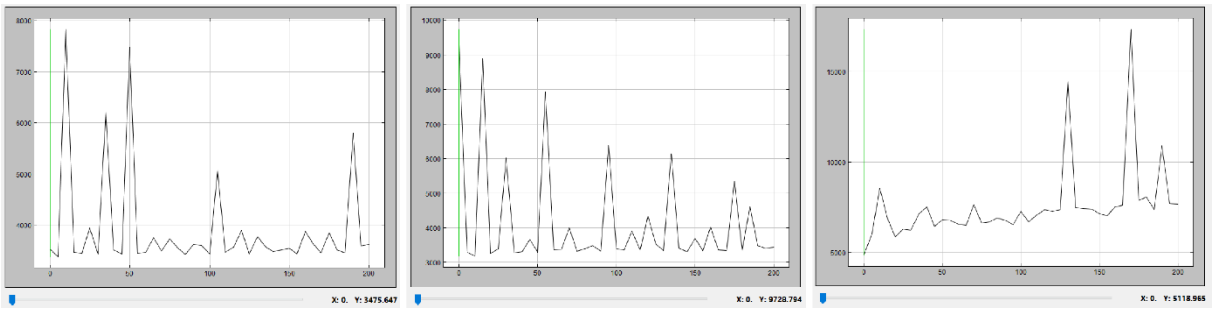

Figure A.1.21. Light scattering intensity changes with the addition of phenol in the system containing 10 mg/mL BSA and different concentrations of CD. (X: the added volume of phenol, Y: the intensity of light scattering signal; the figures from left to right represent the CD concentrations of 10, 50 and 100 mg/mL)

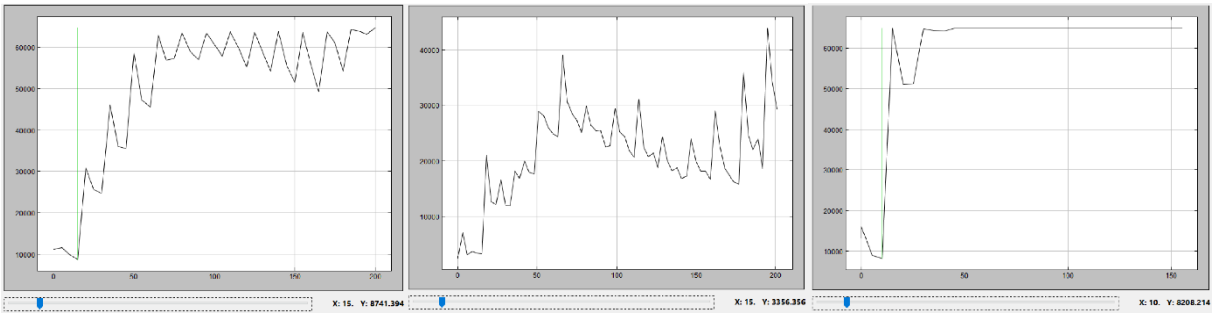

Figure A.1.22. Light scattering intensity changes with the addition of phenol in the system containing 10 mg/mL hGH. (X: the added volume of phenol, Y: the intensity of light scattering signal; data shown in the left two figures are two independent replicates at 4.4% phenol, and in the right figure are at 6.13%)

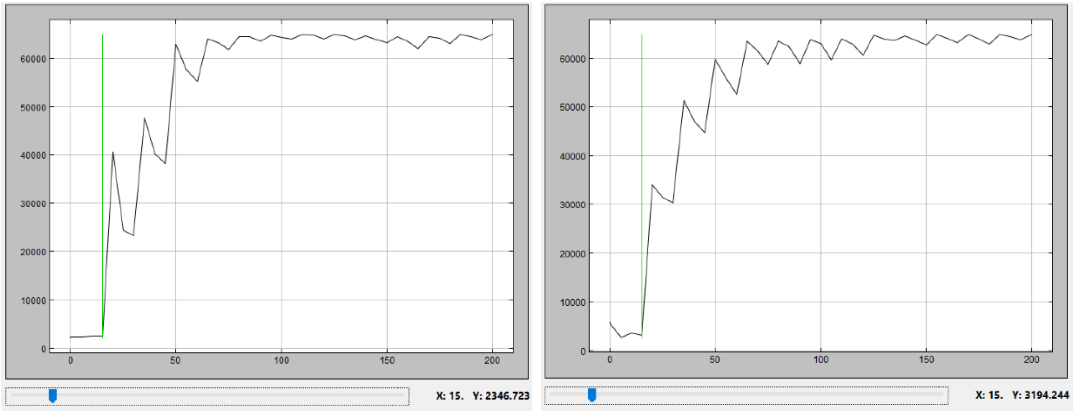

Figure A.1.23. Light scattering intensity changes with the addition of phenol in the system containing 10 mg/mL hGH and 10 mg/mL CD. (X: the added volume of phenol, Y: the intensity of light scattering signal; data shown are two independent replicates)

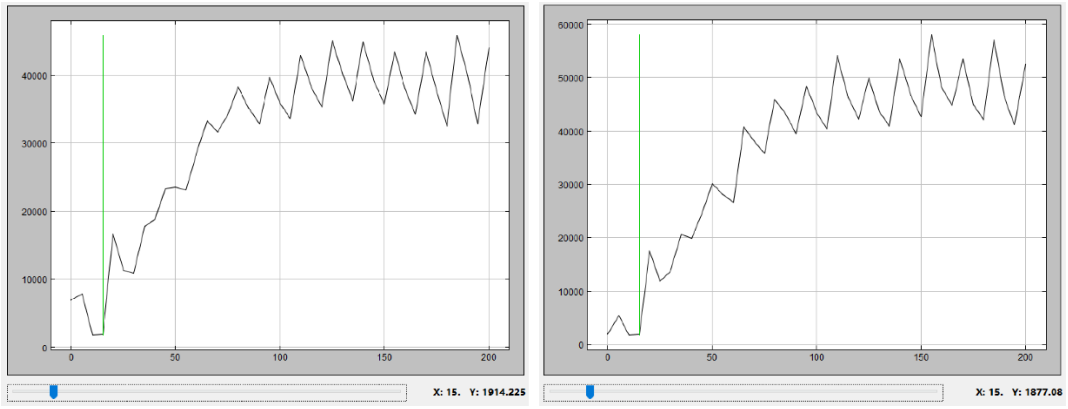

Figure A.1.24. Light scattering intensity changes with the addition of phenol in the system containing 10 mg/mL hGH and 50 mg/mL CD. (X: the added volume of phenol, Y: the intensity of light scattering signal; data shown are two independent replicates)

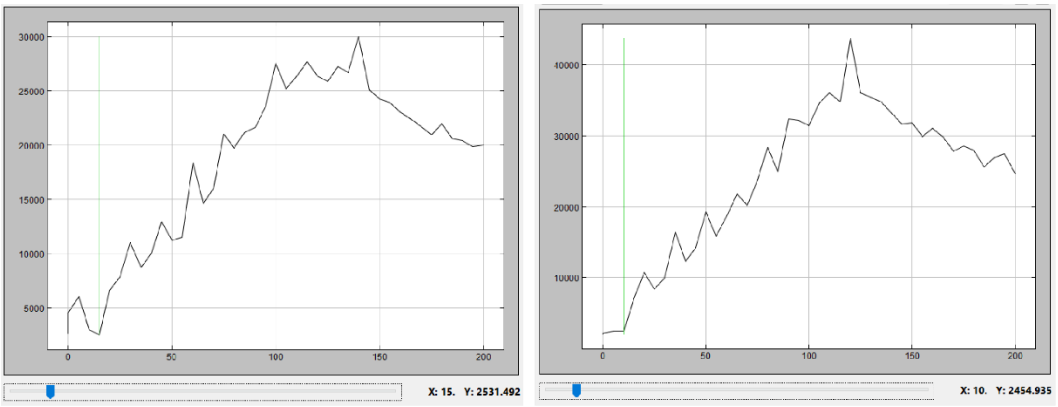

Figure A.1.25. Light scattering intensity changes with the addition of phenol in the system containing 10 mg/mL hGH and 100 mg/mL CD. (X: the added volume of phenol, Y: the intensity of light scattering signal; data shown are two independent replicates)

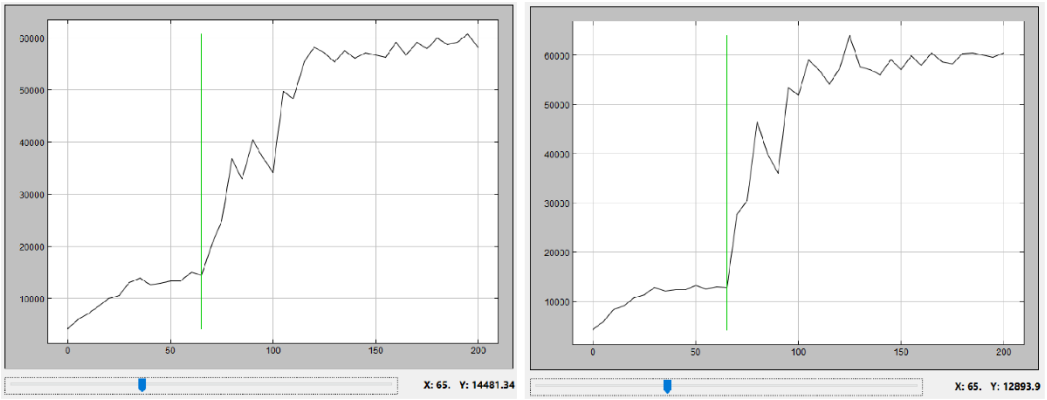

Figure A.1.26. Light scattering intensity changes with the addition of phenol in the system containing 10 mg/mL BSA and 0.01% PS20. (X: the added volume of phenol, Y: the intensity of light scattering signal; data shown are two independent replicates)

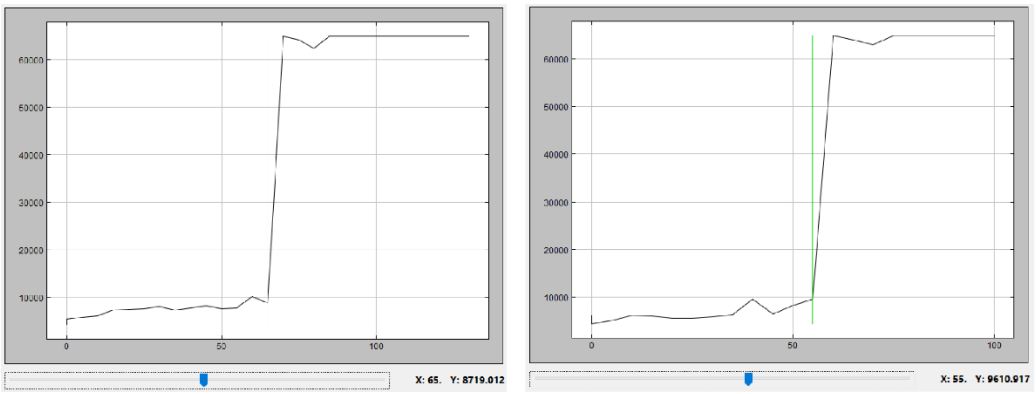

Figure A.1.27. Light scattering intensity changes with the addition of phenol in the system containing 10 mg/mL BSA and 0.1% PS20. (X: the added volume of phenol, Y: the intensity of light scattering signal; data shown are two independent replicates)

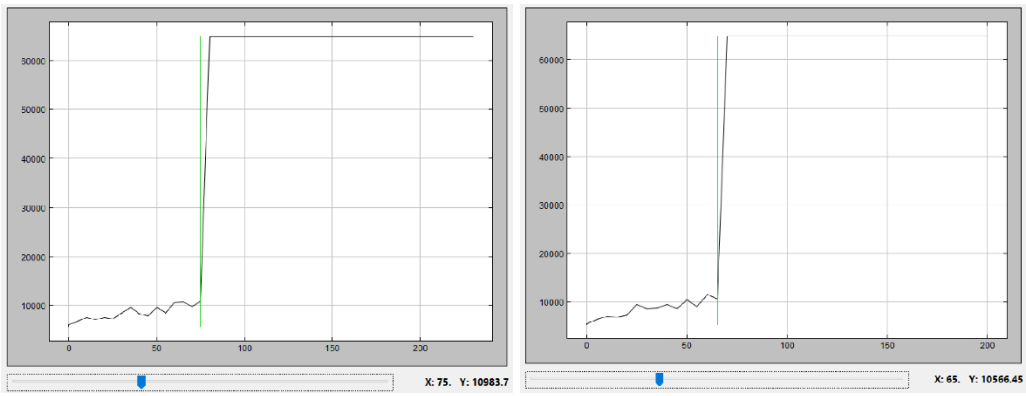

Figure A.1.28. Light scattering intensity changes with the addition of phenol in the system containing 10 mg/mL BSA and 1% PS20. (X: the added volume of phenol, Y: the intensity of light scattering signal; data shown are two independent replicates)

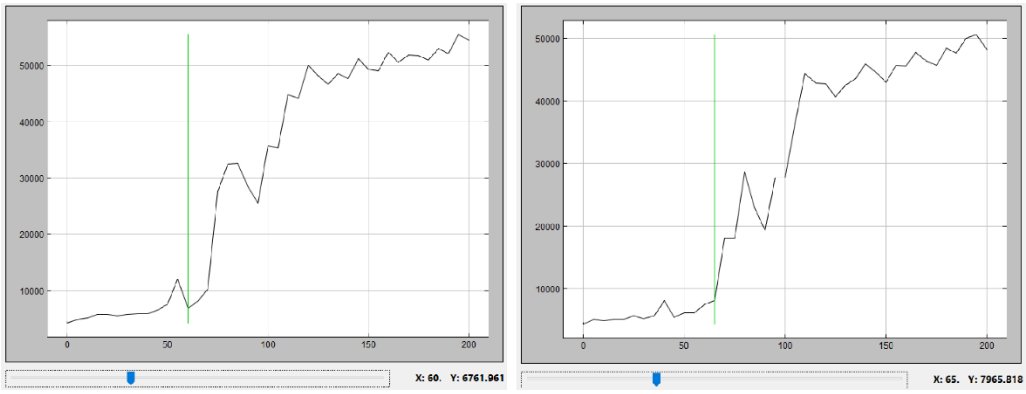

Figure A.1.29. Light scattering intensity changes with the addition of phenol in the system containing 10 mg/mL BSA, 0.01% PS20 and 10 mg/mL CD. (X: the added volume of phenol, Y: the intensity of light scattering signal; data shown are two independent replicates)

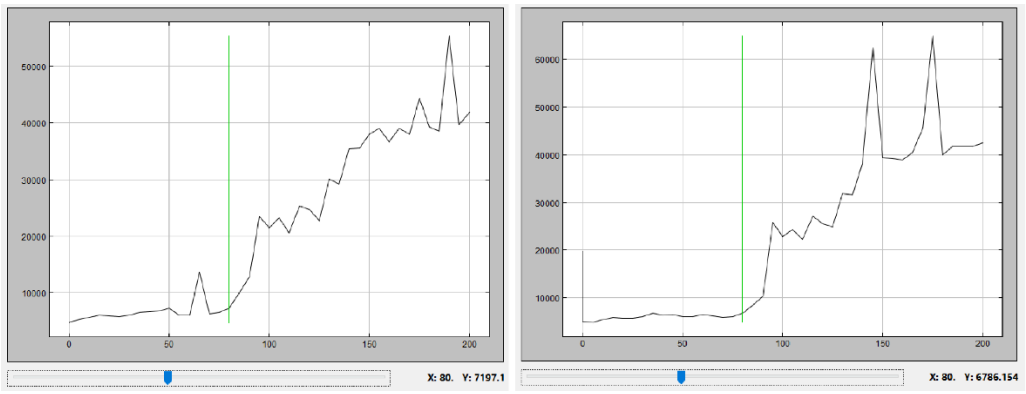

Figure A.1.30. Light scattering intensity changes with the addition of phenol in the system containing 10 mg/mL BSA, 0.01% PS20 and 50 mg/mL CD. (X: the added volume of phenol, Y: the intensity of light scattering signal; data shown are two independent replicates)

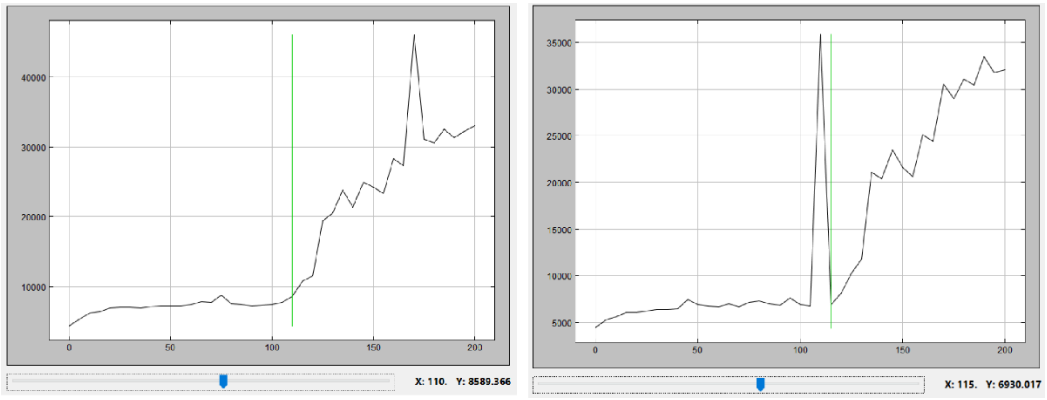

Figure A.1.31. Light scattering intensity changes with the addition of phenol in the system containing 10 mg/mL BSA, 0.01% PS20 and 100 mg/mL CD. (X: the added volume of phenol, Y: the intensity of light scattering signal; data shown are two independent replicates)

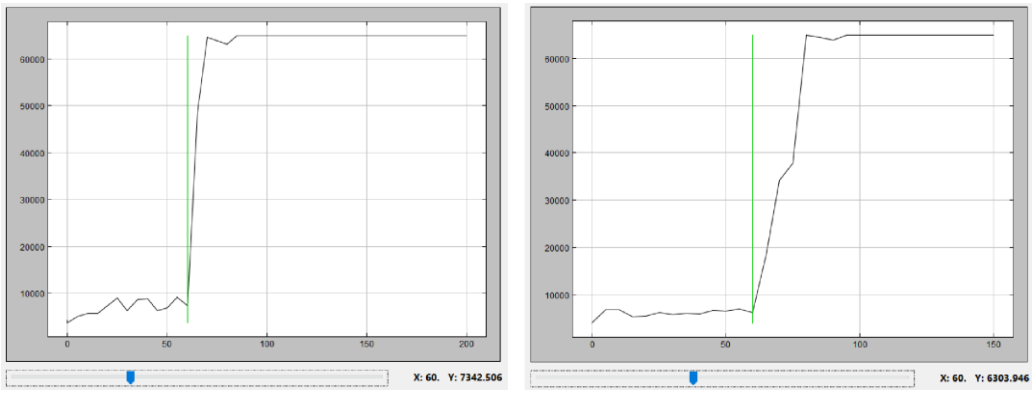

Figure A.1.32. Light scattering intensity changes with the addition of phenol in the system containing 10 mg/mL BSA, 0.1% PS20 and 10 mg/mL CD. (X: the added volume of phenol, Y: the intensity of light scattering signal; data shown are two independent replicates)

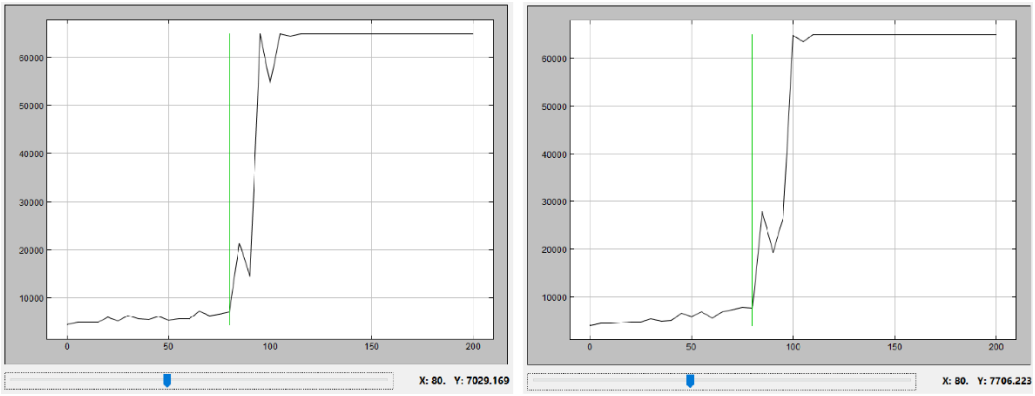

Figure A.1.33. Light scattering intensity changes with the addition of phenol in the system containing 10 mg/mL BSA, 0.1% PS20 and 50 mg/mL CD. (X: the added volume of phenol, Y: the intensity of light scattering signal; data shown are two independent replicates)

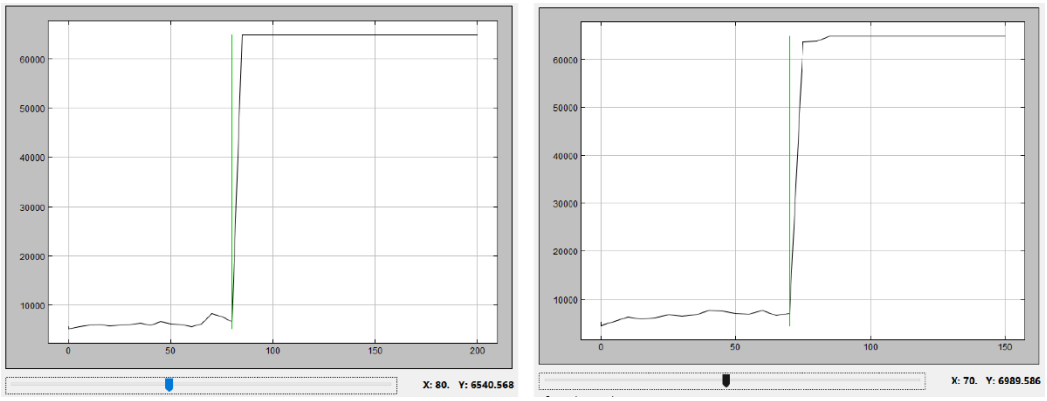

Figure A.1.34. Light scattering intensity changes with the addition of phenol in the system containing 10 mg/mL BSA, 1% PS20 and 10 mg/mL CD. (X: the added volume of phenol, Y: the intensity of light scattering signal; data shown are two independent replicates)

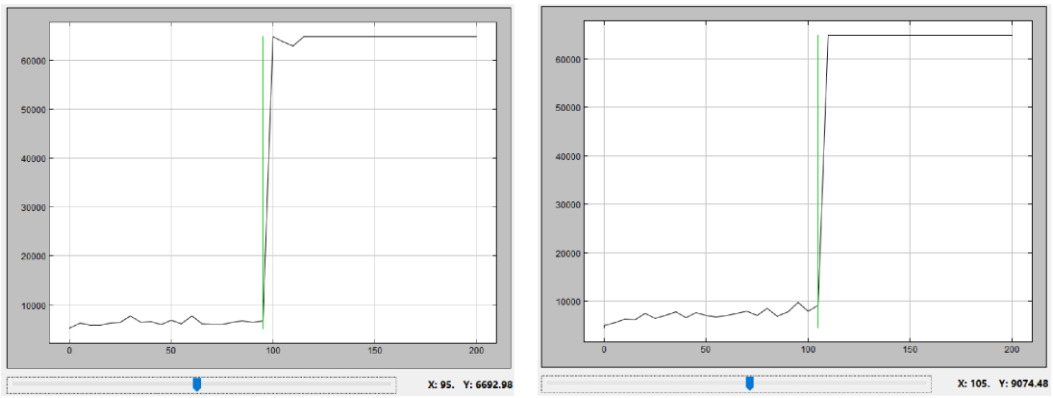

Figure A.1.35. Light scattering intensity changes with the addition of phenol in the system containing 10 mg/mL BSA, 1% PS20 and 50 mg/mL CD. (X: the added volume of phenol, Y: the intensity of light scattering signal; data shown are two independent replicates)

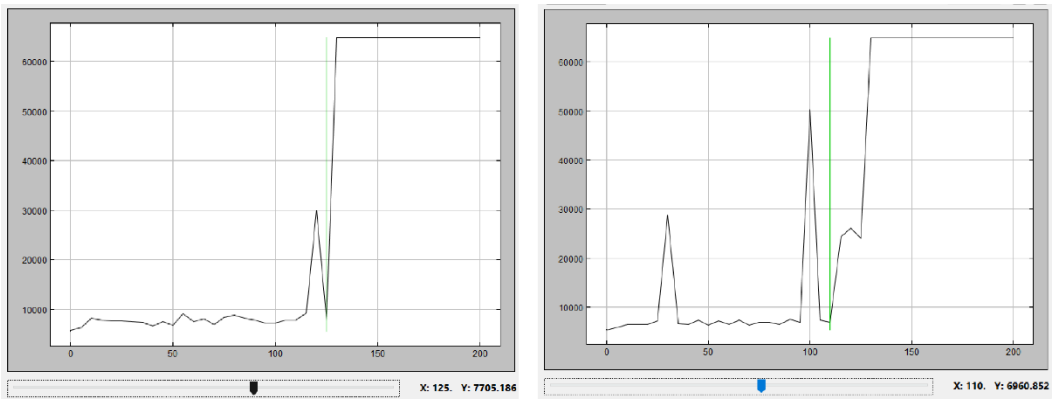

Figure A.1.36. Light scattering intensity changes with the addition of phenol in the system containing 10 mg/mL BSA, 1% PS20 and 100 mg/mL CD. (X: the added volume of phenol, Y: the intensity of light scattering signal; data shown are two independent replicates)

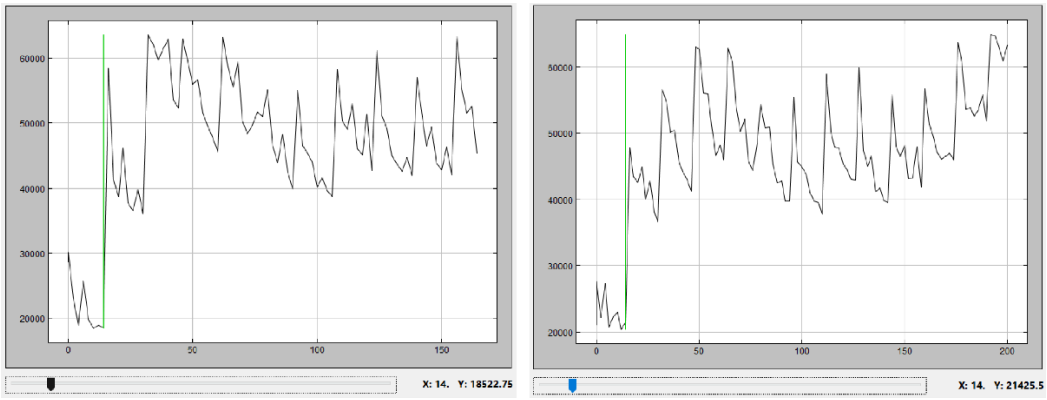

Figure A.1.37. Light scattering intensity changes with the addition of phenol in the system containing 10 mg/mL hGH and 0.01% PS20. (X: the added volume of phenol, Y: the intensity of light scattering signal; data shown are two independent replicates)

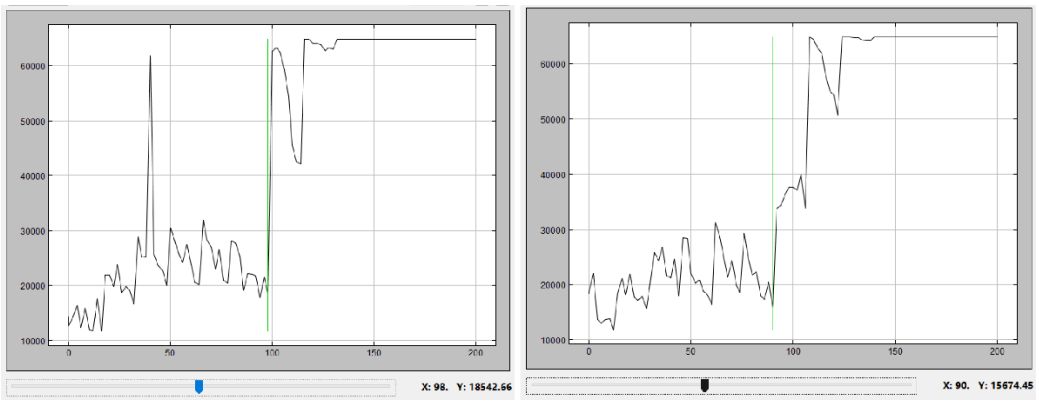

Figure A.1.38. Light scattering intensity changes with the addition of phenol in the system containing 10 mg/mL hGH and 0.1% PS20. (X: the added volume of phenol, Y: the intensity of light scattering signal; data shown are two independent replicates)

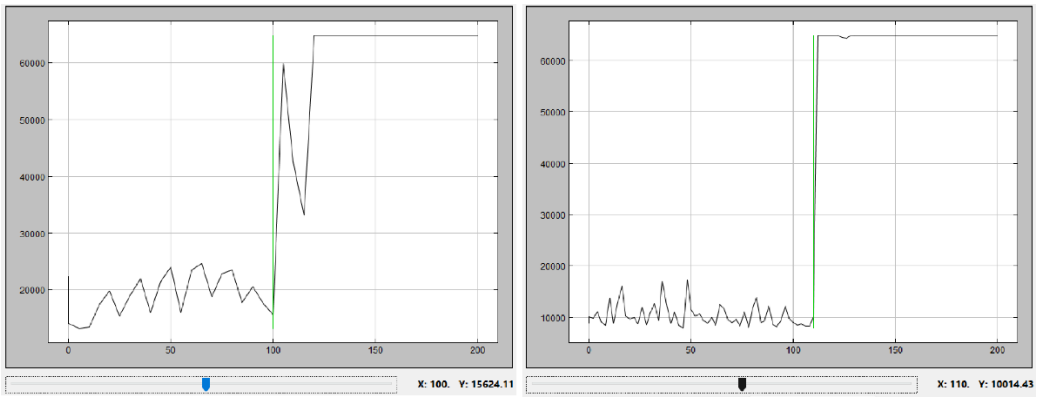

Figure A.1.39. Light scattering intensity changes with the addition of phenol in the system containing 10 mg/mL hGH and 1% PS20. (X: the added volume of phenol, Y: the intensity of light scattering signal; data shown are two independent replicates)

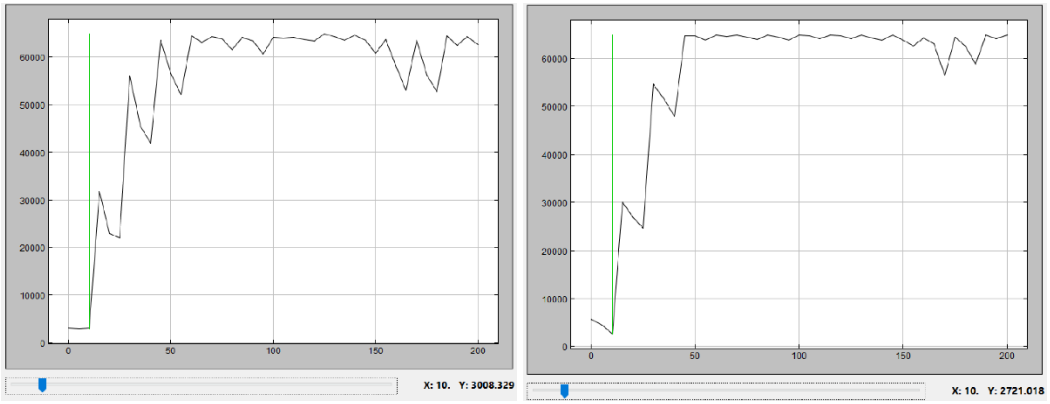

Figure A.1.40. Light scattering intensity changes with the addition of phenol in the system containing 10 mg/mL hGH, 0.01% PS20, and 10 mg/mL CD. (X: the added volume of phenol, Y: the intensity of light scattering signal; data shown are two independent replicates)

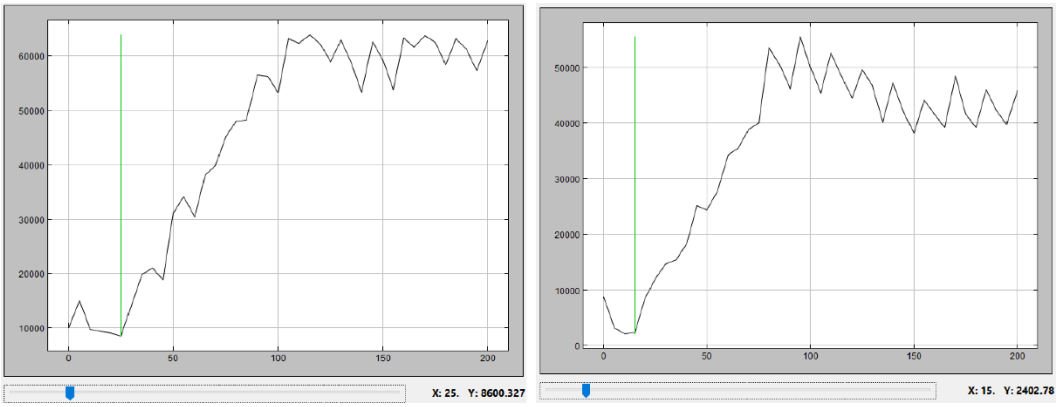

Figure A.1.41. Light scattering intensity changes with the addition of phenol in the system containing 10 mg/mL hGH, 0.01% PS20, and 50 mg/mL CD. (X: the added volume of phenol, Y: the intensity of light scattering signal; data shown are two independent replicates)

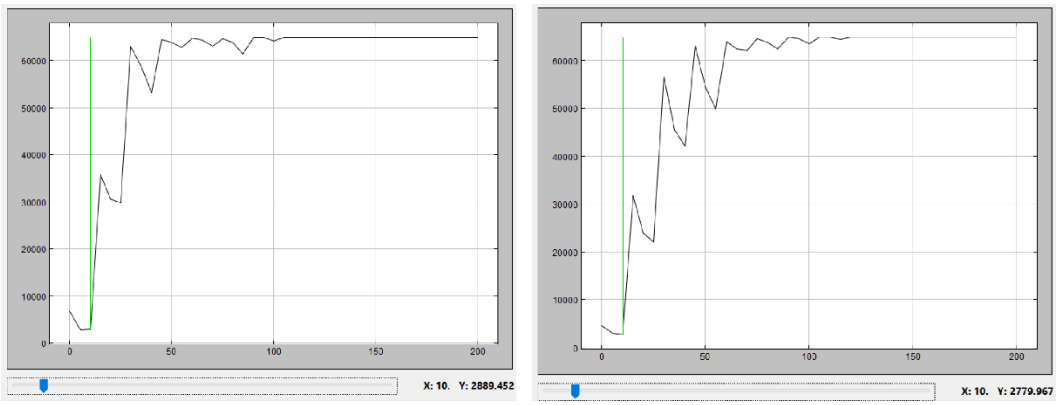

Figure A.1.42. Light scattering intensity changes with the addition of phenol in the system containing 10 mg/mL hGH, 0.1% PS20, and 10 mg/mL CD. (X: the added volume of phenol, Y: the intensity of light scattering signal; data shown are two independent replicates)

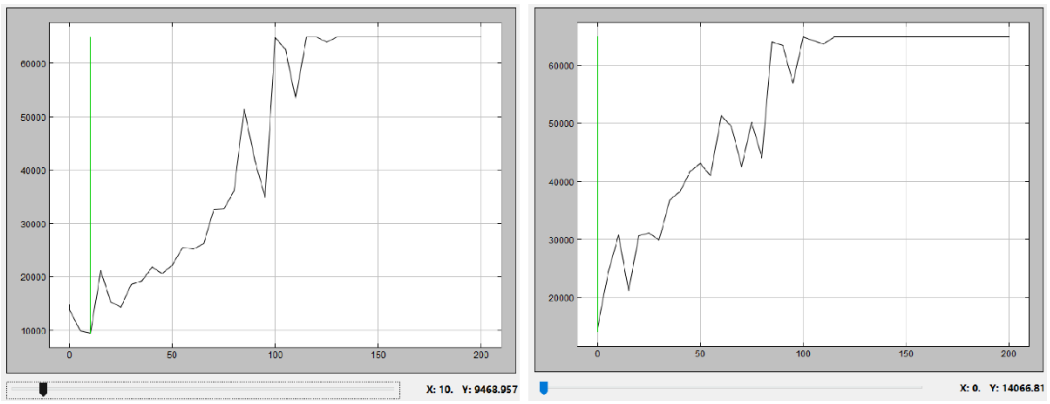

Figure A.1.43. Light scattering intensity changes with the addition of phenol in the system containing 10 mg/mL hGH, 0.1% PS20, and 50 mg/mL CD. (X: the added volume of phenol, Y: the intensity of light scattering signal; data shown are two independent replicates)

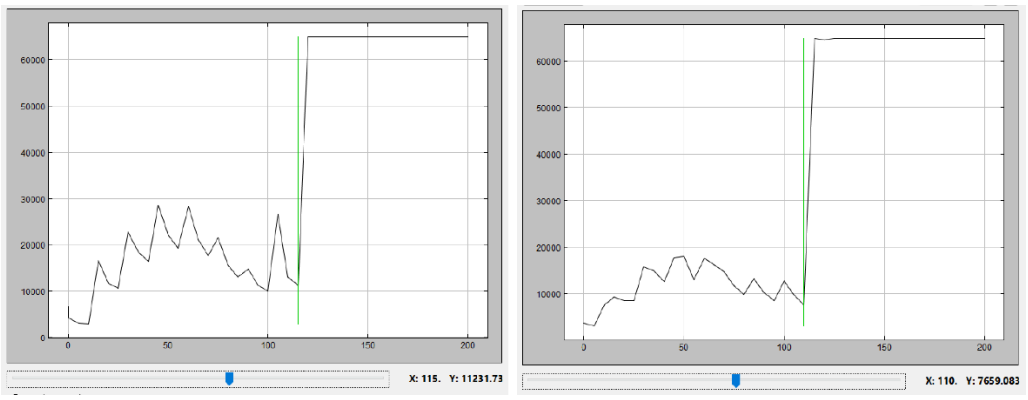

Figure A.1.44. Light scattering intensity changes with the addition of phenol in the system containing 10 mg/mL hGH, 1% PS20, and 10 mg/mL CD. (X: the added volume of phenol, Y: the intensity of light scattering signal; data shown are two independent replicates)

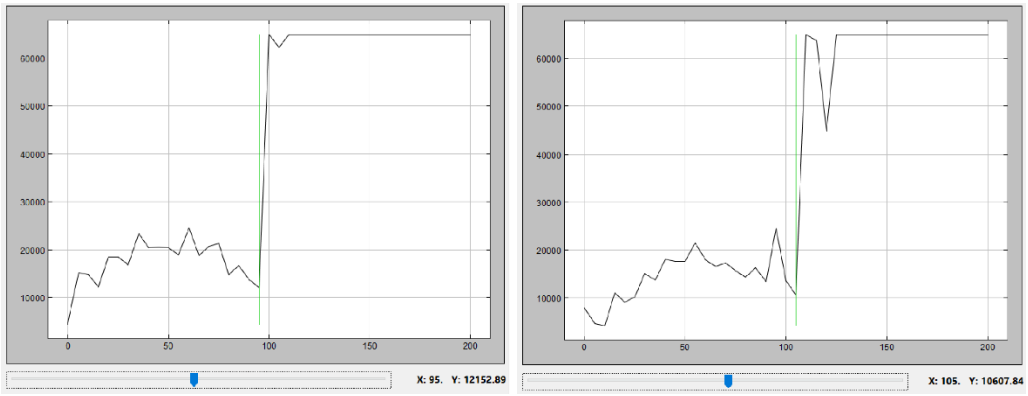

Figure A.1.45. Light scattering intensity changes with the addition of phenol in the system containing 10 mg/mL hGH, 1% PS20, and 50 mg/mL CD. (X: the added volume of phenol, Y: the intensity of light scattering signal; data shown are two independent replicates)

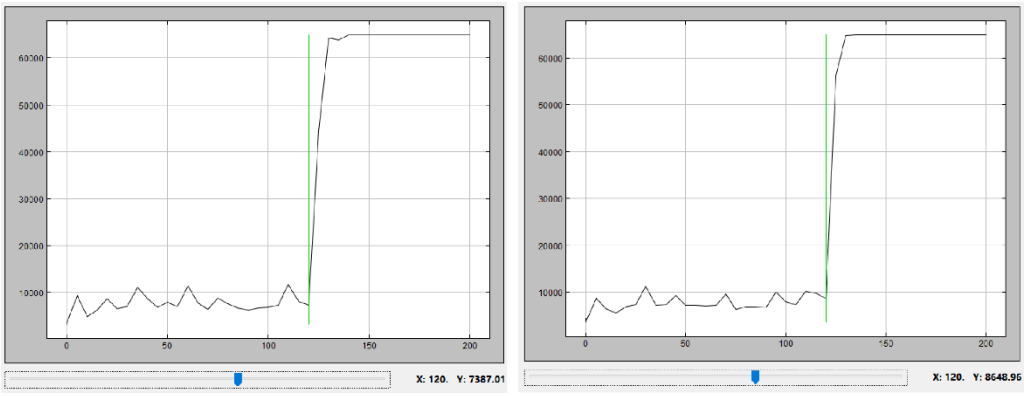

Figure A.1.46. Light scattering intensity changes with the addition of phenol in the system containing 10 mg/mL hGH, 1% PS20, and 100 mg/mL CD. (X: the added volume of phenol, Y: the intensity of light scattering signal; data shown are two independent replicates)

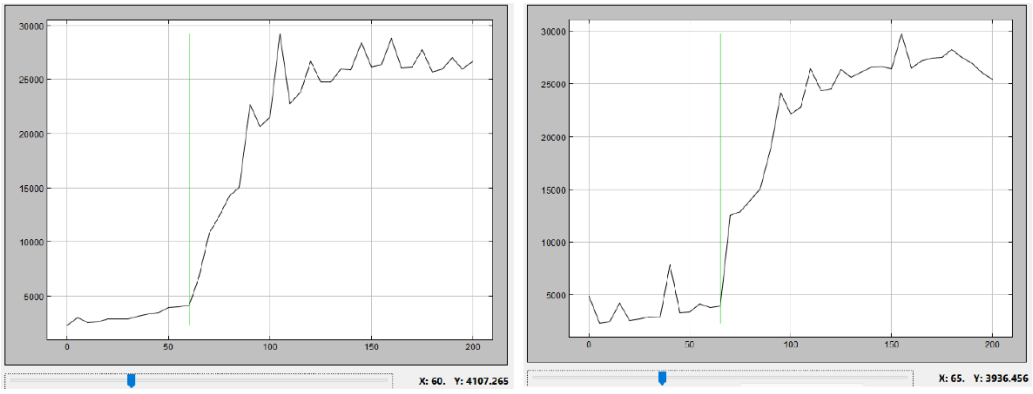

Figure A.1.47. Light scattering intensity changes with the addition of 1M NaCl in the system containing 10 mg/mL hGH. (X: the added volume of NaCl solution, Y: the intensity of light scattering signal; data shown are two independent replicates)

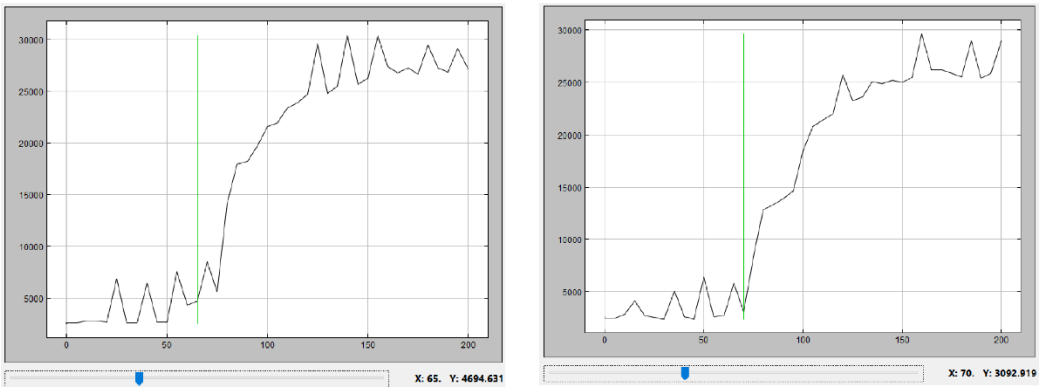

Figure A.1.48. Light scattering intensity changes with the addition of 1M NaCl in the system containing 10 mg/mL hGH and 0.01% PS20. (X: the added volume of NaCl solution, Y: the intensity of light scattering signal; data shown are two independent replicates)

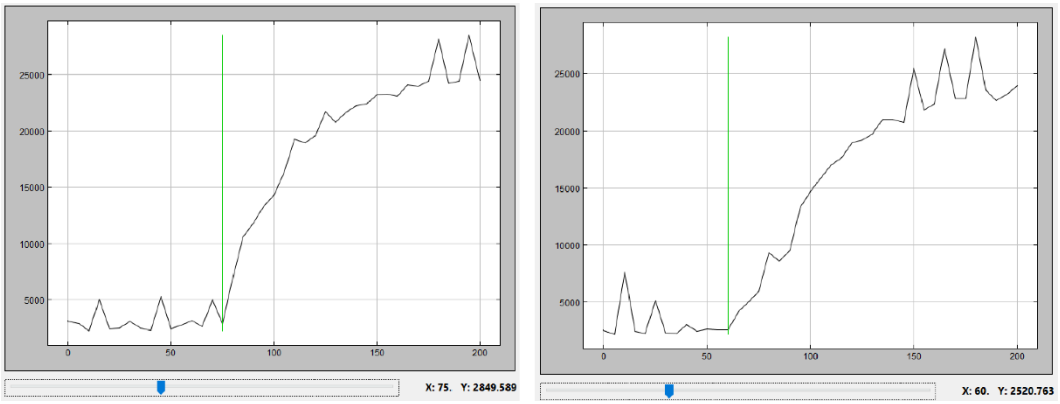

Figure A.1.49. Light scattering intensity changes with the addition of 1M NaCl in the system containing 10 mg/mL hGH and 0.1% PS20. (X: the added volume of NaCl solution, Y: the intensity of light scattering signal; data shown are two independent replicates)

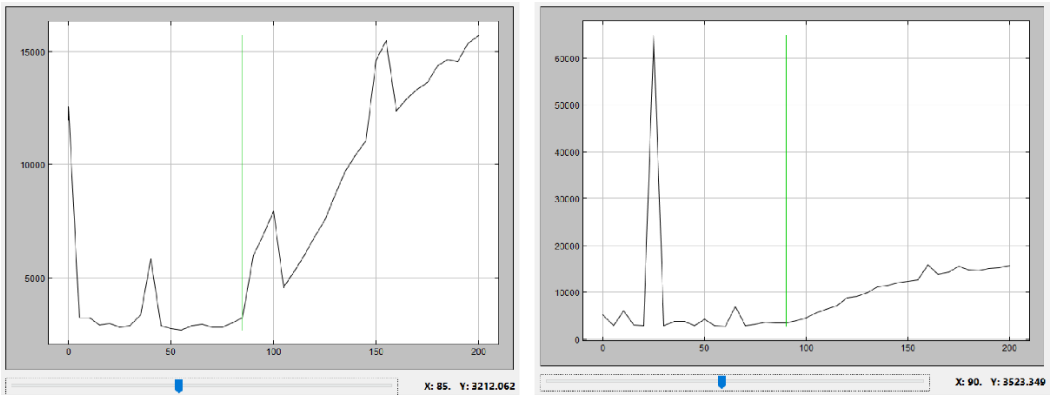

Figure A.1.50. Light scattering intensity changes with the addition of 1M NaCl in the system containing 10 mg/mL hGH and 1% PS20. (X: the added volume of NaCl solution, Y: the intensity of light scattering signal; data shown are two independent replicates)

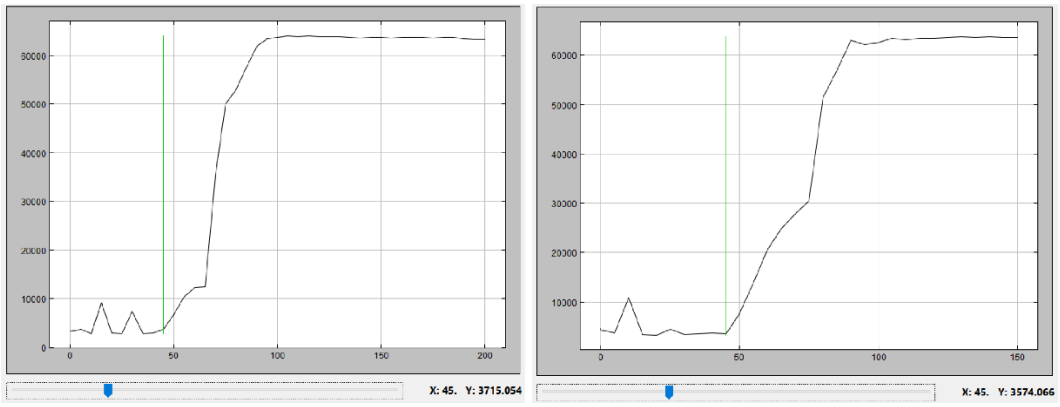

Figure A.1.51. Light scattering intensity changes with the addition of 1M NaCl in the system containing 10 mg/mL hGH, 0.1% PS20, and phenol. (X: the added volume of NaCl solution, Y: the intensity of light scattering signal; data shown are two independent replicates)

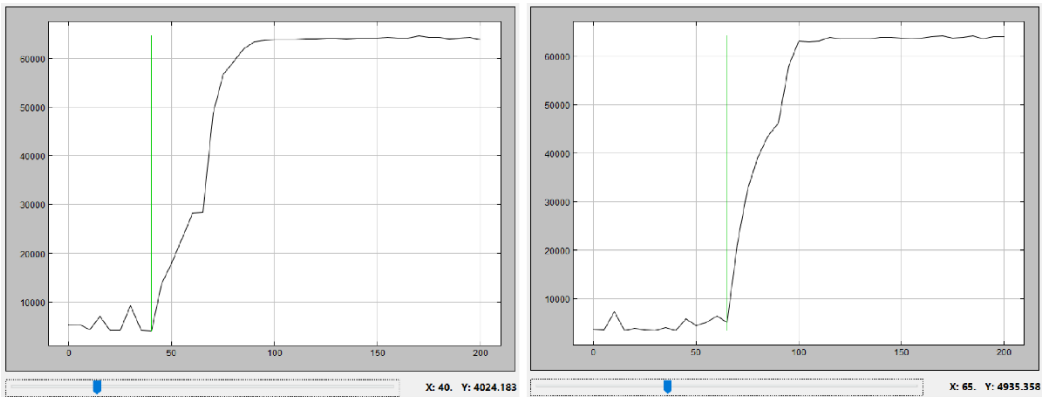

Figure A.1.52. Light scattering intensity changes with the addition of 1M NaCl in the system containing 10 mg/mL hGH, 1% PS20, and phenol. (X: the added volume of NaCl solution, Y: the intensity of light scattering signal; data shown are two independent replicates)

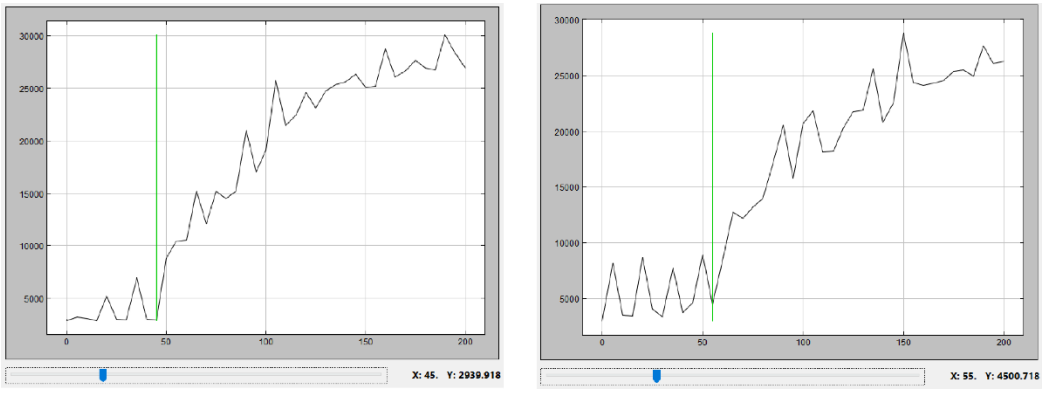

Figure A.1.53. Light scattering intensity changes with the addition of 1M NaCl in the system containing 10 mg/mL hGH, 1% PS20, and 10 mg/mL CD. (X: the added volume of NaCl solution, Y: the intensity of light scattering signal; data shown are two independent replicates)

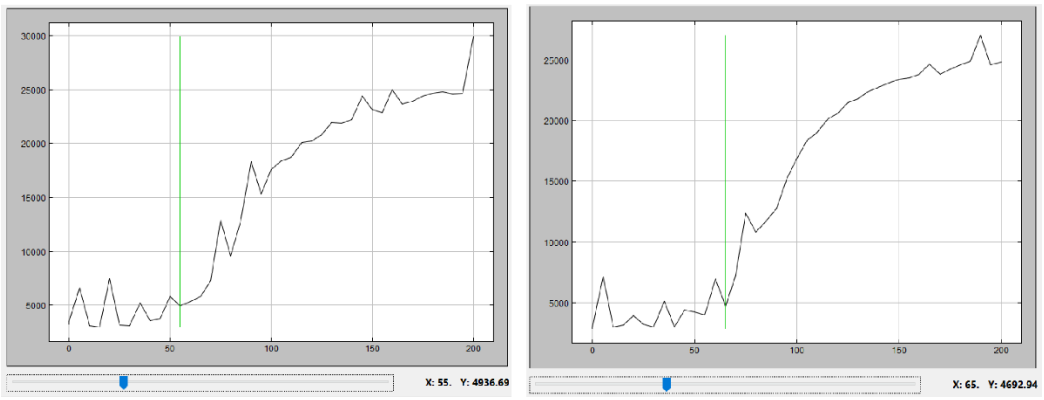

Figure A.1.54. Light scattering intensity changes with the addition of 1M NaCl in the system containing 10 mg/mL hGH, 1% PS20, and 50 mg/mL CD. (X: the added volume of NaCl solution, Y: the intensity of light scattering signal; data shown are two independent replicates)

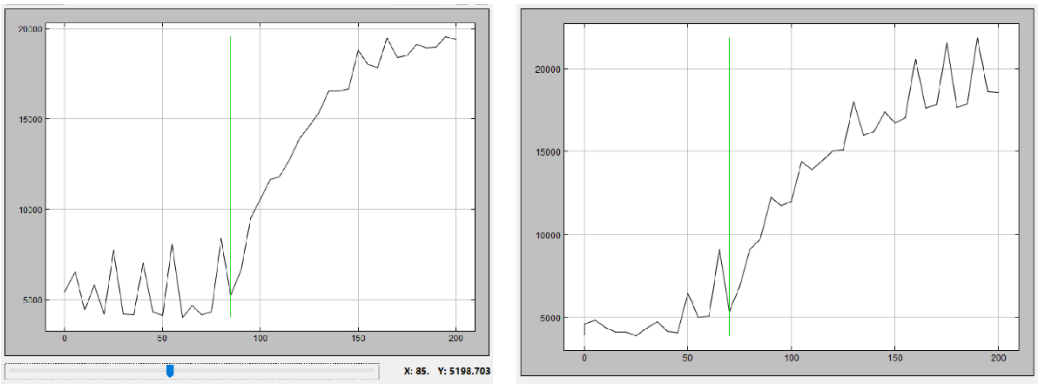

Figure A.1.55. Light scattering intensity changes with the addition of 1M NaCl in the system containing 10 mg/mL hGH, 1% PS20, and 100 mg/mL CD. (X: the added volume of NaCl solution, Y: the intensity of light scattering signal; data shown are two independent replicates)

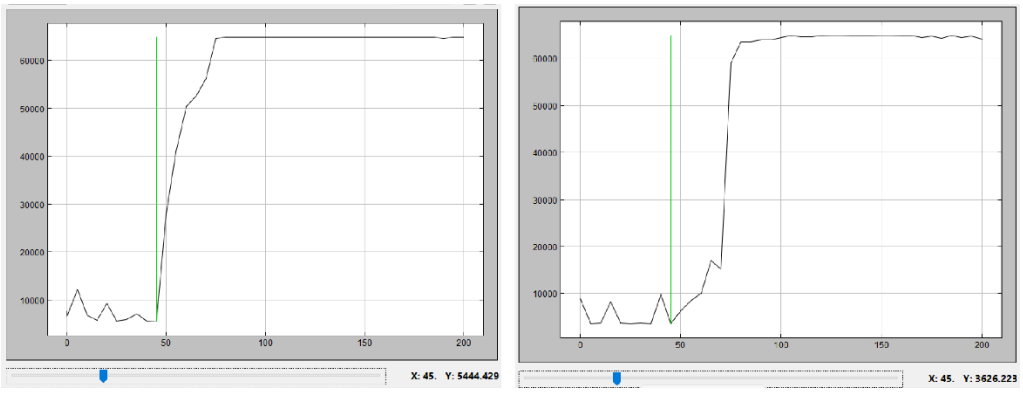

Figure A.1.56. Light scattering intensity changes with the addition of 1M NaCl in the system containing 10 mg/mL hGH, 1% PS20, 10 mg/mL CD, and phenol. (X: the added volume of NaCl solution, Y: the intensity of light scattering signal; data shown are two independent replicates)

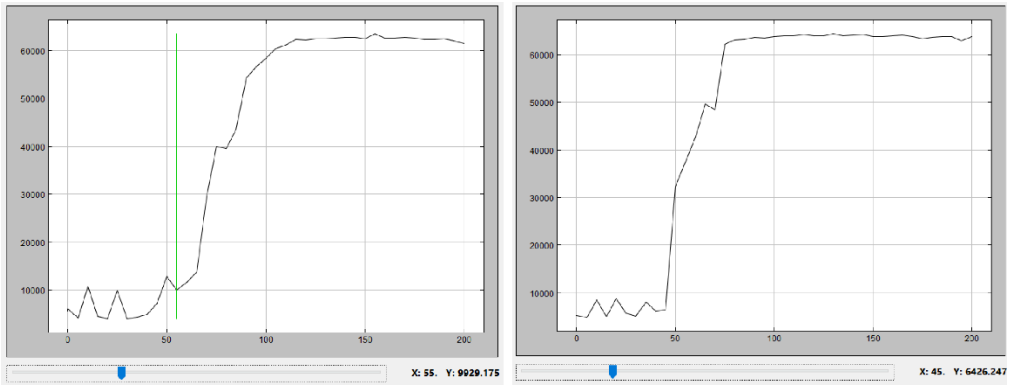

Figure A.1.57. Light scattering intensity changes with the addition of 1M NaCl in the system containing 10 mg/mL hGH, 1% PS20, 50 mg/mL CD, and phenol. (X: the added volume of NaCl solution, Y: the intensity of light scattering signal; data shown are two independent replicates)

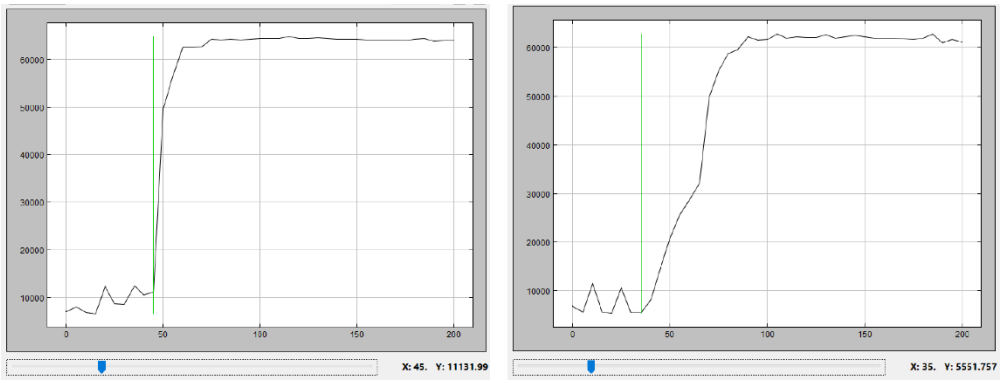

Figure A.1.58. Light scattering intensity changes with the addition of 1M NaCl in the system containing 10 mg/mL hGH, 1% PS20, 100 mg/mL CD, and phenol. (X: the added volume of NaCl solution, Y: the intensity of light scattering signal; data shown are two independent replicates)

10.2 Appendix B: Raw data and results of fluorescence signals

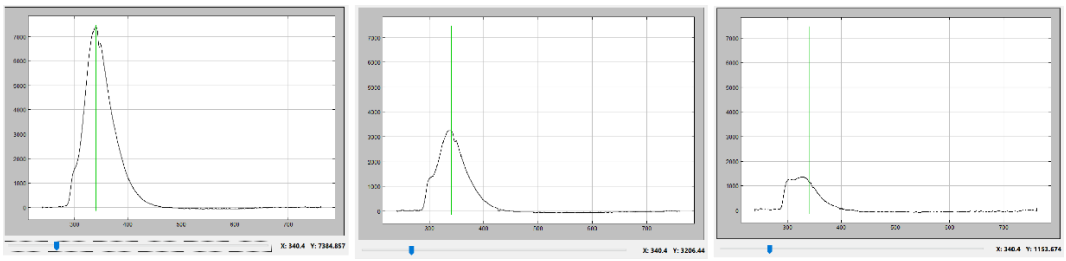

Figure A.2.1. Changes in fluorescence spectra with the addition of phenol in the system containing 10 mg/mL BSA, shown from left to right with increasing phenol volume. (X: emission wavelength, Y: fluorescence intensity)

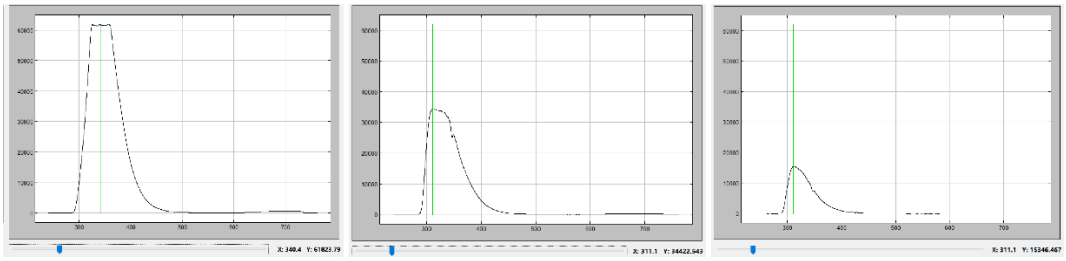

Figure A.2.2. Changes in fluorescence spectra with the addition of phenol in the system containing 10 mg/mL BSA and 10 mg/mL CD, shown from left to right with increasing phenol volume. (X: emission wavelength, Y: fluorescence intensity)

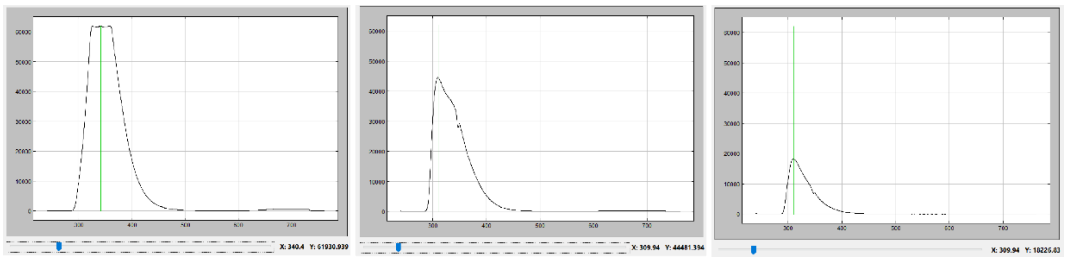

Figure A.2.3. Changes in fluorescence spectra with the addition of phenol in the system containing 10 mg/mL BSA and 50 mg/mL CD, shown from left to right with increasing phenol volume. (X: emission wavelength, Y: fluorescence intensity)

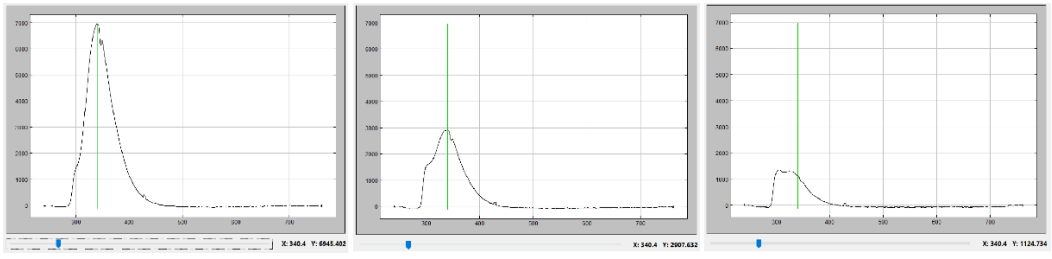

Figure A.2.4. Changes in fluorescence spectra with the addition of phenol in the system containing 10 mg/mL BSA and 100 mg/mL CD, shown from left to right with increasing phenol volume. (X: emission wavelength, Y: fluorescence intensity)

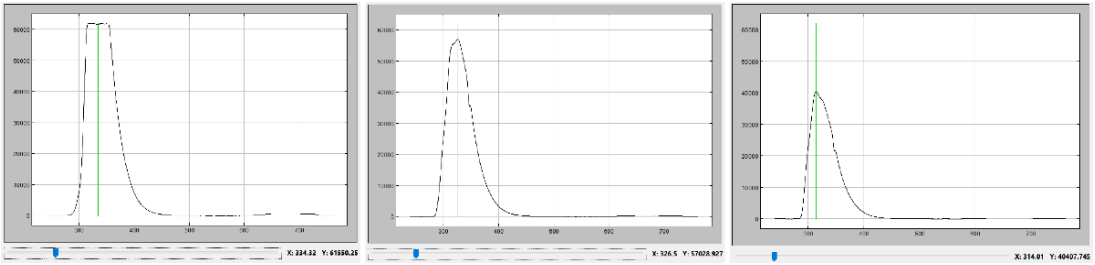

Figure A.2.5. Changes in fluorescence spectra with the addition of 4.4% phenol in the system containing 10 mg/mL hGH, shown from left to right with increasing phenol volume. (X: emission wavelength, Y: fluorescence intensity)

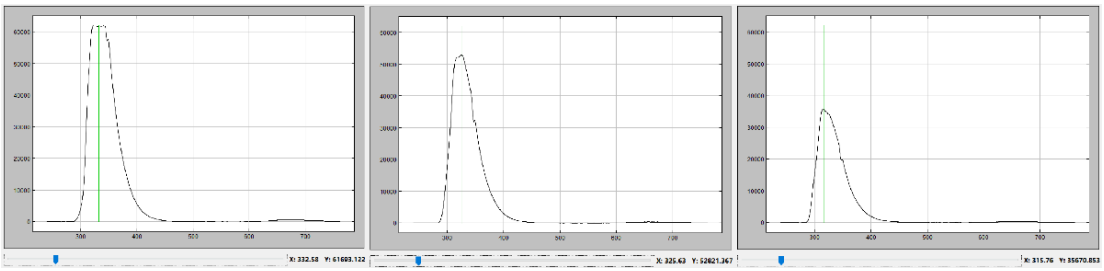

Figure A.2.6. Changes in fluorescence spectra with the addition of phenol in the system containing 10 mg/mL hGH and 10 mg/mL CD, shown from left to right with increasing phenol volume. (X: emission wavelength, Y: fluorescence intensity)

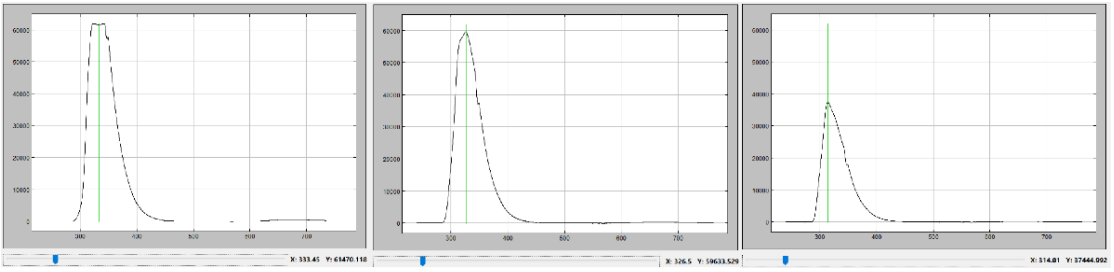

Figure A.2.7. Changes in fluorescence spectra with the addition of phenol in the system containing 10 mg/mL hGH and 50 mg/mL CD, shown from left to right with increasing phenol volume. (X: emission wavelength, Y: fluorescence intensity)

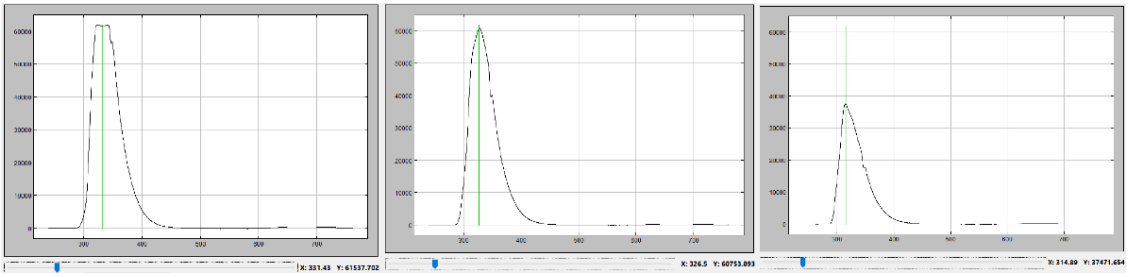

Figure A.2.8. Changes in fluorescence spectra with the addition of phenol in the system containing 10 mg/mL hGH and 100 mg/mL CD, shown from left to right with increasing phenol volume. (X: emission wavelength, Y: fluorescence intensity)

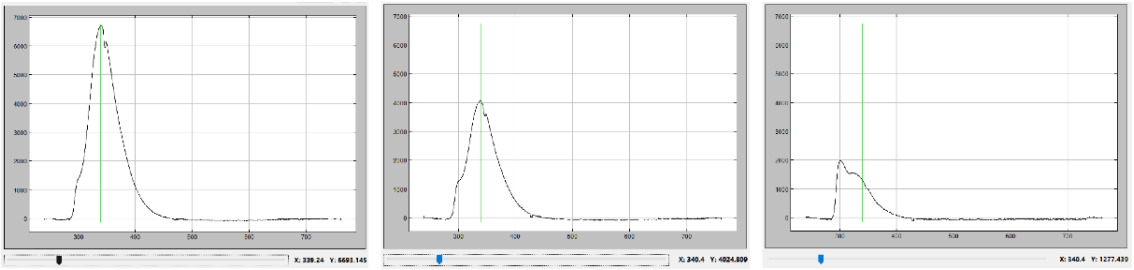

Figure A.2.9. Changes in fluorescence spectra with the addition of phenol in the system containing 10 mg/mL BSA and 0.01% PS20, shown from left to right with increasing phenol volume. (X: emission wavelength, Y: fluorescence intensity)

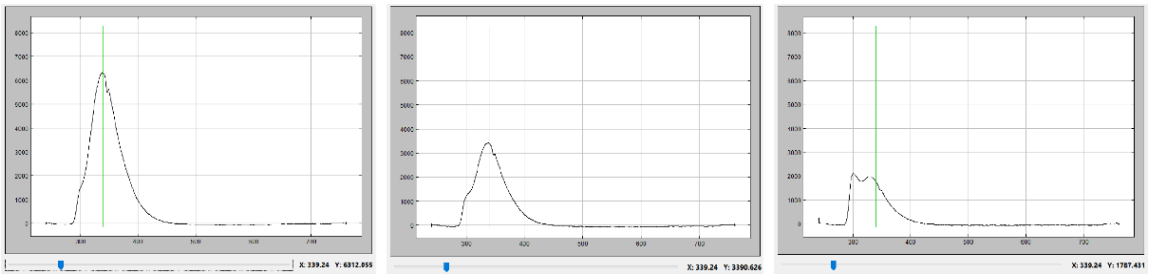

Figure A.2.10. Changes in fluorescence spectra with the addition of phenol in the system containing 10 mg/mL BSA and 0.1% PS20, shown from left to right with increasing phenol volume. (X: emission wavelength, Y: fluorescence intensity)

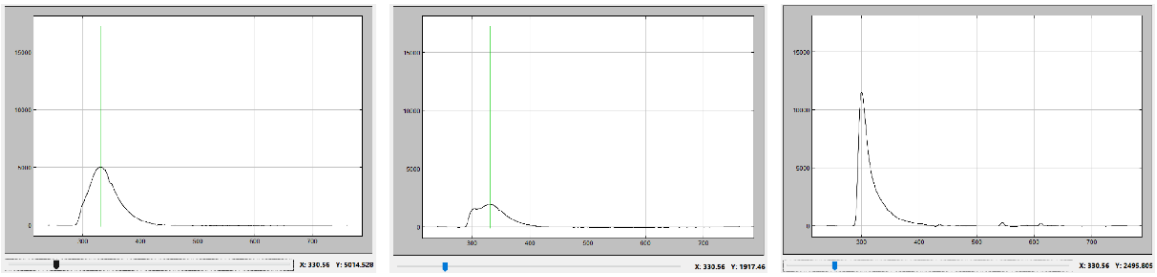

Figure A.2.11. Changes in fluorescence spectra with the addition of phenol in the system containing 10 mg/mL BSA and 1% PS20, shown from left to right with increasing phenol volume. (X: emission wavelength, Y: fluorescence intensity)

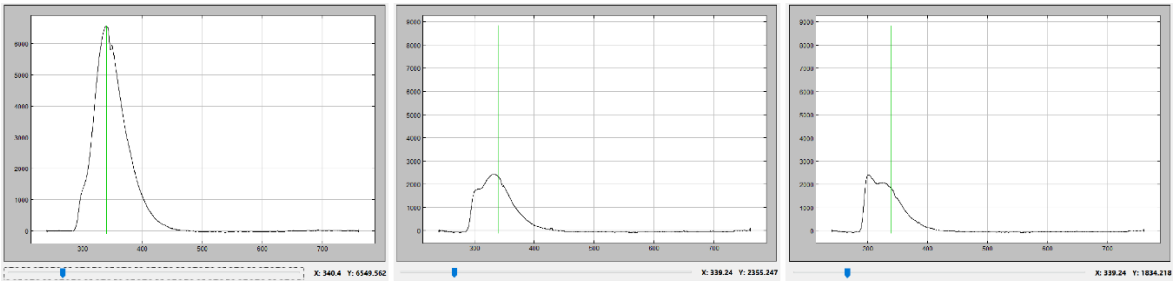

Figure A.2.12. Changes in fluorescence spectra with the addition of phenol in the system containing 10 mg/mL BSA, 0.01% PS20, and 10 mg/mL CD, shown from left to right with increasing phenol volume. (X: emission wavelength, Y: fluorescence intensity)

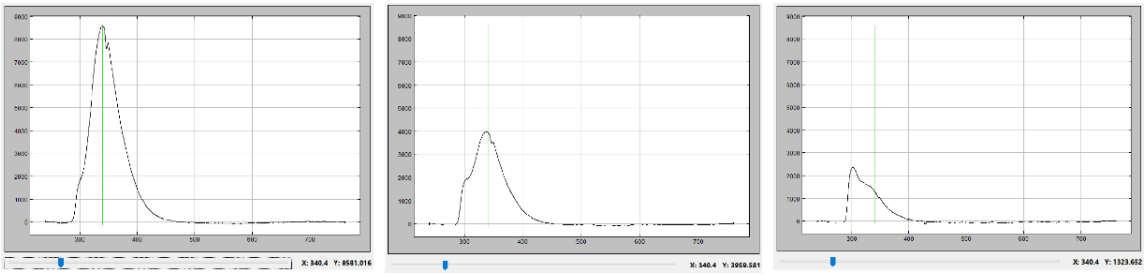

Figure A.2.13. Changes in fluorescence spectra with the addition of phenol in the system containing 10 mg/mL BSA, 0.01% PS20, and 50 mg/mL CD, shown from left to right with increasing phenol volume. (X: emission wavelength, Y: fluorescence intensity)

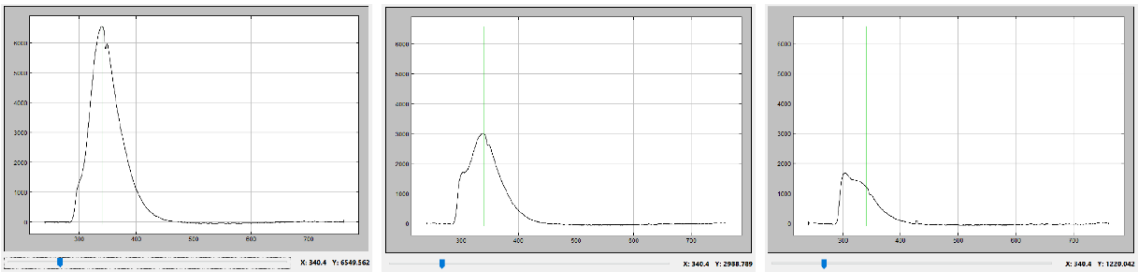

Figure A.2.14. Changes in fluorescence spectra with the addition of phenol in the system containing 10 mg/mL BSA, 0.01% PS20, and 100 mg/mL CD, shown from left to right with increasing phenol volume. (X: emission wavelength, Y: fluorescence intensity)

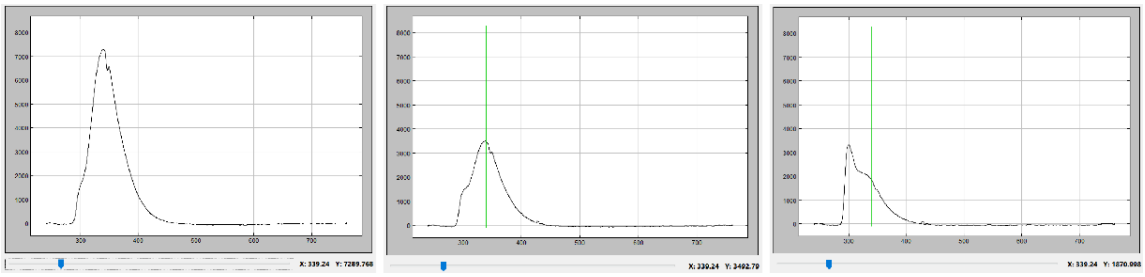

Figure A.2.15. Changes in fluorescence spectra with the addition of phenol in the system containing 10 mg/mL BSA, 0.1% PS20, and 10 mg/mL CD, shown from left to right with increasing phenol volume. (X: emission wavelength, Y: fluorescence intensity)

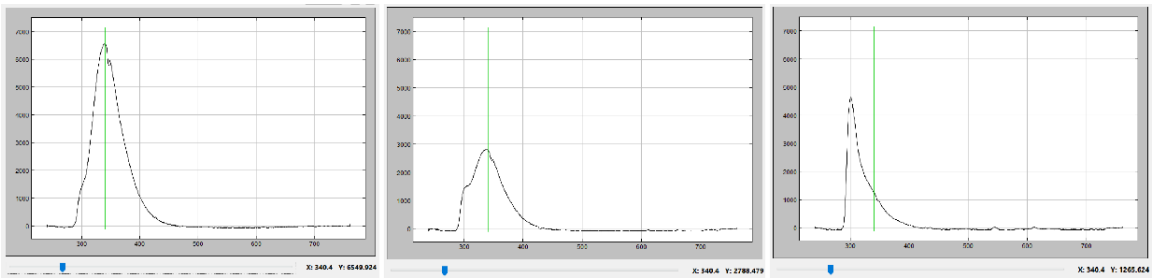

Figure A.2.16. Changes in fluorescence spectra with the addition of phenol in the system containing 10 mg/mL BSA, 0.1% PS20, and 50 mg/mL CD, shown from left to right with increasing phenol volume. (X: emission wavelength, Y: fluorescence intensity)

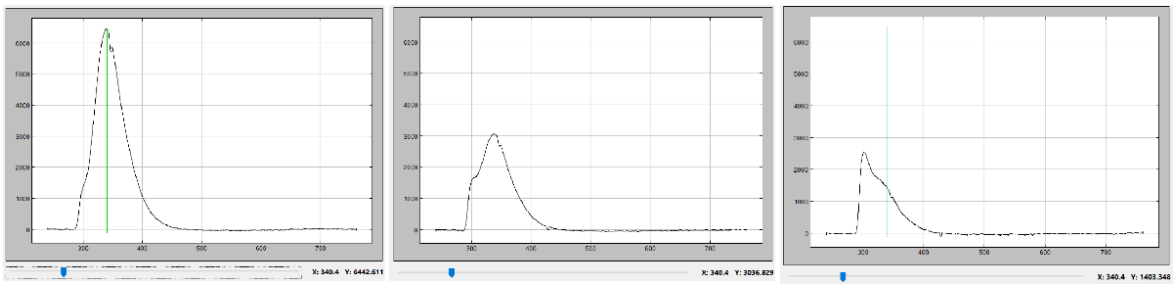

Figure A.2.17. Changes in fluorescence spectra with the addition of phenol in the system containing 10 mg/mL BSA, 0.1% PS20, and 100 mg/mL CD, shown from left to right with increasing phenol volume. (X: emission wavelength, Y: fluorescence intensity)

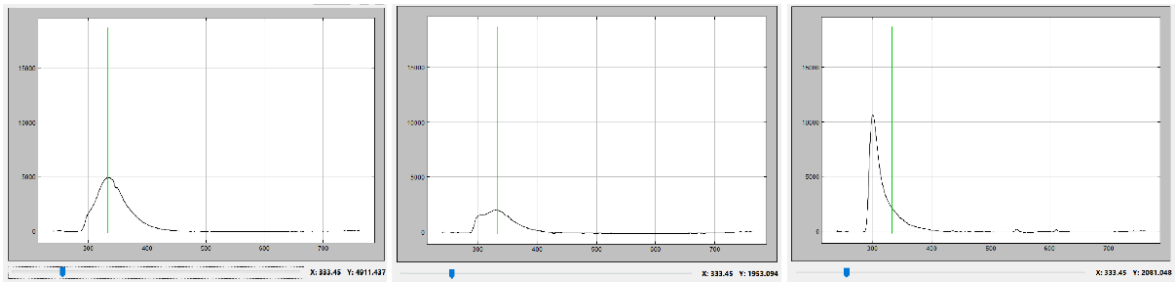

Figure A.2.18. Changes in fluorescence spectra with the addition of phenol in the system containing 10 mg/mL BSA, 1% PS20, and 10 mg/mL CD, shown from left to right with increasing phenol volume. (X: emission wavelength, Y: fluorescence intensity)

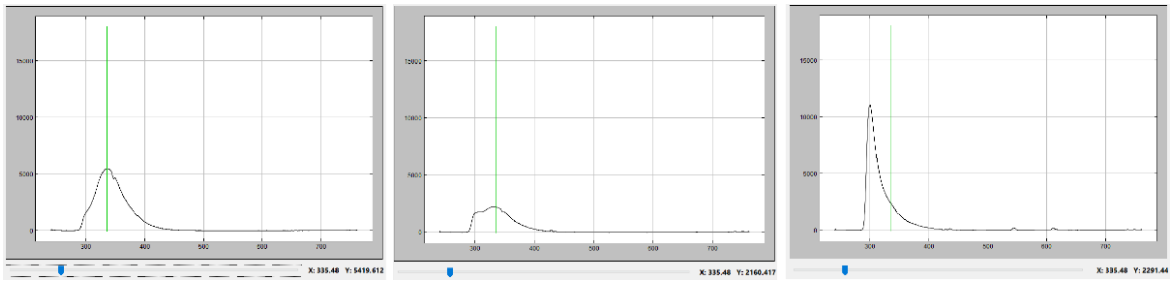

Figure A.2.19. Changes in fluorescence spectra with the addition of phenol in the system containing 10 mg/mL BSA, 1% PS20, and 50 mg/mL CD, shown from left to right with increasing phenol volume. (X: emission wavelength, Y: fluorescence intensity)

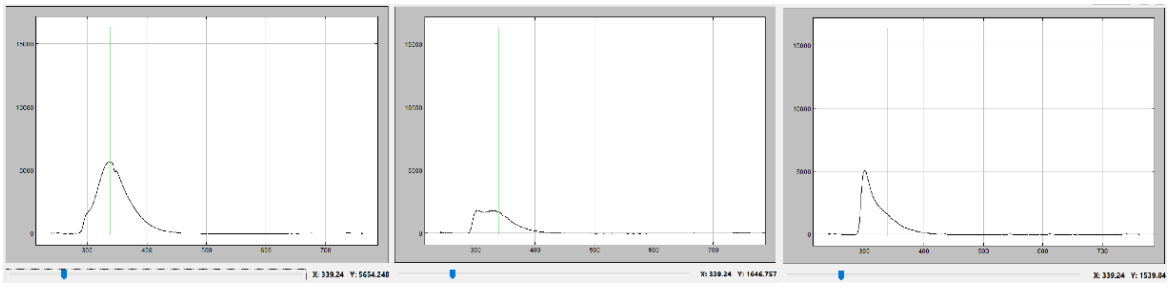

Figure A.2.20. Changes in fluorescence spectra with the addition of phenol in the system containing 10 mg/mL BSA, 1% PS20, and 100 mg/mL CD, shown from left to right with increasing phenol volume. (X: emission wavelength, Y: fluorescence intensity)

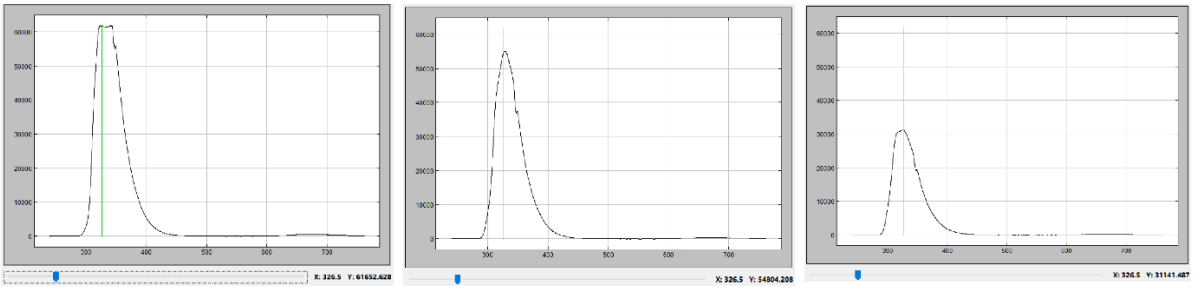

Figure A.2.21. Changes in fluorescence spectra with the addition of phenol in the system containing 10 mg/mL hGH and 0.01% PS20, shown from left to right with increasing phenol volume. (X: emission wavelength, Y: fluorescence intensity)

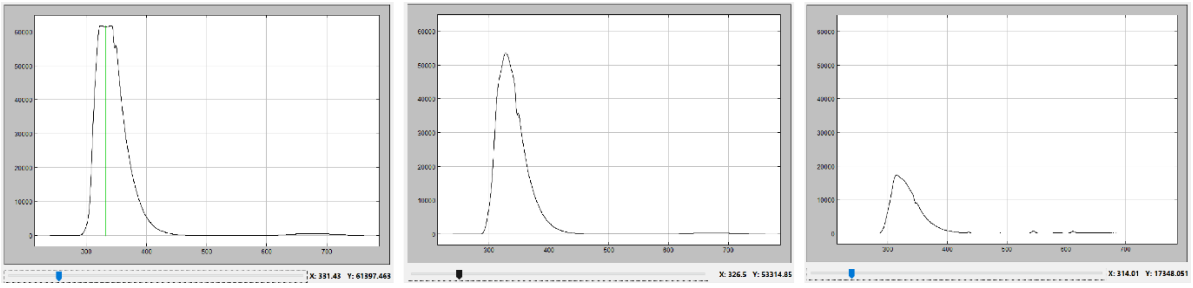

Figure A.2.22. Changes in fluorescence spectra with the addition of phenol in the system containing 10 mg/mL hGH and 0.1% PS20, shown from left to right with increasing phenol volume. (X: emission wavelength, Y: fluorescence intensity)

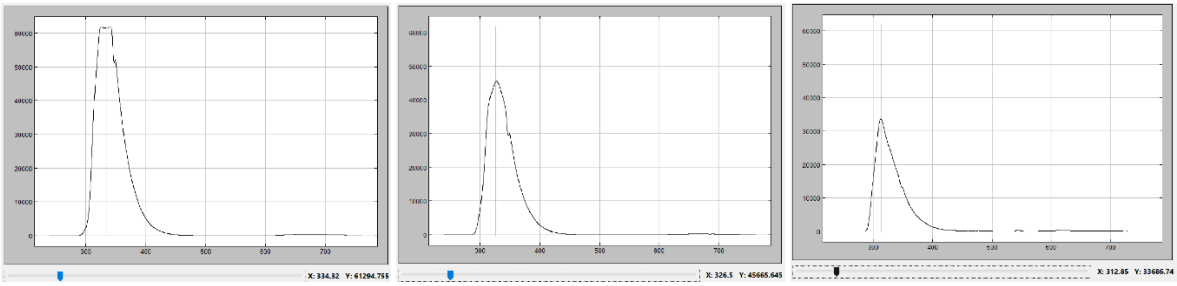

Figure A.2.23. Changes in fluorescence spectra with the addition of phenol in the system containing 10 mg/mL hGH and 1% PS20, shown from left to right with increasing phenol volume. (X: emission wavelength, Y: fluorescence intensity)

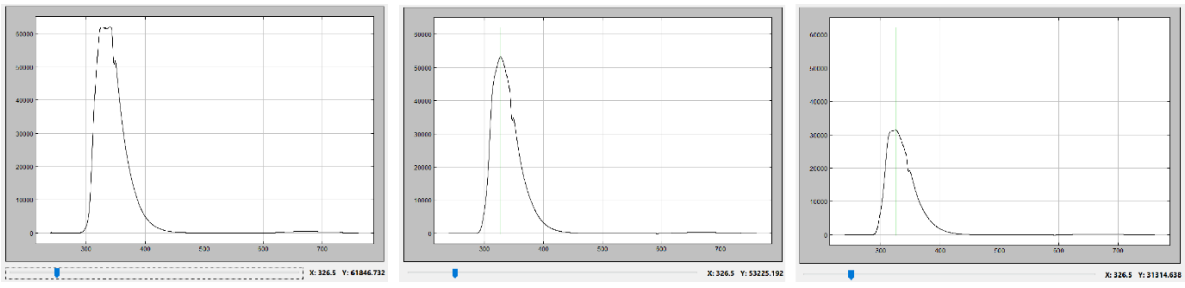

Figure A.2.24. Changes in fluorescence spectra with the addition of phenol in the system containing 10 mg/mL hGH, 0.01% PS20, and 10 mg/mL CD, shown from left to right with increasing phenol volume. (X: emission wavelength, Y: fluorescence intensity)

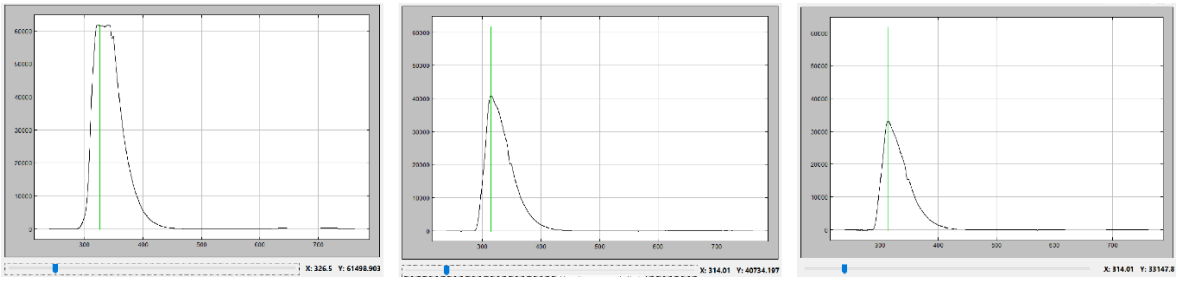

Figure A.2.25. Changes in fluorescence spectra with the addition of phenol in the system containing 10 mg/mL hGH, 0.01% PS20, and 50 mg/mL CD, shown from left to right with increasing phenol volume. (X: emission wavelength, Y: fluorescence intensity)

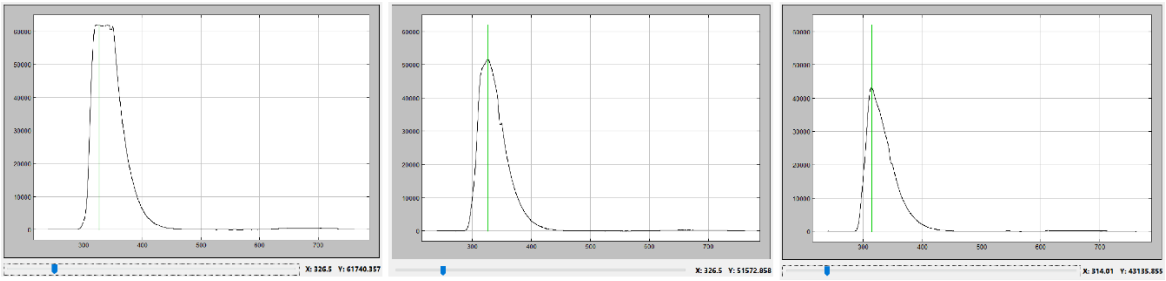

Figure A.2.26. Changes in fluorescence spectra with the addition of phenol in the system containing 10 mg/mL hGH, 0.1% PS20, and 10 mg/mL CD, shown from left to right with increasing phenol volume. (X: emission wavelength, Y: fluorescence intensity)

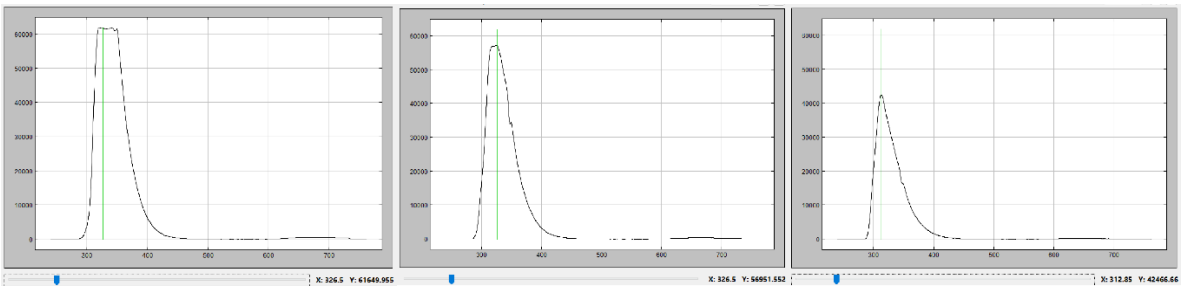

Figure A.2.27. Changes in fluorescence spectra with the addition of phenol in the system containing 10 mg/mL hGH, 0.1% PS20, and 50 mg/mL CD, shown from left to right with increasing phenol volume. (X: emission wavelength, Y: fluorescence intensity)

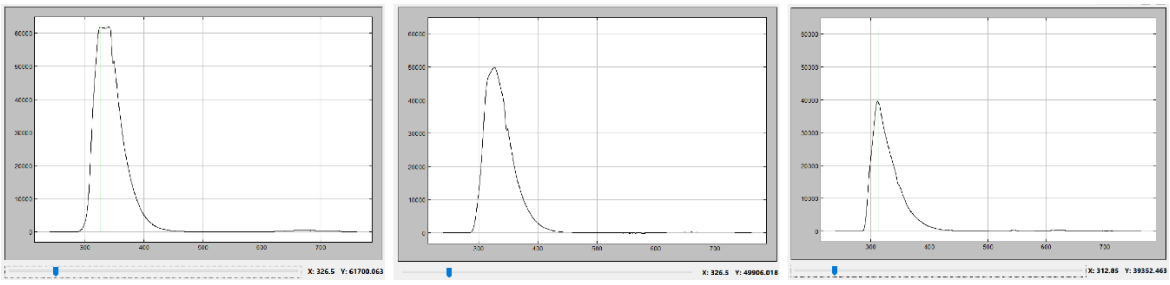

Figure A.2.28. Changes in fluorescence spectra with the addition of phenol in the system containing 10 mg/mL hGH, 1% PS20, and 10 mg/mL CD, shown from left to right with increasing phenol volume. (X: emission wavelength, Y: fluorescence intensity)

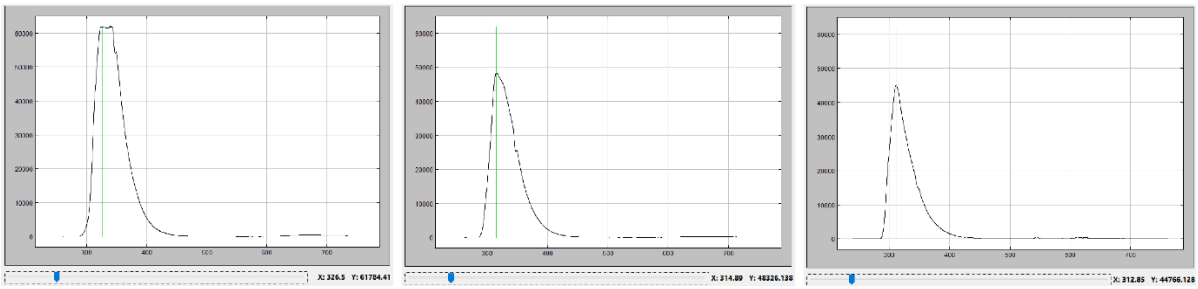

Figure A.2.29. Changes in fluorescence spectra with the addition of phenol in the system containing 10 mg/mL hGH, 1% PS20, and 50 mg/mL CD, shown from left to right with increasing phenol volume. (X: emission wavelength, Y: fluorescence intensity)

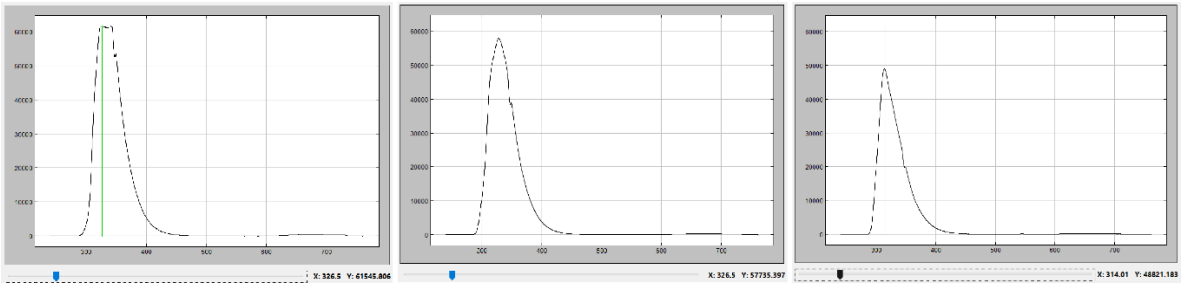

Figure A.2.30. Changes in fluorescence spectra with the addition of phenol in the system containing 10 mg/mL hGH, 1% PS20, and 100 mg/mL CD, shown from left to right with increasing phenol volume. (X: emission wavelength, Y: fluorescence intensity)

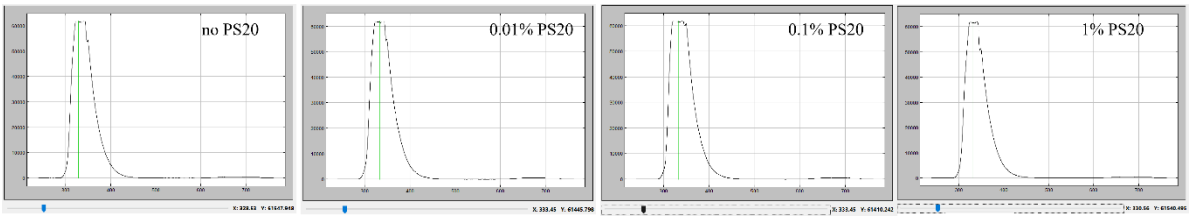

Figure A.2.31. Fluorescence spectra during the addition of 1M NaCl in the system containing 10 mg/mL hGH and different concentrations of PS20, and figures shown from left to right are 0, 0.01%, 0.1%, and 1% PS20 inside. (X: emission wavelength, Y: fluorescence intensity)

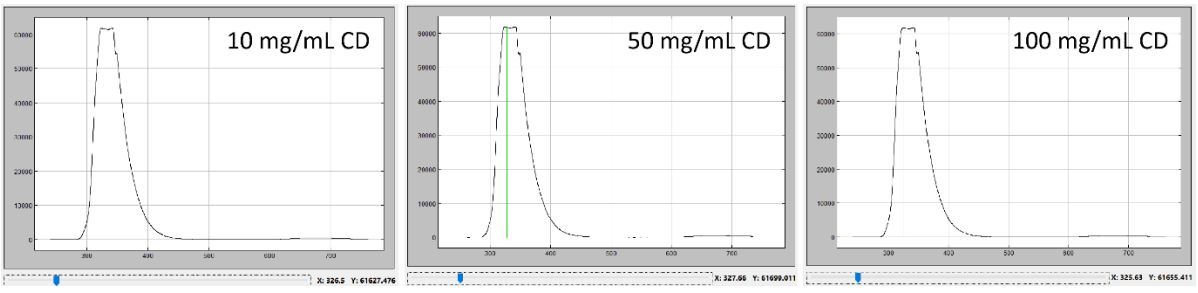

Figure A.2.32. Fluorescence spectra during the addition of 1M NaCl in the system containing 10 mg/mL hGH, 1% PS20, and different concentrations of CD, and figures shown from left to right are 10 mg/mL, 50 mg/mL, and 100 mg/mL inside. (X: emission wavelength, Y: fluorescence intensity)

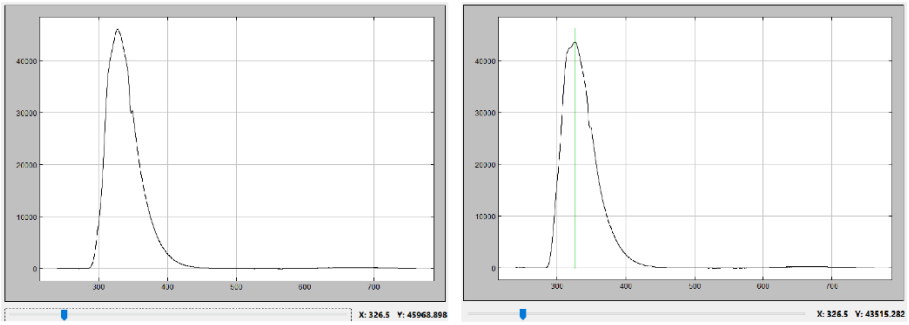

Figure A.2.33. Changes in fluorescence spectra with the addition of 1M NaCl in the system containing 10 mg/mL hGH, 0.1% PS20, and phenol, shown from left to right with increasing phenol volume. (X: emission wavelength, Y: fluorescence intensity)

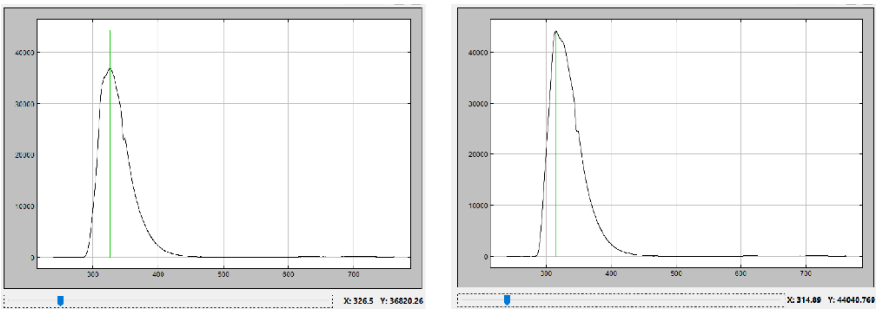

Figure A.2.34. Changes in fluorescence spectra with the addition of 1M NaCl in the system containing 10 mg/mL hGH, 1% PS20, and phenol, shown from left to right with increasing phenol volume. (X: emission wavelength, Y: fluorescence intensity)

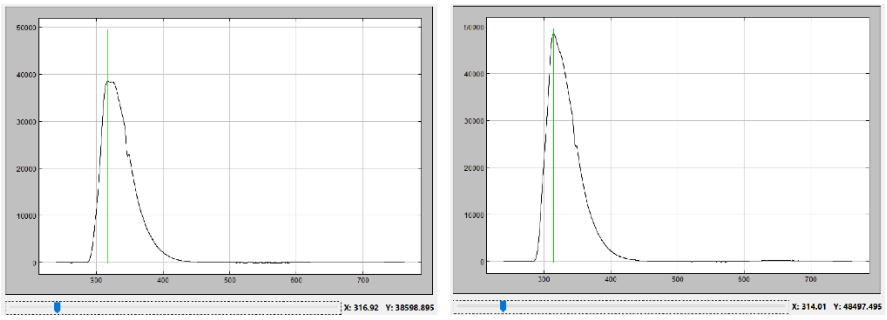

Figure A.2.35. Changes in fluorescence spectra with the addition of 1M NaCl in the system containing 10 mg/mL hGH, 1% PS20, 10 mg/mL CD and phenol, shown from left to right with increasing phenol volume. (X: emission wavelength, Y: fluorescence intensity)

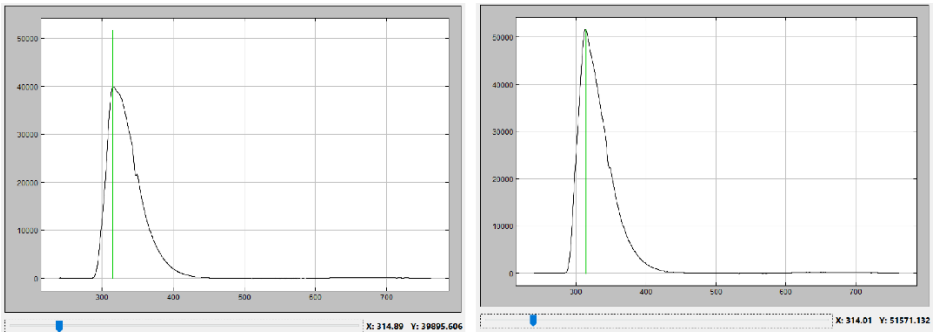

Figure A.2.36. Changes in fluorescence spectra with the addition of 1M NaCl in the system

containing 10 mg/mL hGH, 1% PS20, 50 mg/mL CD and phenol, shown from left to right with increasing phenol volume. (X: emission wavelength, Y: fluorescence intensity)

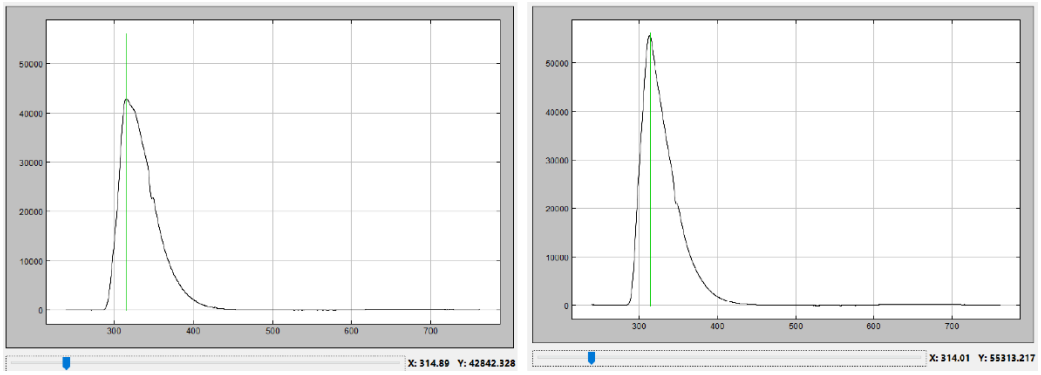

Figure A.2.37. Changes in fluorescence spectra with the addition of 1M NaCl in the system containing 10 mg/mL hGH, 1% PS20, 100 mg/mL CD and phenol, shown from left to right with increasing phenol volume. (X: emission wavelength, Y: fluorescence intensity)